2008

A study of saturated induction motor starting performance

Muhammad Choudhary
University of Windsor

A STUDY OF SATURATED INDUCTION MOTOR STARTING PERFORMANCE

by

Muhammad Choudhary

A Thesis
Submitted to the Faculty of Graduate Studies
through the Department of Electrical and Computer Engineering
in Partial Fulfillment of the Requirements for the
Degree of Master of Applied Science at the
University of Windsor

Windsor, Ontario, Canada

2008

Your file Votre référence
ISBN: 978-0-494-82098-8
Our file Notre référence
ISBN: 978-0-494-82098-8

AUTHOR'S DECLARATION OF ORIGNALITY

I hereby certify that I am the sole author of this thesis and that no part of this thesis has been published or submitted for publication.

I certify that, to the best of my knowledge, my thesis does not infringe upon anyone's copyright nor violate any proprietary rights and that any ideas, techniques, quotations, or any other material from the work of other people included in my thesis, published or otherwise, are fully acknowledged in accordance with the standard referencing practices. Furthermore, to the extent that I have included copyrighted material that surpasses the bounds of fair dealing within the meaning of the Canada Copyright Act, I certify that I have obtained a written permission from the copyright owner(s) to include such material(s) in my thesis and have included copies of such copyright clearances to my appendix.

I declare that this is a true copy of my thesis, including any final revisions, as approved by my thesis committee and the Graduate Studies office, and that this thesis has not been submitted for a higher degree to any other University or Institution.

ABSTRACT

The use of induction motors in modern industry become increasingly high. Induction motor starting phenomenon has an important impact on the industrial loads and dynamics of the power system. Induction motor consumes tremendous amount of reactive power during starting, resulting in considerable drop in the terminal voltage. The starting current of the motor increases six to seven times of the rated current and starting time extends. This voltage depression during the starting transient period affects the starting and acceleration torque of the motor, as it is a function of the voltage. In this research work, starting performance of induction motor is investigated and analyzed comprehensively.

To minimize the terminal voltage drop of the motor during starting, reactive power compensation is required. Static VAR compensator (SVC) and shunt capacitors are used as a source of reactive power for both 50 hp and 500 hp motors. By employing SVC and shunt capacitors, significant improvement in the terminal voltage is achieved with less starting time for different loading conditions.

The saturation takes place in almost all induction electrical machines and induction motors are no exceptions. Transient saturated induction motor (50 hp) model is developed to investigate the effect of main flux saturation on the starting performance for different loading conditions.

DEDICATION

To my parents

&

To my wife & kids

ACKNOWLEDGEMENTS

First of all, I would like to thank my God who gave me courage to stay away from my family and still fully concentrate on my research with full capacity. Secondly, I would like to express my sincere thanks to Dr. Narayan Kar for his extremely valuable guidance and suggestions throughout this project. His technical assistance and personal advice have been invaluable. Also special thanks to my examining committee Dr. K. Tepe and Dr. T. Bolisetti for reviewing my research work. I would also like to thank my fellow graduate students for their technical help and suggestions.

I am very much obliged to my wife due to her continuous unyielding support during my whole study period. I would also like to have special thanks to my loving wife who took care of my three kids in my absence and gave me all possible encouragements towards my degree.

TABLE OF CONTENTS

LIST OF TABLES

LIST OF FIGURES

LIST OF SYMBOLS

ψ_{ds}, ψ_{qs} : d-and q-axis stator flux linkages, respectively.

ψ_{dr}, ψ_{qr} : d-and q-axis rotor flux linkages, respectively.

V_{ds}, V_{qs} : d-and q-axis stator voltages, respectively.

V_{dr}, V_{qr} : d-and q-axis stator voltages, respectively.

i_{ds}, i_{qs} : d-and q-axis rotor currents, respectively.

i_{dr}, i_{qr} : d-and q-axis rotor currents, respectively.

R_s, R_r : stator and rotor resistances, respectively.

L_s, L_r : stator and rotor inductances, respectively.

L_{ls}, L_{lr} : stator and rotor leakage inductances, respectively.

L_m, L_{ms} : unsaturated and saturated magnetizing inductances, respectively

i_m : magnetizing current.

i_{md}, i_{mq} : d-and q-axis magnetizing currents, respectively.

T_e, T_L : electromagnetic torque and load torque, respectively.

ω_s, ω_r : synchronous and rotor speed, respectively.

B : friction coefficient.

J : inertia coefficient.

σ : conduction angle.

α : firing angle.

Q_{lmax} : maximum inductive reactive power.

Q_{cmax} : maximum capacitive reactive power.

V_m : measured voltage.

V_{ref} : reference voltage.

B_α : effective susceptance.

1. Introduction

1.1 Background

The rotating magnetic field is a fundamental principle on which induction motors are based. Faraday discovered the electromagnetic induction law around 1831 and Maxwell formulated the laws of electricity (Maxwell's equations) around 1860. By using these basic laws Galileo Ferrari (1885) in Italy and Nicola Tesla (1886) in United States initially invented induction machine [1].

Both induction machines based their designs on two-phase systems. In Fig. 1 Ferrari's patent the rotor was made of by using a copper cylinder In Fig. 2 Tesla's patent the rotor was made of by using a ferromagnetic cylinder with short-circuited winding In 1889 Dolivo-Dobrovolsky invented the induction motor with the wound rotor and subsequently the cage rotor in a topology very similar to that used today. General Electric began installation of three-phase systems in 1893. But with the passage of time the three-phase system led to its eventual adoption as a nearly universal standard for generation, transmission, and distribution [2].

Multiphase induction machines, especially with squirrel-cage rotors, are the simplest and least expensive electrical machines devised. Small power induction motors, in most home appliances, are fed from a local single phase AC power grid. Now after over a century from its invention, the induction motor steps into the 21st century which is mostly used motor in industry. This is due to the fact that induction machines are rugged, simple in construction, easy to maintain and reliable.

Basically, electric motors are divided into three broad horsepower categories small, medium and large. The most common motors are considered to be fractional-horsepower motors with ratings from 1/20 to 1 hp and are categorized as small motors. Also included in the small category are motors with smaller ratings, which are commonly classified as sub-fractional or miniature. Medium size motors are considered to be in the range of 1 hp to 100 hp, with large motors occupying the 100 hp to 50,000 hp range.

In United States and Canada for both AC and DC motors, the Institute for Electrical and Electronic Engineers (IEEE) establishes the standards for motor testing and test methodologies, while the National Electrical Manufacturers Association (NEMA) prepares the standards for motor performance and classifications. Besides the industry

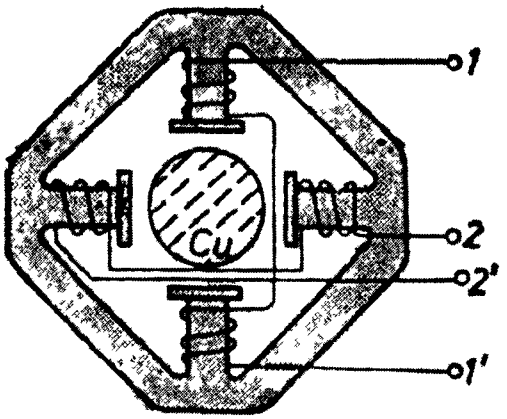

Fig. 1. Ferrar's induction motor [1].

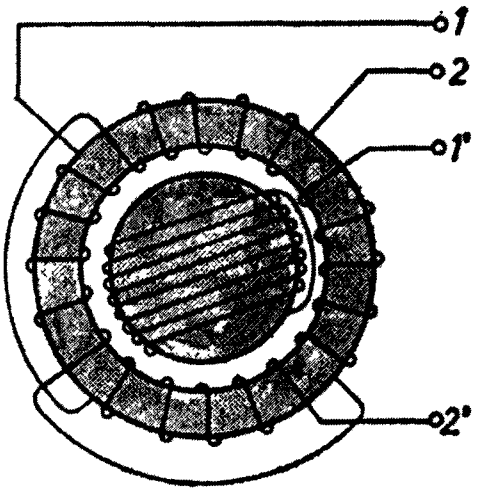

Fig. 2. Tesla's induction motor [1].

usage, the induction motors are widely used in home appliances (fans, washing machines, dryers, refrigerators, freezers, etc.). In industry, induction machines have variety of applications, like pumps, compressor and other drives. Induction motors are mostly used for variable speed applications in association with PWM converters. Besides being used as drives in the industries, the induction machines are extensively used for wind turbines. Nearly 85% of wind power generation is being done by induction generators, both squirrel-cage and wound rotor type.

Induction motors draw large reactive power during starting and as a result, initial inrush current is high, which is undesirable during starting. Due to high starting current, motor terminal voltage drops considerably, causing a drop in the accelerating torque [3], [4]. The reduction in the starting torque extends the acceleration time of the motor, which might cause a heating problem in the winding [5]. To overcome all these starting issues, researchers have been using different starting methods, such as reduced voltage methods and full voltage methods [6]. The main objective of using different starters is to reduce starting current, to stabilize the terminal voltage, to develop sufficient accelerating torque and also to reduce the starting time of the motor [7], [8]. If these starters are not used during starting, especially for large starting motors in an isolated power system, voltage instability problem may arise [9], [10]. In any power system transient and steady state stabilities are very crucial for the power system. Starting transients of induction motors have significant importance for the voltage stability [11]-[14]. To fulfill the demand of

reactive power required by the induction motor, Shunt capacitors are one of the economical ways of providing necessary VARs (volt-ampere reactive) [15]. Solid state devices like static VAR compensators (SVC) are another mean of controlling the reactive current drawn by the motor during starting [16]. Different starting methods can be used to start the large induction motors depending on the different applications [5], [6].

1.2 Brief Review of Induction Motors

The induction motor essentially consists of two parts:

- Stator
- Rotor

The power supply is connected to the stator and the rotor receives power by induction caused by the rotating stator flux, hence the motor is called as induction motor. The stator consists of a cylindrical laminated and slotted core placed in a frame of rolled or cast steel [17]. The frame provides mechanical protection, carries the terminal box and the end covers with bearings. The rotor consists of a laminated and slotted core tightly pressed on the shaft as shown in the Fig. 3. There are two general types of rotors:

- The squirrel-cage rotor
- The wound (or slip-ring) rotor

Squirrel-Cage - In squirrel-cage motors, the rotor consists of a permeable metal containing embedded strips of magnetic material. As the stator magnetic field rotates, the field interacts with the magnetic field established by the magnetic poles of the rotor, causing the rotor to turn at nearly the speed of the rotating stator magnetic field [1].

Wound-Rotor - In wound-rotor designs, the permanent magnets used in the squirrel-cage motor are replaced by a rotor having windings. In this motor, when the stator magnetic field rotates and the rotor windings are shorted, the stator magnetic field motion induces a field into the wound-rotor, once again causing the rotor to turn at nearly the speed of the rotating stator magnetic field. However, if the rotor windings are connected externally through slip rings on the shaft, the winding current can be controlled to increase or decrease the slip speed of the rotor [1].

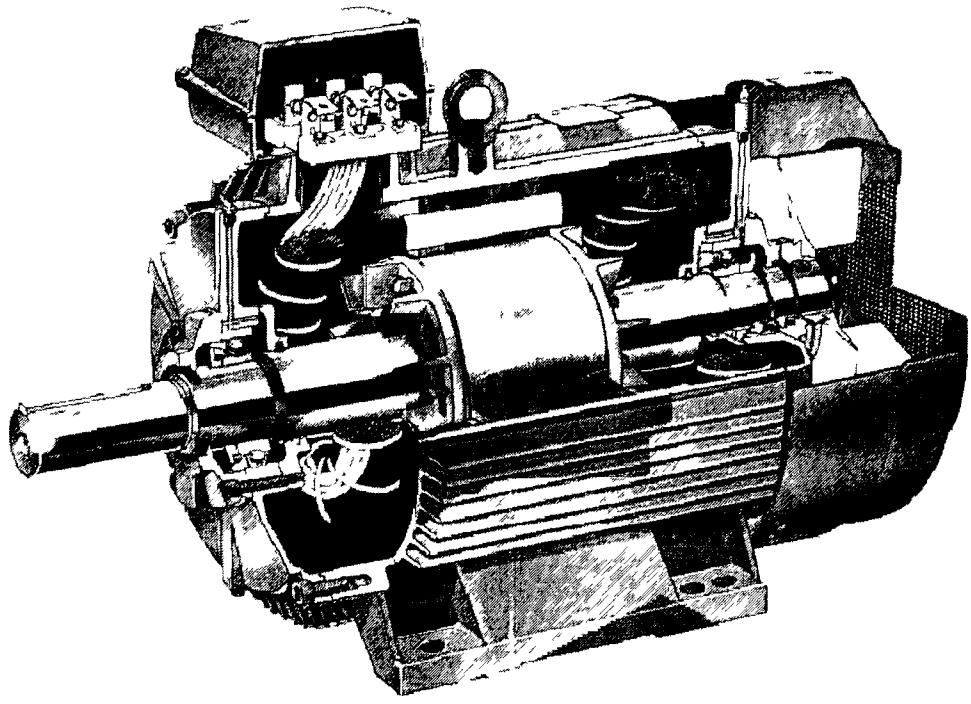

Fig. 3. A state-of-the-art three-phase induction motor [1].

1.3 Induction Motor Starting Issues

Induction motor loads are becoming increasingly larger in overall modern industrial systems. Voltage instability in power system recently gained an increasing importance. Voltage instability characterized by progressive fall in the magnitude of the voltage at particular nodes and may finally result in complete voltage collapse [10]. The starting of large induction motors causes significant drop in the terminal voltage due to high inrush current, as motor draws large reactive power from the system. This transient voltage depression can substantially reduce the motor torque [18], and extends the starting period of the motor. Also, if these voltage dips are severe, may cause deceleration of the other motors feeding on the same bus, which increase the demand of reactive power.

Induction motors typically have very low power factor during starting, and draw approximately six to seven times of the rated current [19]. This causes significant voltage drop at the terminal of the motor and severely influence the operation of locally connected loads in parallel. Recently these starting issues discussed above attracted great

attention from the researchers. During starting of induction motors, the key factors which influence the starting performance are:

- draw large reactive power
- high inrush current
- high voltage drop
- low accelerating torque

Induction motors consume large reactive power during starting. Because of the highly inductive nature of the motor circuit at rest, the power factor is quite low and consequently draws higher inrush current [8].This undesirable high starting current decays slowly during the transient period. The large inrush current causes problems for the equipment connected to the electrical system. The terminal voltage drops significantly, which further reduces the accelerating torque and thus increases the acceleration time of the motor. The motor needs sufficient starting and accelerating torque to gain the operating speed, with less acceleration time without any overheating [20]. Induction motor starting torque is a function of the voltage, as it reduces by the square of the voltage during starting period.

Induction motor must generate a torque greater than the torque required to accelerate the load. The motor needs the time to accelerate the required load is a function of load inertia and it depends on the margin between the torque of the motor and the load curve, as shown in the Fig. 4 [6]. During starting of the motor, high inertia loads may prolong the starting time due to terminal voltage drop and also heating in the motor due to high currents drawn [21]. Starting torque requirements of some loads may not permit the use of motors with low inrush current in order to reduce the voltage dip caused by the starting of the motor [22].

To reduce the reactive current drawn by the motor during starting, injection of VARs (volt-ampere reactive) is absolutely important to stabilize the terminal voltage of the motor and this phenomenon is called the reactive power compensation [23]. Series and shunt VAR compensation can be used to modify the electrical behavior of AC power system.

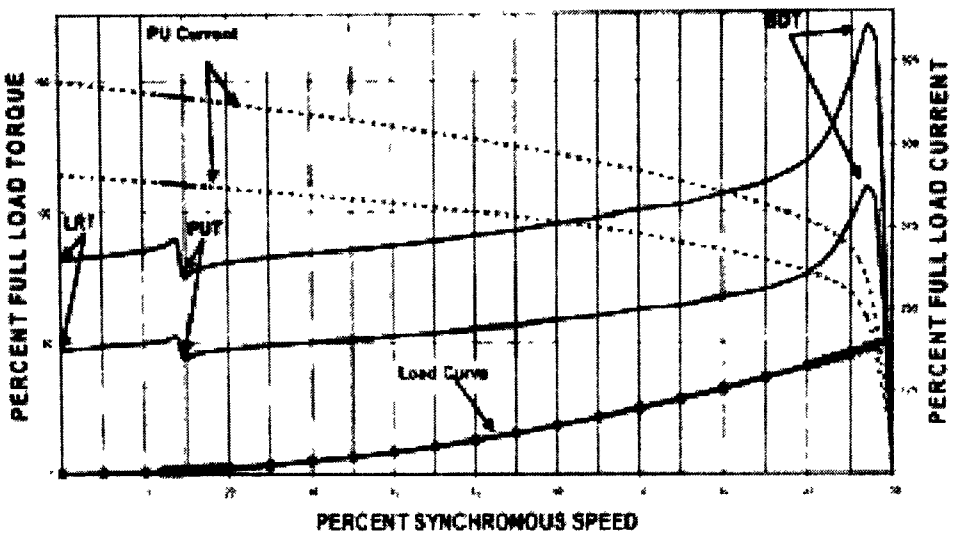

Fig. 4. Typical speed torque, current curves with load curve [6].

Series compensation can be used to modify the transmission or distribution parameter of the system [24]. Shunt compensation may be applied to change the equivalent impedance of the load. The main objectives of both methods is to manage the reactive power to improve the performance of AC system. In load compensation, the main goals are to increase the value of the system power factor, to balance the real power drawn from A.C supply and voltage regulation [25].

In the past, different methodology has been used to solve this voltage dip problem during starting of induction motors [26]. While starting, the motor draws inrush current which is directly proportional to the terminal voltage. Therefore the current limiting starting methods also called reduced voltage methods can be applied to reduce the voltage dip. In all reduced voltage starting methods, as explained earlier, the torque available for accelerating the load is the most critical consideration, especially when high inertial loads are involved. So by taking this important factor into account, full voltage or 'direct starting' method is the most economical and frequently used method these days in an industry. As discussed before, to limit the high inrush currents, and to minimize the voltage dip, reactive power compensation can be done [5], [6].

Shunt capacitors are one of the economical ways of supplying reactive power to the system to boost the terminal voltage of induction motor [27], [28]. By using this method,

the high inductive component of the starting reactive current can be reduced considerably by addition of capacitor bank to the motor bus [14], [15], [19]. The significant advantage of this approach is, it does not reduce the starting torque during the starting period. The starting transient characteristics of induction motor while using the different starting methods can be observed [5]. It has been noticed that the inrush currents during the stating period influence the induction motor starting performance during the transient's period. A fast and recursive solution for induction motor transients has been discussed in [13].

Static VAR compensators (SVC), solid-state switching devices provide continuous reactive power support and maintain stable utility and plant voltages [15], [29]. SVC improves the starting performance of induction motor, by controlling the flow of reactive power during the starting transient period [30], [31]. SVC is a best solution for the voltage flicker or transient voltage drop occurs at the pumping stations, during starting of large induction motors [15]. Moreover, SVC helps to prevent the voltage instability which may results from the presence of large induction motors under some system conditions. These voltage instabilities may further lead to the uncontrolled transient voltage collapse [32]-[36].

The induction motor starting performance with constant parameters has traditionally been used in the past. The effects of magnetic saturation in induction motors cannot be avoided as the saturation takes place in almost all the electrical machines. So for the determination of accurate starting behavior of an induction motor, inclusion of saturation effects is important [37]-[47]. The magnetic saturation effect is significant during the starting transient and steady state period of induction motor. The impact of saturation on 'direct start' of induction motor is very vital while considering the torque oscillations during transient state [48].

1.4 Objective

The main objective of this research work is to investigate the starting performance of induction motor by employing shunt capacitors and SVC for different loading conditions. In this research work it will be comprehensively analyzed the role of reactive power and

voltage profile during starting transient and impact of these effects on the motor performance and the system stability.

Moreover, another goal of this work is to investigate the reduction in starting and accelerating torque with the drop in the terminal voltage, and its influence on the motor acceleration performance during the starting transient period. Induction motors draw large reactive power while starting which results in significant drop in the terminal voltage that leads to voltage instability. To improve the starting voltage, injection of reactive power is performed by using two different methods with shunt capacitors and SVC.

In this research work, main flux saturation has been incorporated in the motor modeling in order to investigate further, how the starting behavior of induction motor can be affected by saturation. Also, the effect of considering and ignoring main flux saturation has been analytical compared while employing SVC and shunt capacitors for direct starting of induction motor.

Also, another attempt has been made to investigate starting performance of unsaturated model of larger motor (500 hp). During the transient period voltage and reactive power characteristics of 500 hp motor are analyzed and compared with 50 hp motor for unsaturated model.

1.5 Scope

A d-q model of induction motor with squirrel-cage rotor considering and ignoring saturation has been developed to investigate the starting performance. For certain values of voltage, load, and frequency, and machine parameters, the starting behavior of induction motor has been investigated and analyzed. During the starting period the drop in the terminal voltage has been noted for different loading conditions. Starting inrush current envelope, starting torque oscillations and motor starting time have been observed. Induction motor demands significant amount of reactive power during starting period. There are many methods to support VARs requirements. In this research work, shunt capacitors of known capacitance values and static VAR compensator (SVC) of known susceptance values have been used to supply the necessary reactive power.

MATLAB/Simulink program has been used in order to perform the simulations and numerical investigations. Simulated results have been used to analyze the starting performance. Also, comparative analysis of the starting performance by employing shunt capacitors and SVC has been discussed. It has been noticed that injection of reactive power by capacitor or SVC improves the starting performance of the motor by stabilizing the terminal voltage during transient and steady state.

The main flux saturation has been included in the model to analyze the starting performance. The dynamic performance of induction motor during direct starting, with capacitor and SVC has been analytically investigated, while ignoring and considering the main flux saturation.

The starting characteristics of bigger motor (500 hp) have been investigated. The behavior of terminal voltage and reactive power consumption has been analyzed and compared with a 50 hp motor for different loading conditions.

2. Problem Definition

2.1 Methods of Starting Induction Motors

Different starting methods can be used to start the induction motor, depending upon the applications and requirements. The primary objective of all the starting methods is to minimize the voltage drop at the motor terminals and to provide soft start of the driven equipment, along with adequate accelerating torque to the load. The selection of the method depends on the overall power system constraints, equipment cost and the driven load. Each of these methods requires some kind of mechanical switch or contact. These methods are divided into two main categories [6].

- Reduced voltage starting
- Full voltage starting

2.2 Reduced Voltage Starting

As stated in previous chapter, the induction motor during starting draws six to seven times its rated current, when rated voltage is applied to the stator terminals of the motor. If the terminal voltage is reduced, the motor starting current will be reduced linearly with the voltage [5]. In all reduced voltage methods, the accelerating torque is the most critical factor to be considered. The common reduced voltage methods include:

- Autotransformer starting
- Wye-Delta starting
- Part winding starting
- Solid state voltage controller starting

2.2.1 Autotransformer Starting

The standard taps ranging from 50-80% of normal rated voltage are used for autotransformer starting of induction motor as shown in the Fig.5. Practically as the motor gains speed these taps are changed to increase the terminal voltage [6]. However, there will be transient period due to switching of these taps. The torque transient period of the motor is also a function of this current peak, which may cause problem to the

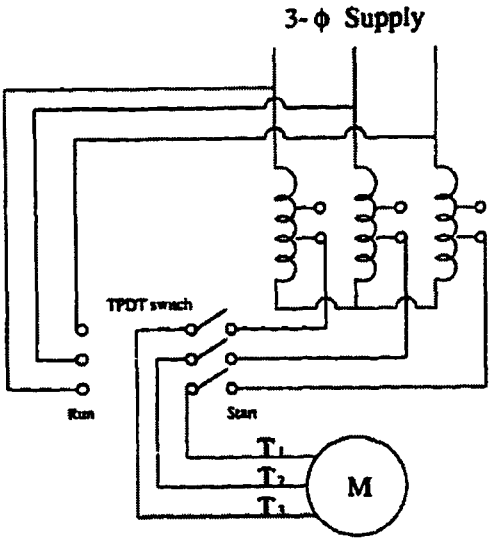

Fig. 5. Auto-transformer motor starting [49].

driven equipment [8]. This method is more costly than any other reduced voltage starting methods and, also another disadvantage is low starting torque [49].

2.2.2 Wye-Delta Starting

The Wye-Delta starting method is used extensively with wye–start and delta-run configuration as shown in the Fig. 6. Initially during the start-up phase, the delta connected stator is connected in wye, which reduces the voltage by a factor of $1/\sqrt{3}$ and results in only $1/\sqrt{3}$ of nominal current draw [6]. But also reduces the starting torque roughly 2/3. However, the switching from wye to delta can be done at 50-60% of full load speed of the motor [49].

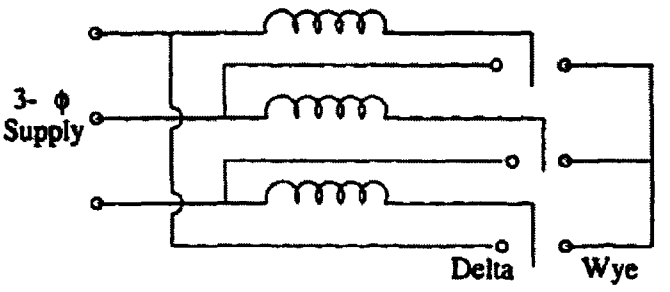

Fig. 6. Wye-Delta motor starting [49].

2.2.3 Part-Winding Starting

In this method, the stator of the motor is designed with two part windings, in such a way that each of windings produces same number of poles and same amount of rotating magnetic field. For starting of the motor, full voltage is applied to one circuit of each phase as shown in the Fig. 7.

By using this method a considerable reduction in both starting current (50 to 60%) and starting torque (nearly 45%) can be achieved. This method is more suitable for light loads or at no load conditions. [6].

2.2.4 Solid-State Voltage Controller Starting

This method of starting is the simplest form of soft starting of induction motor by using solid state devices for variable speed drives as shown in Fig. 8. Thyristors or silicon controlled rectifiers (SCRs) can be used to control the line voltage during starting of the motor [10], [49].

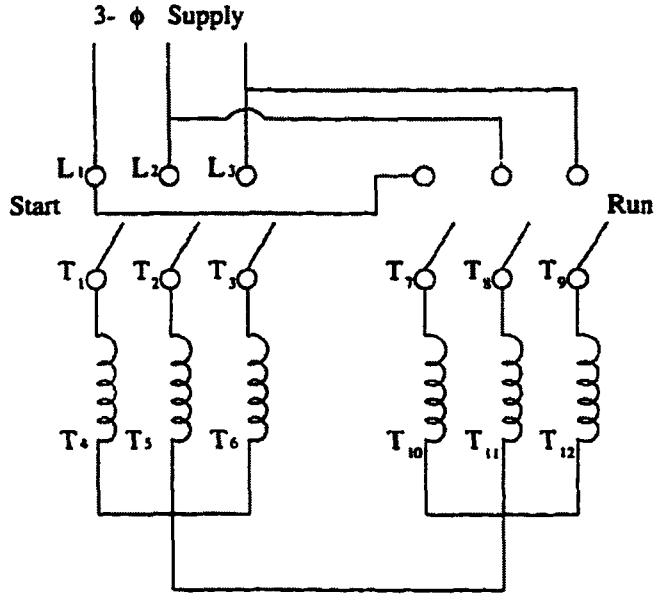

Fig. 7. Part-winding motor starting [49].

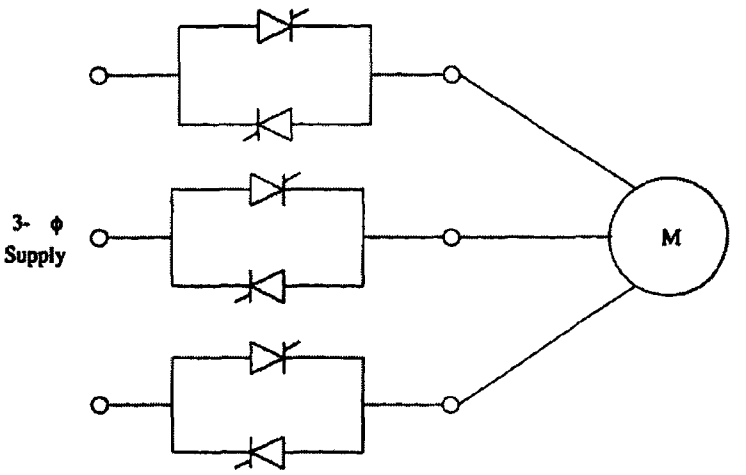

Fig. 8. Solid-state voltage controller motor starting [49].

2.3 Full Voltage Starting

2.3.1 Direct Starting

The full voltage starting method or 'direct starting' is the simplest and most frequently used method for starting a motor. This method is the most reliable and economical way of starting the motor. However, it requires a stable voltage source (network) in order to meet the high inrush currents at the starting period. The voltage is applied directly to the motor terminals by closing a switch or contactor. The advantage of this method is that the motor generates its highest starting torque and can provide shortest acceleration time. High starting torque is generally required to start high inertia load with less acceleration time. However, this high starting torque put undesirable stress on the mechanical system, like gears and chains can be damage [3], [8].

The injection of VARs to the system is extremely necessary to stabilize the voltage during starting. A weak network needs a significant amount of reactive power support to maintain the voltage to minimum permissible level at a certain node. For large induction motors in an isolated power system, reactive power compensation can be done by different methods depending on the applications, loading conditions and system configuration.

2.3.2 Direct Starting with Shunt Capacitors

Direct starting of large induction motor by employing shunt capacitors can be a useful means of controlling the voltage dip. Induction motor demands large reactive power during starting which results in significant drop at the terminal voltage. Shunt capacitors supply the reactive power (VARs) required by the large induction motors to relieve the system voltage. The leading current drawn by the shunt capacitors compensates the lagging current drawn by the load. Installing shunt capacitors in the load area or at the point that they are needed will increase the voltage stability. The system benefits due to application of shunt capacitors [27] are;

- Reactive power support
- Voltage profile improvement
- Line and transformer loss reduction
- Release of power system capacity
- Saving due to increase energy loss

The shunt capacitors can reduce the amount of inductive current by providing the necessary reactive power support (capacitive current) to maintain the acceptable voltage level [49]. The value of the capacitive reactive power is a function of steady state voltage. The line current decreases by employing the shunt capacitors, which results in reduction of I^2R and I^2X. The shunt capacitors are used extensively in distribution system for power factor correction. The selection of the shunt capacitor depends on factors like, the amount of lagging reactive power drawn by the load and adequate size of the capacitor bank. The switching time of capacitor bank at the instant when the motor is starting is very important. To effectively reduce the flicker problem, a control and switching system must be provided to energize the capacitors at the instant when the motor is started and turned off when the motor has reached its rated speed [19].

Mechanically-switched shunt capacitor banks have the advantage of much lower costs, variety of sizes, flexibility of installation compared to the other methods of compensation like static VAR systems [15]. However, shunt capacitors have a number of disadvantages and limitations from the voltage stability and control viewpoint. For example, unlike SVCs, they do not provide precise and rapid voltage control of the system. Also in systems heavily compensated by shunt capacitors, voltage regulation

tends to be poor and stable operation is not possible beyond a certain level of compensation. The most important shortcoming of shunt capacitor banks is their inability to provide fast compensation under voltage contingencies. The reactive power output of these banks is proportional to the square of the voltage. Consequently, in conditions where the voltage is dropping, the VAR support also drops, thus not serving its primary purpose. For transient voltage instability, the capacitor banks are not fast enough to prevent induction motor stalling.

2.3.3 Direct Starting with SVC

Static VAR compensator (SVC) can also be employed as a source of reactive power while starting large induction motors. Direct starting with shunt capacitors can effectively provide the required VARs support during starting of induction motors but it does not have continuous control on the demand of the reactive power. To overcome this problem, SVC can be an effective means of supplying controlled reactive power on cycle by cycle basis [9], [10]. SVC of phasor model has been used in this research work by using phasor simulation method in MATLAB/Simulink.

2.3.3.1 Static VAR Compensator (SVC)

A shunt connected static VAR generator or absorber whose output is adjusted to exchange capacitive or inductive current so as to maintain or control specific parameters of the electrical power system [29].

A Static VAR Compensator is a regulated source of leading or lagging reactive power. By varying its reactive power output in response to the demand of an automatic voltage regulator, an SVC can maintain virtually constant voltage at the point in the network to which it is connected [23]. An SVC is comprised of standard inductive and capacitive branches controlled by thyristor valves connected in shunt to the transmission network as shown in the Fig .9. Thyristor control gives the SVC the characteristic of a variable shunt susceptance. In terms of its steady state performance, an SVC acts much like a synchronous condenser. Unlike a synchronous condenser, however an SVC has no inertia and contributes nothing to the network short circuit level. Unlike mechanically switched compensation, an SVC can operate repeatedly and is not encumbered by the

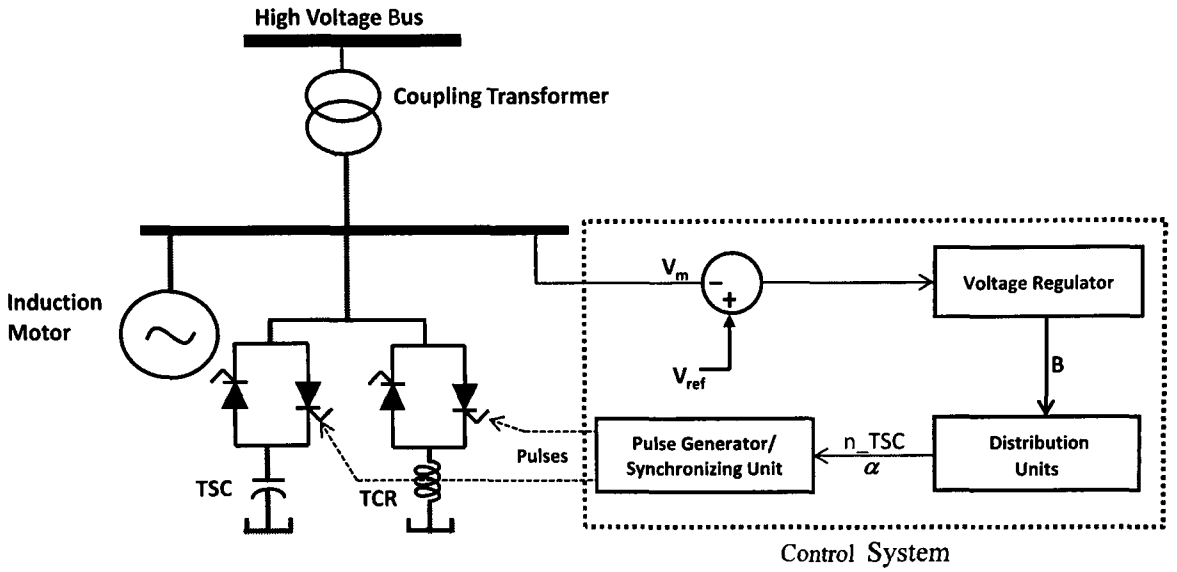

Fig. 9. Single line diagram of SVC and control system block.

delays associated with mechanical switching. This is the reason SVC respond very rapidly to changing network conditions such as line or generator outage contingencies [30]. Static VAR Compensators (SVCs) are more effective in preventing transient voltage oscillations in areas with concentrated induction motor loads, when compared to shunt capacitors. The SVCs performance is critical in cases of low voltage where the shunt capacitor's output is lower than their rating.

2.3.3.2 Basic Configuration of SVC

Basic configuration of SVC includes the following reactive power control elements:

- Thyristor-controlled reactor (TCR)
- Thyristor-switched capacitor (TSC)
- Thyristor-switched reactor (TSR)

The most common configuration used for static VAR control system consists of a controllable inductive reactor TCR in parallel with a fixed capacitor bank. The second type of SVC in which variable capacitor (thyristor switched capacitor TSC) is connected in parallel with thyristor controlled reactor [15], [29]. The controllable inductive reactor and variable capacitors are monitored by thyristors.

For both capacitors and inductors, the appropriate switching time occurs at the zero crossing of the current. Capacitors are switched completely in or out of the system as needed. However, the current through the inductor can be controlled continuously providing a variable susceptance.

Thyristor-controlled reactor (TCR):

Thyristor-controlled reactor (TCR) is a shunt connected thyristor-controlled inductor whose effective reactance is varied in a continuous manner by partial conduction control of the thyristor valve [29]. Current in a thyristor-controlled reactor can be continuously varied from zero to maximum by gating or conducting signal to the thyristors. The reactor is connected in series with two opposite poled thyristors. One of these thyristors conducts in each positive half cycle of the supply frequency, while the other conducts in the corresponding negative half cycle [50], [51]. The gating or 'turn on' signal to each thyristor is delayed by α, the firing or conduction angle, from the zero crossing of the source voltage. As current lags the voltage across the reactor by ninety degrees, so a firing angle of ninety degrees results in maximum, that is, continuous reactor current. For a firing angle of 180°, the reactor current will be zero. As the thyristor firing angle is increased from 90° towards 180° degrees, the current in the reactor is reduced. Therefore, the firing angle must be in the range 90° o $\leq \alpha \leq$ 180° as shown in the Fig. 10. The effect of increasing the gating angle is to reduce the fundamental harmonic component of the current. The effect of increasing the inductance of the reactor is equivalent to reducing the reactive power and the current.

Let σ be the conduction angle related to α by;

$$\sigma = 2(\pi - \alpha) \tag{1}$$

Fourier analysis of the current waveform gives the fundamental component;

$$I = \frac{V}{X_L}\frac{\sigma - \sin\sigma}{\pi} \tag{2}$$

Where I and V are RMS values and X_L is the reactance of the reactor at fundamental frequency. As the firing angle α increases, the conduction angle σ decreases and the fundamental component of current I reduces. The effective susceptance is a function of firing angle α and can be expressed as,

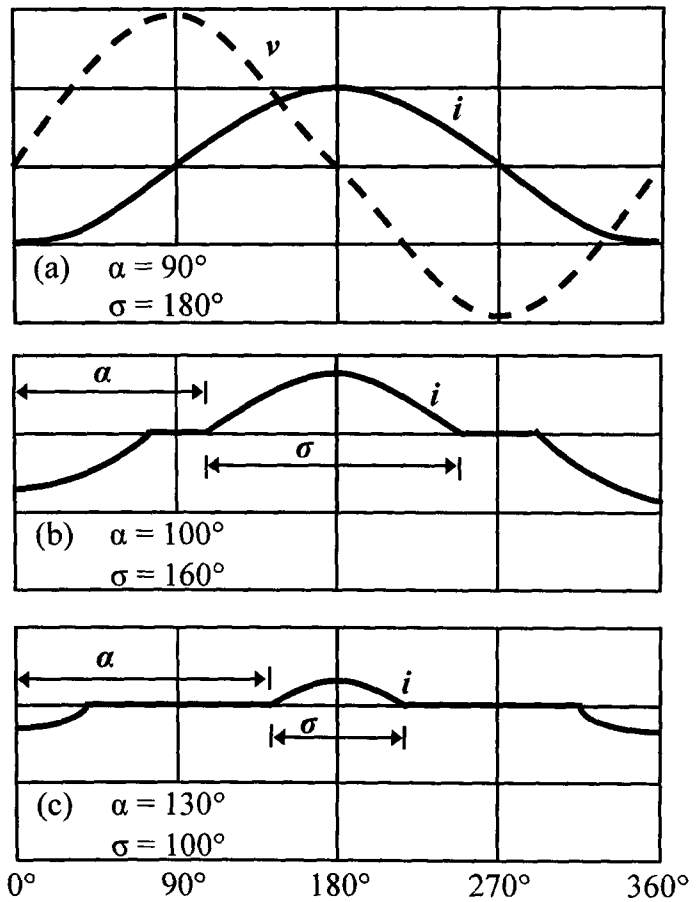

Fig. 10. TCR firing angles and current waveform [15].

$$B(\alpha) = \frac{I}{V} = \frac{\sigma - \sin\sigma}{\lambda X_L} \tag{3}$$

$$B(\alpha) = \frac{2(\lambda - \alpha) + \sin 2\alpha}{\lambda X_L} \tag{4}$$

The maximum value of susceptance will be at full conduction at α=90° or σ=180° and the minimum value will be at α=180° or σ=0°

Thyristor-switched capacitor (TSC):

A thyristor-switched capacitor (TSC) is a capacitor connected in series with two back to back thyristors. One thyristors conducts in each positive half cycle of the supply frequency, while the other conducts in the corresponding negative half cycle. The current

flowing through the capacitor may be controlled by blocking the thyristors. The TSC configuration can be used for different numbers and different sized capacitor banks. The switching of capacitors causes transients which can be large or small depending on the resonant frequency of the capacitors with the circuit [52], [53].

One disadvantage in utilizing a TSC is the switching transients produced. Since a TSC blocks the current when the thyristors are blocked and allows current to flow when the thyristors are gated. Severe transients will occur if a TSC is switched off while the current through it is not zero. Similarly, to avoid generation of transients during switching on, the thyristor must receive its firing pulse at a particular instant of the voltage cycle. That is, transient free switching may be obtained when the voltage across a capacitor is either at its positive peak or negative peak such that the current through the capacitor is zero. Also for some applications, in order to limit the switching transients, a small inductor can be used in series with the thyristors [15], [29].

2.3.3.3 Control Strategy of SVC

The primary purpose of SVC control system is to produce firing signals to thyristor for phase angle control of the reactor in such a manner that a continuous controllable output of reactive power is obtained on a cycle by cycle basis [54]. When the thyristors are fully conducting, the reactor consumes more than the reactive power generated in the fixed capacitor bank and the net output from the compensator is inductive. When the thyristors are blocked, there is no current in the reactor and the output from the compensator will be all the reactive power generated in the capacitor bank. A SVC control system as shown in Fig. 9 consists of:

- A measurement and comparison system
- Automatic voltage regulator (AVR)
- Distribution unit
- Pulse generator/Synchronizing unit

The measurement system measures the positive sequence voltage V_m to be controlled and compares with the reference voltage V_{ref}. The difference is the voltage error, which determines the voltage response of the SVC. Automatic voltage regulator that uses the voltage error (difference between measured voltage V_m and the reference voltage V_{ref}) to

determine the SVC susceptance B needed to keep the system voltage constant. A distribution unit which determines the TSCs switching in and out and also computes the firing angles of TCRs. The pulse generator sends the appropriate pulses to the thyristors and synchronizing unit synchronize the voltage by using the phase locked loop [55].

3. Induction Motor Transient Modeling

3.1 Introduction

The magnetic induction creates a current in the secondary or rotor circuit of induction motor when primary or stator circuit supplied with a three-phase power [56]. This makes induction motor more unique, as compared to the other motors, when they require DC supply or other external source for field as in synchronous or DC motors. When stator is excited by balanced three-phase supply, a synchronously revolving magnetic field in the air gap is produced, which rotates around the air gap at synchronous speed N_S, which can be calculated as

$$N_s = \frac{120f}{P} \tag{5}$$

f : excitation frequency in cycle per seconds (Hz)

P : number of pole pairs

N_S: synchronous speed in revolutions per minute (rpm)

The slip of the motor can be written as:

$$S = \frac{N_s - N_r}{N_s} \tag{6}$$

N_r : rotational speed of the rotor

If the speeds are expressed in radians per seconds, the slip is given by

$$S = \frac{\omega_s - \omega_r}{\omega_s} \tag{7}$$

where

ω_s: synchronous speed in radian per second (rad/sec)

ω_r: rotor speed in (rad/sec)

3.2 d-q Model Representation of Induction Motor

The conventional steady state models and equivalent circuits are useful for studying the performance of induction motor in steady state which shows that electrical transients are neglected during load changes and stator frequency variations. We need to evaluate

the dynamic model that considers the instantaneous effects of varying voltages, currents, stator frequency and torque disturbance. The dynamic model of induction motor is derived by using a two-phase motor in direct and quadrature (d-q axes) axes as shown in the Fig. 11. The advantage of the d-q axes model is conceptual simplicity and less computational time for analyzing the transient and steady state conditions. The voltages, currents, and flux linkages transformation is derived in a generalized way. The power must be equal in three-phase machine and its equivalent two-phase model.

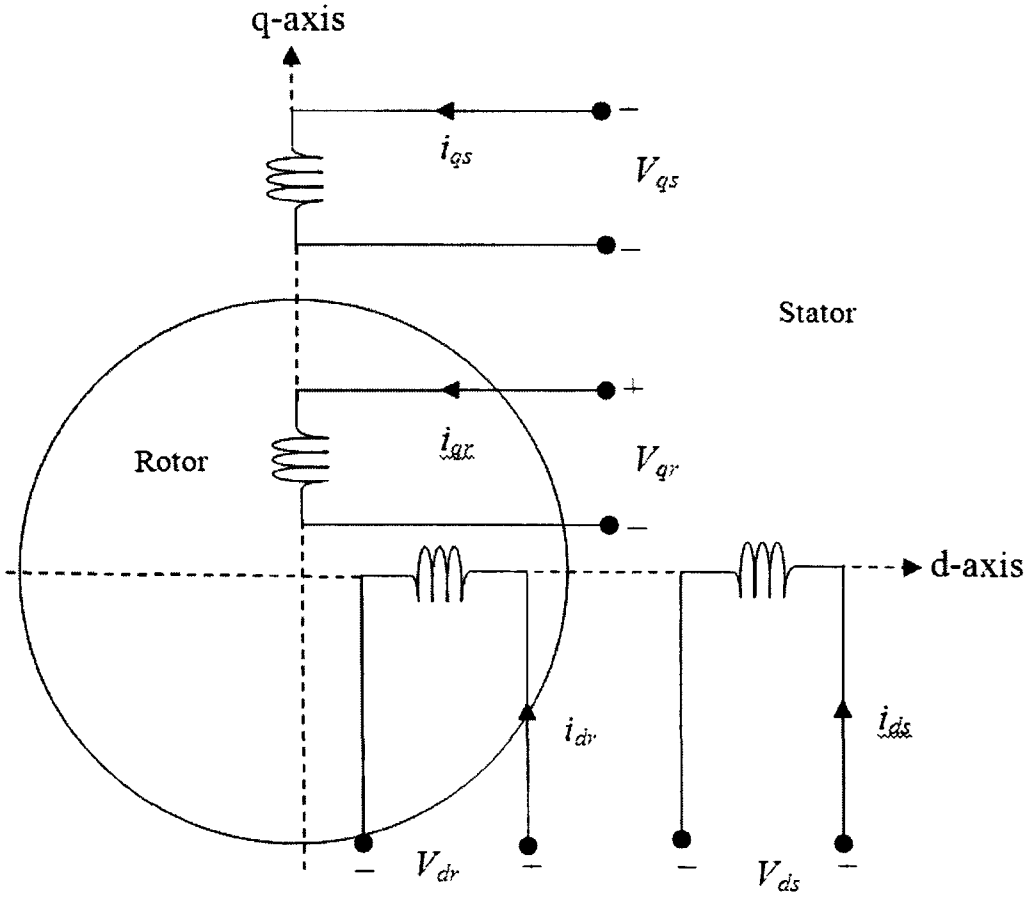

Fig. 11. d-q axes representation of induction motor.

The idealized three-phase induction motor is assumed to be having symmetrical air gap, balanced stator and rotor windings with sinusoidally distributed mmf and including main flux saturation. The two common reference frames can be used for the analysis of induction motors, stationary, and synchronously rotating reference frame [57]. The windings are displaced in space by 90 electrical degrees, and the rotor winding is at an angle of θ_t from the stator d-axes winding. The differential equations describing the induction motor are non linear.

3.3 Unsaturated Transient Model

To investigate the starting performance of induction motor during starting, d-q axes motor model has been used [22]. The d-q equivalent circuits of squirrel-cage induction motor are shown in Fig. 12. The general equations for the d-q representation of an induction motor in the stationary reference frame is given as,

$$\begin{bmatrix} V_{ds} \\ V_{qs} \\ V_{dr} \\ V_{qr} \end{bmatrix} = \begin{bmatrix} R_s + pL_s & 0 & pL_m & 0 \\ 0 & R_s + pL_s & 0 & pL_m \\ pL_m & \omega_r L_m & R_r + pL_r & \omega_r L_r \\ -\omega_r L_m & pL_m & -\omega_r L_r & R_r + pL_r \end{bmatrix} \begin{bmatrix} i_{ds} \\ i_{qs} \\ i_{dr} \\ i_{qr} \end{bmatrix} \tag{8}$$

where,

R_s : stator winding resistance in Ω.

R_r : rotor winding resistance in Ω.

L_m : magnetizing inductance in H.

L_r : stator leakage inductance in H.

L_s : rotor leakage inductance in H.

ω_r : electrical rotor angular speed in rad/sec.

p : *d/dt*, the differential operator.

Equation (8) can be written in arbitrary rotating reference frame by changing it to first order differential equation form, which gives the following matrix equation

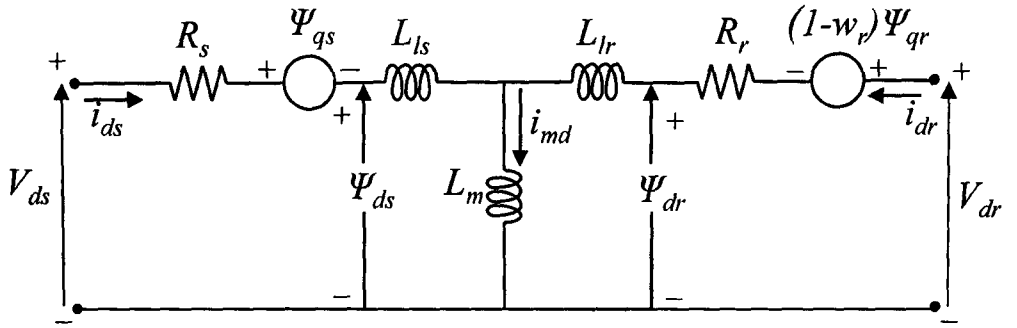

(a)

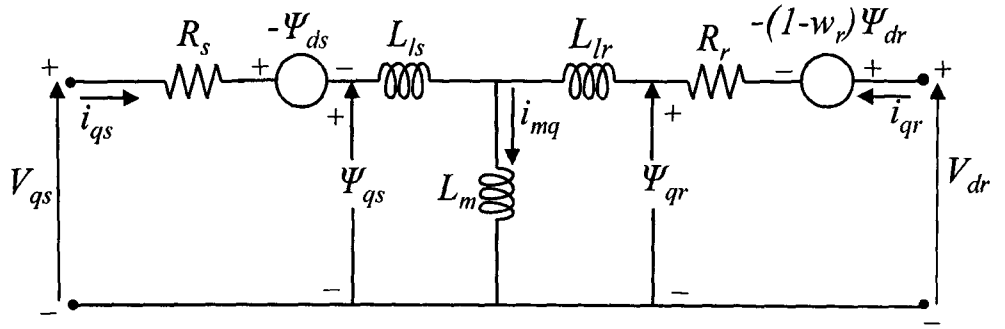

(b)

Fig. 12. Equivalent circuits of induction motor in synchronously rotating reference frame (a) d-axis equivalent circuit. (b) q axis equivalent circuit.

$$\begin{bmatrix} V_{ds} \\ V_{qs} \\ V_{dr} \\ V_{qr} \end{bmatrix} = \begin{bmatrix} R_s & 0 & 0 & 0 \\ 0 & R_s & 0 & 0 \\ 0 & 0 & R_r & 0 \\ 0 & 0 & 0 & R_r \end{bmatrix} \begin{bmatrix} i_{ds} \\ i_{qs} \\ i_{dr} \\ i_{qr} \end{bmatrix} + \begin{bmatrix} p & -\omega_s & 0 & 0 \\ \omega_s & p & 0 & 0 \\ 0 & 0 & p & -(\omega_s - \omega_r) \\ 0 & 0 & (\omega_s - \omega_r) & p \end{bmatrix} \begin{bmatrix} \psi_{ds} \\ \psi_{qs} \\ \psi_{dr} \\ \psi_{qr} \end{bmatrix} \quad (9)$$

The dynamic equations in which d- and q-axes components of stator and rotor voltages can be expressed as a function of flux linkages are given in (10)-(13). The equivalent circuit of the induction motor in synchronous reference frame is shown in Fig. 12. The d-and q-axes components of the stator and rotor voltages can be expressed as a function of flux linkages and are given as (10) to (13).

$$V_{ds} = R_s i_{ds} - \psi_{qs} + p\psi_{ds} \quad (10)$$

$$V_{qs} = R_s i_{qs} + \psi_{ds} + p\psi_{qs} \quad (11)$$

$$V_{dr} = R_r i_{dr} - (1-\omega_r)\psi_{qr} + p\psi_{dr} \quad (12)$$

$$V_{qr} = R_r i_{qr} + (1-\omega_r)\psi_{dr} + p\psi_{qr} \quad (13)$$

The d-and q-axes components of the stator and rotor currents are related to the d- and q-axes components of the stator and rotor fluxes by

$$\psi_{ds} = L_s i_{ds} + L_m i_{dr} \quad (14)$$

$$\psi_{qs} = L_s i_{qs} + L_m i_{qr} \quad (15)$$

$$\psi_{dr} = L_m i_{ds} + L_r i_{dr} \quad (16)$$

$$\psi_{qr} = L_m i_{qs} + L_r i_{qr} \quad (17)$$

The stator and rotor currents are obtained as follows

$$i_{ds} = \frac{1}{D}(L_r\psi_{ds} - L_m\psi_{dr}) \quad (18)$$

$$i_{qs} = \frac{1}{D}(L_r\psi_{qs} - L_m\psi_{qr}) \quad (19)$$

$$i_{dr} = \frac{1}{D}(-L_m\psi_{ds} + L_s\psi_{dr}) \quad (20)$$

$$i_{qr} = \frac{1}{D}(-L_m\psi_{qs} + L_s\psi_{qr}) \quad (21)$$

where

$$D = (L_s L_r - L_m^2) \quad (22)$$

$$L_s = L_m + L_{ls} \quad (23)$$

$$L_r = L_m + L_{lr} \quad (24)$$

The electromagnetic torque developed by the motor is given by

$$T_e = \frac{3}{2}\frac{p}{2}L_m(i_{qs}i_{dr} - i_{ds}i_{qr}) \quad (25)$$

The mechanical equation is given as

$$T_e = J\frac{d\omega_r}{dt} + B\omega_r + T_L \tag{26}$$

Where

T_e : electromagnetic torque , Nm.

T_L : mechanical torque in shaft, Nm.

ω_r: mechanical shaft speed, rad/sec.

B : friction coefficient, Nm/rad/sec.

J : inertia coefficient, Kg.m^2

3.4 Saturation in Induction Motor

The performance and operation of induction motors have been under investigation since the first invention in 1890. Researchers have well investigated the steady state performance of induction motors, but dynamic performance during starting needs more research. Direct starting of induction motor has been investigated only by a few researchers [44]. The determination of starting performance of induction motor has traditionally been based on constant parameters models for both steady state and most transient conditions. Magnetic saturation cannot be ignored in all electrical machines, so unavoidable in induction motors as well. The saturation effects of both stator and rotor core and teeth play significant role while considering the transient performance of the induction motor. It has been found that inclusion of saturation in induction motor model gives more accurate and realistic results [37] .In this research work main flux saturation has been incorporated to analyze the effects of saturation on the starting behavior of induction motor. In order to achieve a better representation and understanding of the induction motors, saturation should be taken into account.

3.5 Saturated Transient Model

A d-and q-axes saturated transient model of induction motor can be developed by considering the main flux saturation in unsaturated transient model previously developed

in section 3.3. For this unsaturated d-and q-axes magnetizing inductances L_m in (14)-(21) are replaced by their corresponding saturated value [42]. The total magnetizing current can be used to locate the operating point on the d-and q-axes saturation characteristics. The total magnetizing current can be calculated by:

$$i_m = \sqrt{i_{md}^{\ 2} + i_{mq}^{\ 2}} \tag{27}$$

Where,

$$i_{md} = i_{ds} + i_{dr}, i_{mq} = i_{qs} + i_{qr} \tag{28}$$

i_{md}: d-axis magnetizing current.

i_{mq}: q-axis magnetizing current.

4. Numerical Analysis

4.1 System Studied and Motor Parameters

The three-phase induction motor which has been under investigation for the starting performance is connected through system network, as shown in the Fig. 13. The three-phase power is supplied by the source (infinite bus) through transmission line and a step-down transformer. Two motors (50 hp and 500 hp) will be investigated for their starting performance, using the same system network but different parameters. The network parameter varies with the requirement of rated terminal voltage and rated current of the motor.

4.1.1 Motor Parameters and Operating Conditions for 50 hp Motor

To analyze the starting performance of 50 hp induction motor, the proposed d-q model has been used. The motor parameters, operating conditions, SVC parameters and shunt capacitors parameters are presented in Table 1, 2, and 3 below, respectively: The motor starting performance will be investigated for both saturated and unsaturated models for different loading conditions. The value of capacitance illustrated in Table. 3 is the capacitance of each capacitor of the capacitor bank. The transformer ratio as mentioned in Table. 2 is the step-down voltage from the transmission line to supply at the terminal of the motor.

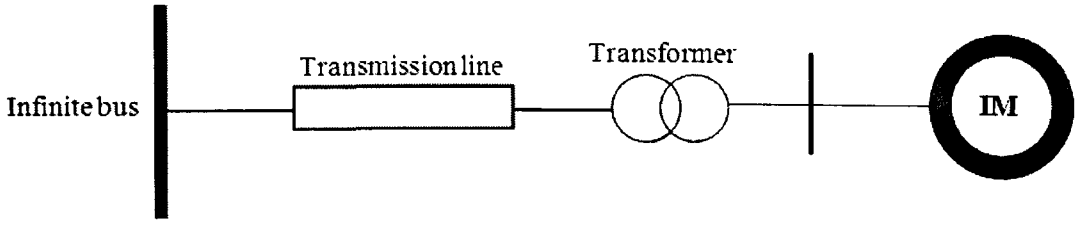

Fig. 13. Single diagram for the system studied.

Table 1. 50 hp Induction motor parameters.

Rated Voltage	460 Volts	L_m	13.08 H
Rated Current	46.84 Amperes	R_s	0.087 Ω
Rated Torque	198 N-m	R_r	0.0228 Ω
Rated Speed	1800 (rpm)	L_{ls}	0.302 Ω
No of Poles	4	L_{lr}	0.302 Ω
Frequency	60 Hz	Inertia	1.662 $Kg.m^2$

Table 2. Operating conditions.

Base Voltage	25 *KV*	Base Power	100 *MVA*
P	10 Watts	Transformer Ratio	$25e^3$:460 *V*

Table 3. SVC and shunt capacitors parameters.

Nominal Voltage	25 *KV*	Base Power	100 *MVA*
Capacitance	0.03939*F*	B_{ref}	0.0313 pu/Pbase
Q_{lmax}	-100 *MVA*	Q_{cmax}	200 *MVA*

4.1.2 Simulations Procedures Using MATLAB/Simulink

The proposed model of induction motor and system network has been constructed by using MATLAB/Simulink SimPowerSystems tool box. The Power System Blockset has been used to build the power system network part and induction motor of the proposed model as in represented Fig. 14. The phasor method of simulation will be used for performing the simulations of different parameters.

The power system network part includes the infinite bus, transmission line, and transformer. The infinite bus (three-phase source) block provides a balanced three-phase RMS phase to phase voltage of 25 KV with internal R-L impedance. The transformer used to step-down phase to phase voltage (RMS) from 25 KV to 460 V A three phase V-I measurement block has been used to measure three phase voltage and current in the circuit. Then the three-phase balanced voltage is supplied to the induction motor block set. MATLAB/Simulink representation of induction motor subsystem is shown in Fig 15. The loading conditions of the motor can be changed by putting the value of the load torque in the block.

The inputs of squirrel cage induction motor are, three-phase balanced voltage, fundamental frequency and the load torque. While the outputs are, three-phase currents, the electrical torque and the rotor speed. The balanced three-phase voltage supplied to the motor is transformed to new d-q axes. The d-q model requires all three-phase variables should be transformed into two-phase synchronously rotating reference frame.

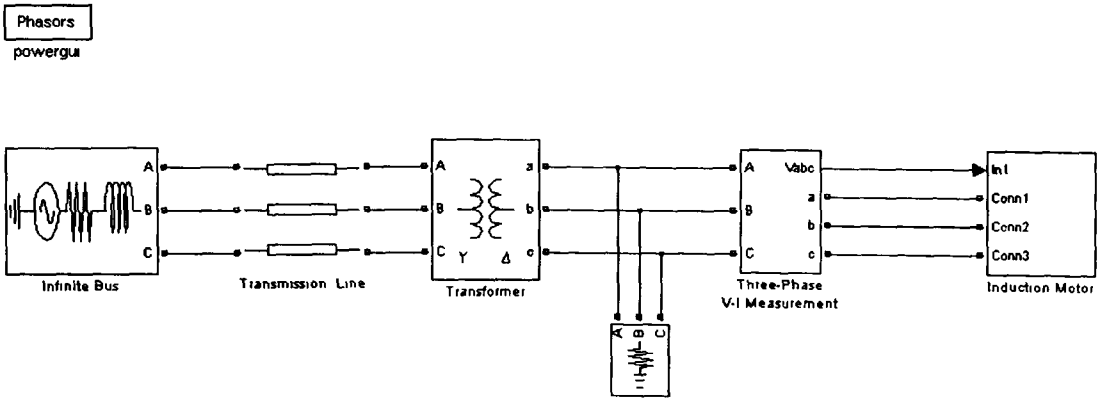

Fig. 14. MATLAB/Simulink block representation of power system and induction motor.

The voltage equations (10) to (13) are solved to calculate the flux linkages. It is important to calculate flux linkages first, then easy to calculate all other variables. Equations (18) to (21) use flux linkages to solve the stator and rotor d-and q-axes currents. The electrical torque calculations can be done from rotor speed, which can be calculated from equations from (25) and (26).

The inputs of squirrel cage induction motor are the three-phase balanced voltage, fundamental frequency and the load torque. While the outputs are, three-phase currents, the electrical torque and the rotor speed. The balanced three-phase voltage supplied to the motor is transformed to new d-q axes. The d-q model requires all three-phase variables should be transformed into two-phase synchronously rotating frame.

The voltage equations (10) to (13) are solved to calculate the flux linkages. It is important to calculate flux linkage first, then easy to calculate all other variables. Equations (18) to (21) use flux linkages to solve the stator and rotor d-and q-axes currents. The electrical torque calculations can be done from rotor speed, which can be calculated from equations from (25) and (26).

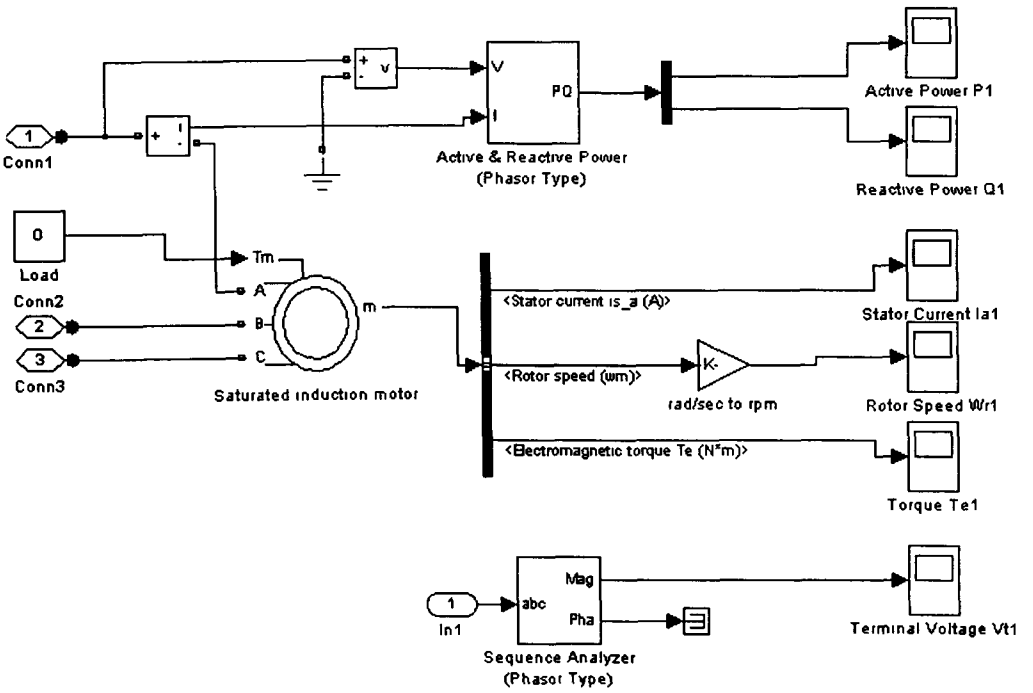

Fig. 15. MATLAB/Simulink representation of induction motor block.

4.1.2.1 Simulation Procedure with Shunt Capacitors

The simulation procedure with shunt capacitor is shown in the Fig. 16. The shunt capacitors bank of each capacitor of 0.03939 F is connected via switch (circuit breaker). The shunt capacitor bank will be switched on at 4ms.The maximum reactive power supplied by the bank is 15 MVARs. As the reactive power supplied is the function of steady state voltage of the induction motor.

4.1.2.2 Simulation Procedure with SVC

The SVC (phasor Type) block used for the simulation process is connected as shown in Fig. 17. The phasor simulation method activated with Powergui block has been used to carry out the simulations. The susceptance value used for SVC is 0.0313 pu/P_{base} and the maximum value for reactive power supplied by SVC is 15 MVARs.

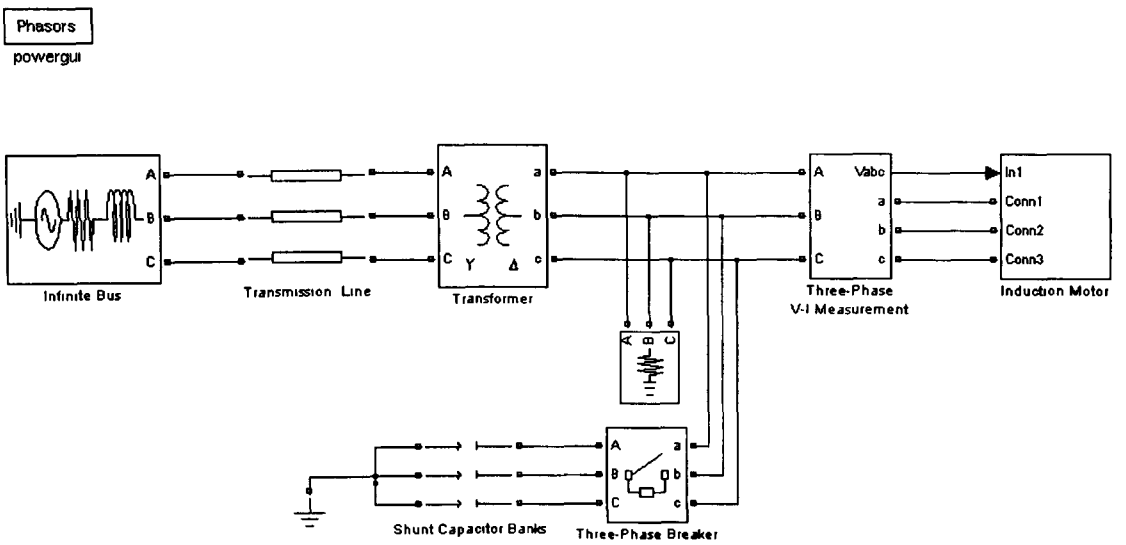

Fig. 16. Simulink model representation with shunt capacitors.

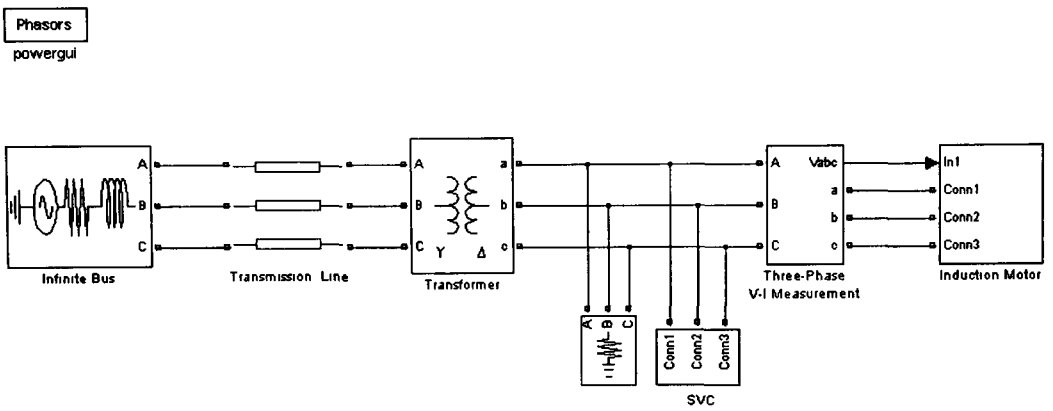

Fig. 17. Simulink model representation with SVC

4.2 Numerical Simulation Results for 50 hp Motor

In this section, the starting performance of 50 hp induction motor will be investigated for different loading conditions. Numerical calculations will be performed for ignoring and considering the main flux saturation. The three cases will be investigated, and analytically calculated results will be compared. For each case, terminal voltage, reactive power, active power, stator current, rotor speed and electromagnetic torque of the motor have been simulated for time t=1 sec. The main objective is to investigate the voltage profile and reactive power during transient period of the motor.

- Direct starting
- Direct starting with shunt capacitors
- Direct starting with SVC

4.2.1 Direct Starting at No Load

In this section, the starting performance of induction motor at no load will be investigated for both saturated and unsaturated cases. As previously demonstrated in Fig. 14, a three-phase balance voltage is supplied to the induction motor terminal. The initial conditions for all parameters are zero. Fig. 18(a) shows the simulated result for terminal voltage at no load for time t=1.0 sec, while in Fig. 18(b) the zoomed in part of the motor terminal voltage during transient period for time t=0.05 sec has been demonstrated. It has been noted, that due to high starting current, the voltage drops to 358.8 volts in case of saturated and 359.8 volts for unsaturated case at time t=0.008 sec during transient period

from the initial 460 volts. The motor reach steady state at time 0.75 sec for voltage value of 366.25 volts in case of saturated and 366.9 volts for unsaturated case. The motor can be under tremendous stress for these conditions, especially when it is driving high inertia loads. This phenomenon further leads to voltage stability problem.

The reactive power consumed by the motor during starting is illustrated in Fig. 19 (a). For both statured and unsaturated cases, to understand the consumption of reactive power during first few cycles it is shown in Fig. 19(b) by zooming in for time 0 to 0.05 sec. It has been investigated that, during early transient period from 0 to 0.05 sec, the discrepancy between the reactive power calculated by the saturated and unsaturated models is considerable. The initial value of reactive power consumed by the motor for saturated case is 0.112 MVAR and for unsaturated case is 0.098 MVAR. The same proportional discrepancy exists for steady state between saturated and unsaturated cases. The large reactive power drawn by the motor can lead to higher starting current which is an undesirable phenomenon during starting period.

The simulated result for active power being consumed by the motor during starting at no load condition is shown in Fig. 20. It can be seen that the steady state values calculated for both saturated and unsaturated cases are same, but during transient period the unsaturated model has slightly higher consumption (bigger oscillations) for some time. Initially motor needs more active power during starting to overcome iron and copper losses, but the active power consumption by the motor decreases to zero as motor gains steady state. The motor gains its rated speed for both cases at t=0.9 sec as shown in the Fig. 21. The phase 'a' stator current has been plotted in Fig. 22 to analyze the starting current characteristics for both saturated and unsaturated cases. The effect of saturation on the stator current has been investigated during starting period for no load condition. The initial peak value of starting stator current is 670 amperes for saturated case, while 615 amperes for unsaturated case. The high discrepancy between the steady state values for both cases is due to the saturation in the motor. The electromagnetic torque calculated by the unsaturated and saturated models is shown in Fig. 23. It can be seen that there is a small discrepancy between the results by the two models. The initial torque oscillations are higher for unsaturated case, during the transient period as compared to the saturated case.

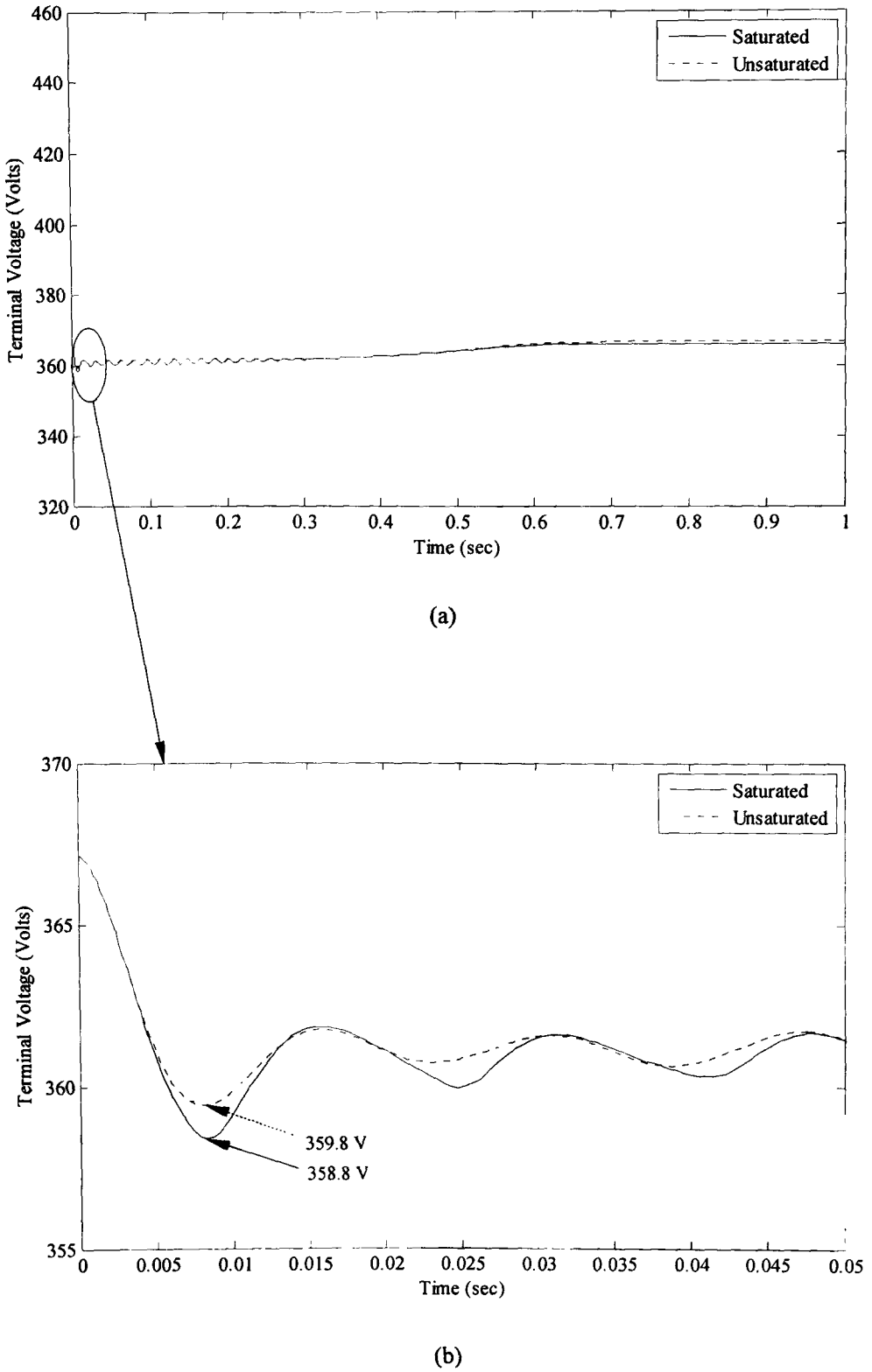

Fig. 18. Terminal voltage calculated by saturated and unsaturated models at no load. (a) Plot for 1 sec. (b) Plot (zoomed in) for 0.05 sec.

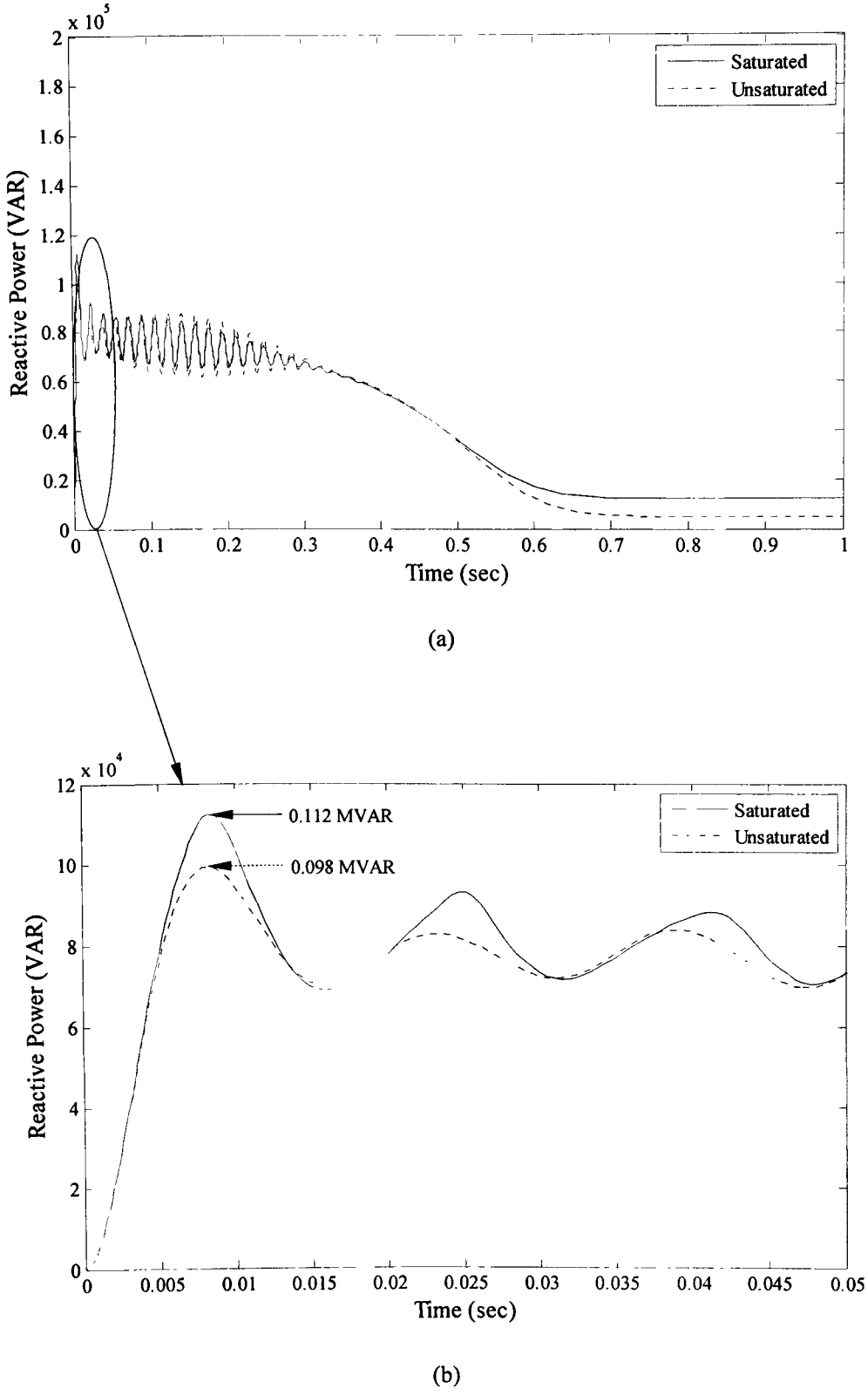

Fig. 19. Reactive power calculated by saturated and unsaturated models at no load (a) Plot for 1sec. (b) Plot (zoomed in) for 0.05 sec.

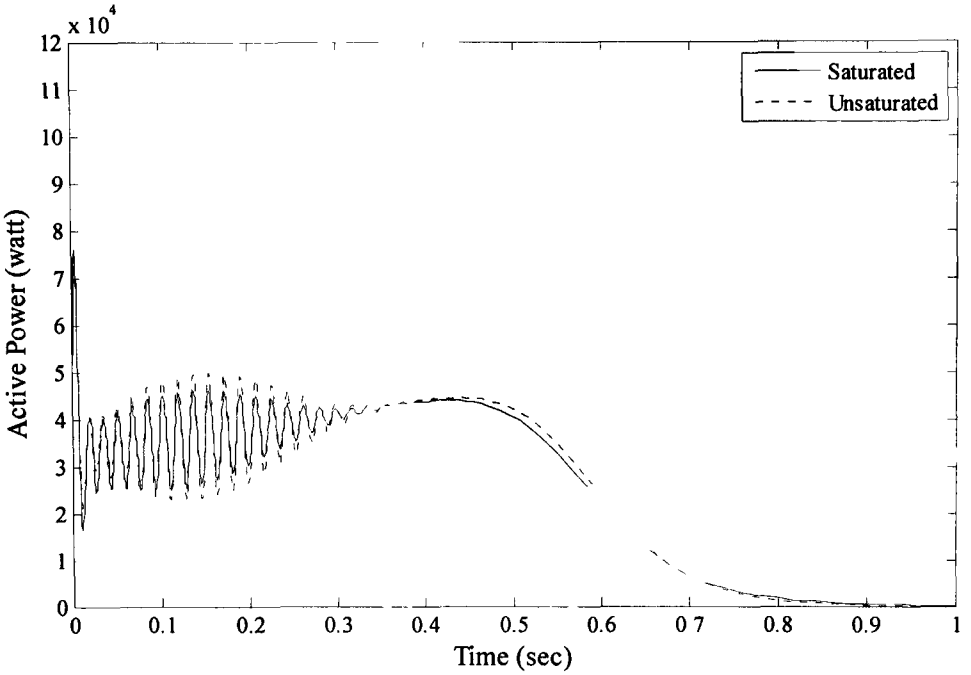

Fig. 20. Active power calculated by saturated and unsaturated models at no load.

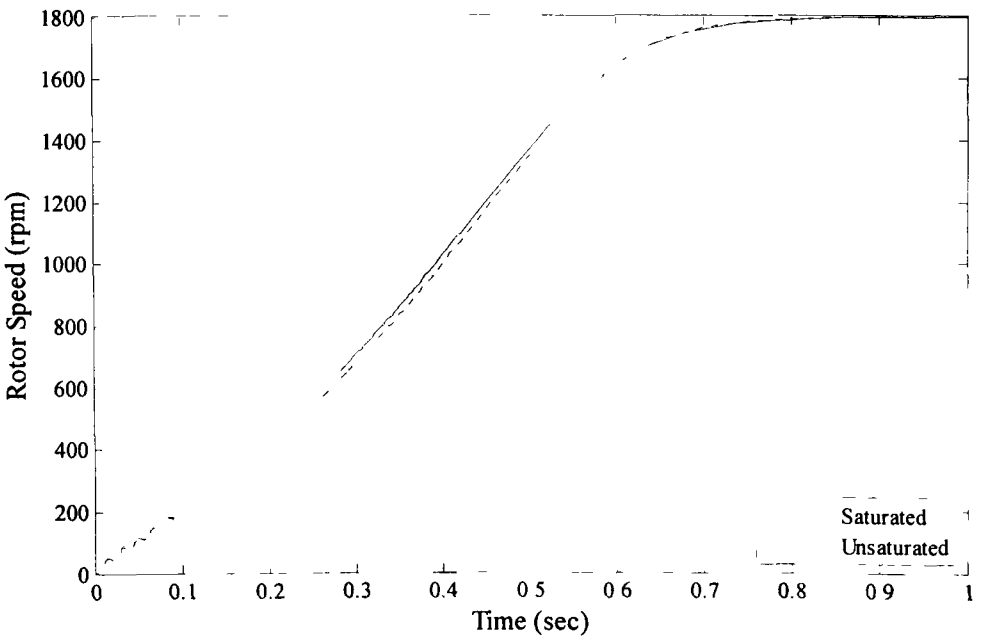

Fig. 21. Rotor speed calculated by saturated and unsaturated models at no load.

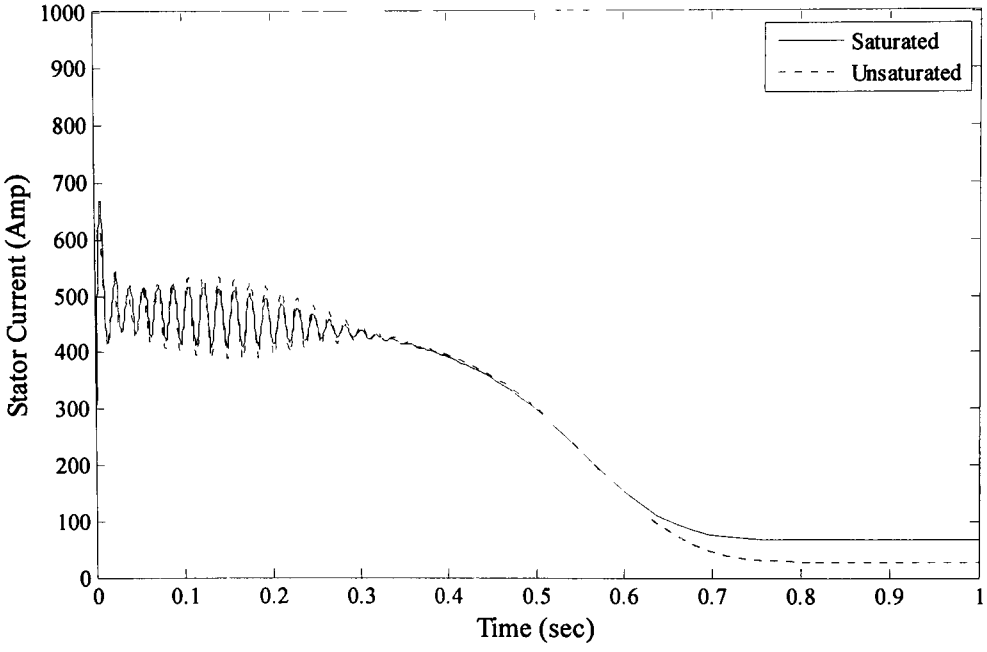

Fig. 22. Phase 'a' stator current calculated by saturated and unsaturated models at no load.

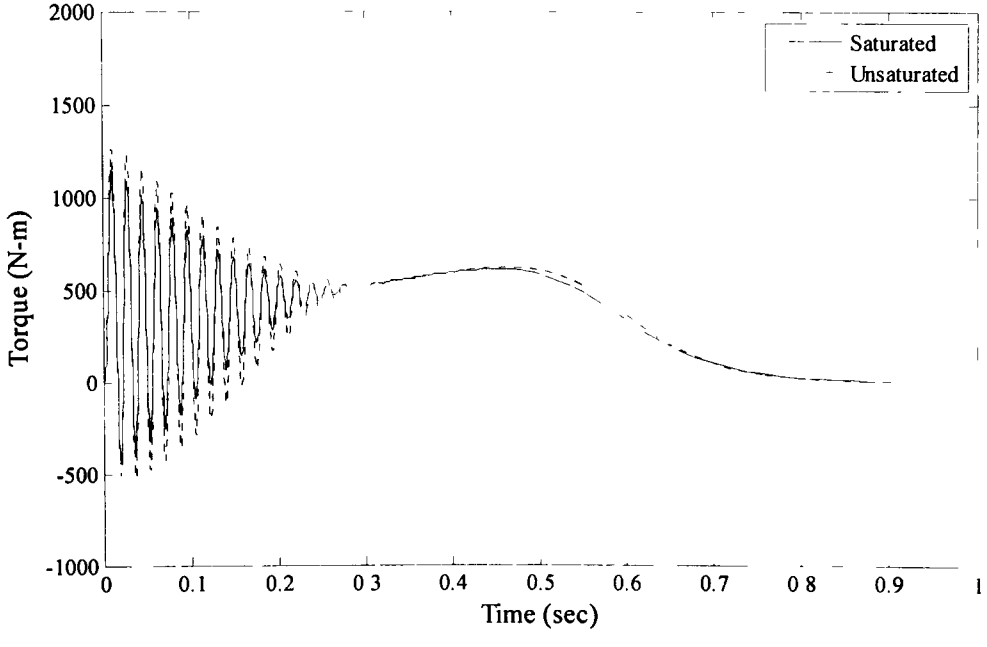

Fig. 23. Electro-magnetic torque calculated by saturated and unsaturated models at no load.

4.2.2 Direct Starting at Full Load

The starting performance of induction motor at full rated load will be investigated in this section while ignoring and considering saturation. For the same operating condition, the balanced three-phase voltage is supplied to the motor terminal at full load. To analyze the voltage behavior during transient period, simulated result of starting voltage dip is shown in the Fig. 24(a). It has been seen that nearly same voltage behavior during early transient period for saturated and unsaturated models for both loading conditions. The voltage versus time plot at t=0.008 sec shows in Fig. 24(b), that the maximum voltage dip for saturated case is 358.4 volts, and for unsaturated case is 359.4 volts. But the starting time has prolonged considerably to more than 1 sec due to the loading condition, which is the most concerning issue while starting of induction motor. Longer acceleration time means that motor terminal voltage dip remains for longer time, and consequently, the starting current will be high for the same period.

The reactive power consumed by the motor at full load is plotted in Fig. 25. It has been calculated that reactive power consumed by unsaturated and saturated models are nearly same for both loading conditions as explained in the previous section. The maximum reactive power consumed by the induction motor during transient period at time t=0.008 sec is calculated as 0.113 MVAR for saturated model and 0.099 MVAR is calculated for unsaturated model as illustrated in Fig. 25(b). At full load, the steady state values calculated for saturated and unsaturated cases are 0.013 MVARs, and 0.006 MVARs respectively, which show the discrepancy of 0.007 MVARs between the two models. As discussed earlier in section 4.2.1 that steady state value of reactive power being consumed by the motor is higher for saturated model because of main flux saturation in the motor.

The active power consumed by the motor during transient period at full load is nearly same as previously calculated for no load condition, but for steady state very small discrepancy has been seen as shown in the Fig. 26. At full load, the rotor speed calculated for saturated model is 1715 (rpm) and for unsaturated model, it is 1708 (rpm) as illustrated in Fig. 27. For saturated case, the motor drop less speed because of relatively higher current in the stator. Transient and steady state values calculated for phase 'a' stator current for both saturated and unsaturated induction motor model is same at no load

and full load as represented in Fig. 28. The steady state value has large discrepancy for both cases due to saturation effect. The magnetizing current of the motor is equal to stator current while taking saturation into account. This high stator current is undesirable component for the motor, especially during starting as well as for steady state. The electromagnetic torque calculated at full load during the transient period is higher for unsaturated motor model as compared to the saturated motor model. The acceleration time significantly accounts for starting torque when driving high inertia load. The torque versus time plot in Fig. 29 shows that the acceleration time is extended to more than 1 sec, which can be big problem for the motor winding due to heating problem.

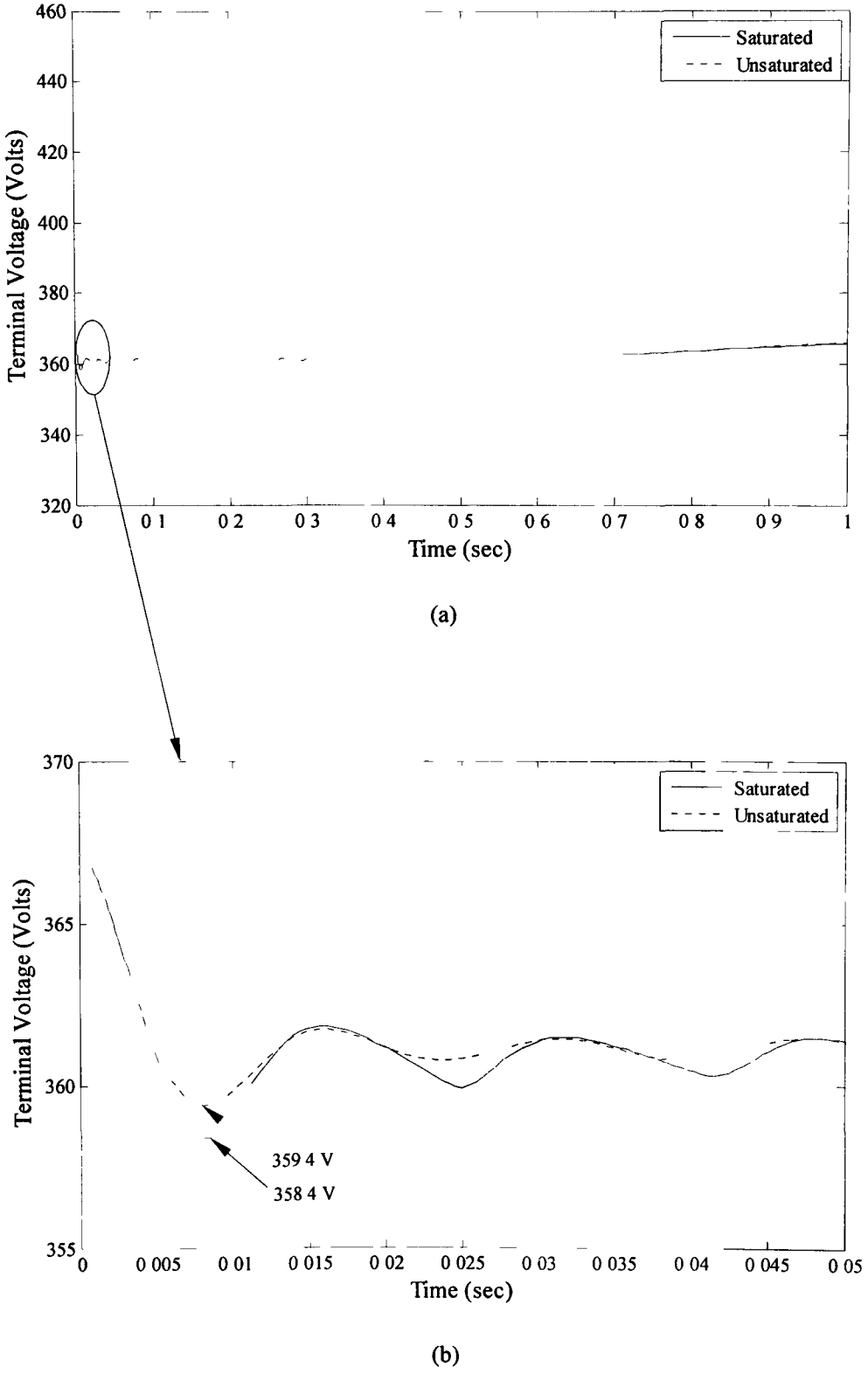

Fig. 24. Terminal voltage calculated by saturated and unsaturated models at full load. (a) Plot for 1sec. (b) Plot (zoomed in) for 0 05 sec.

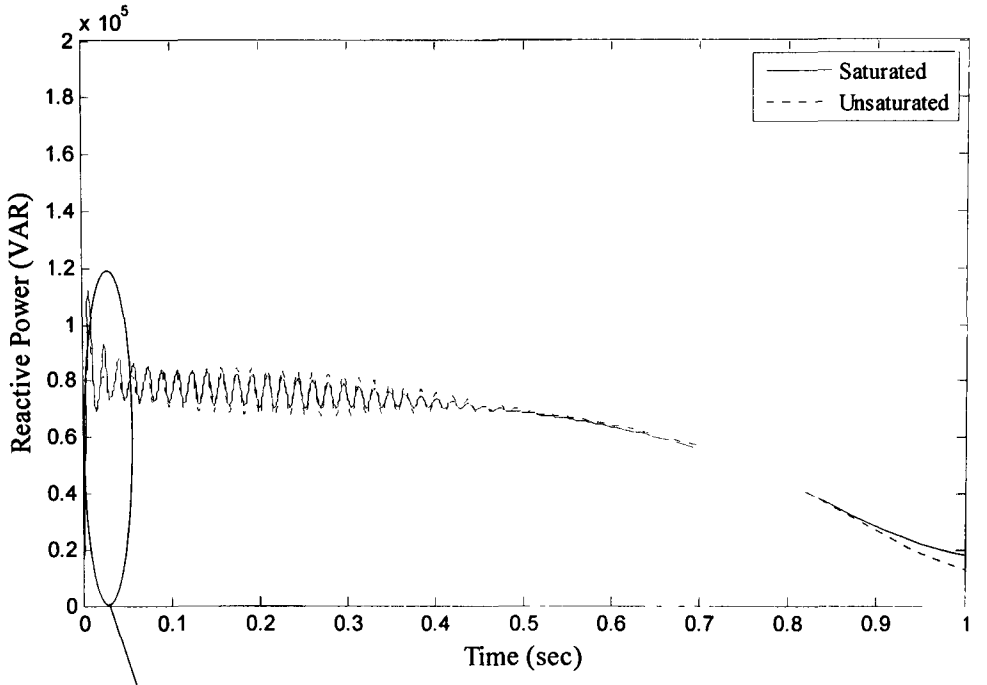

(a)

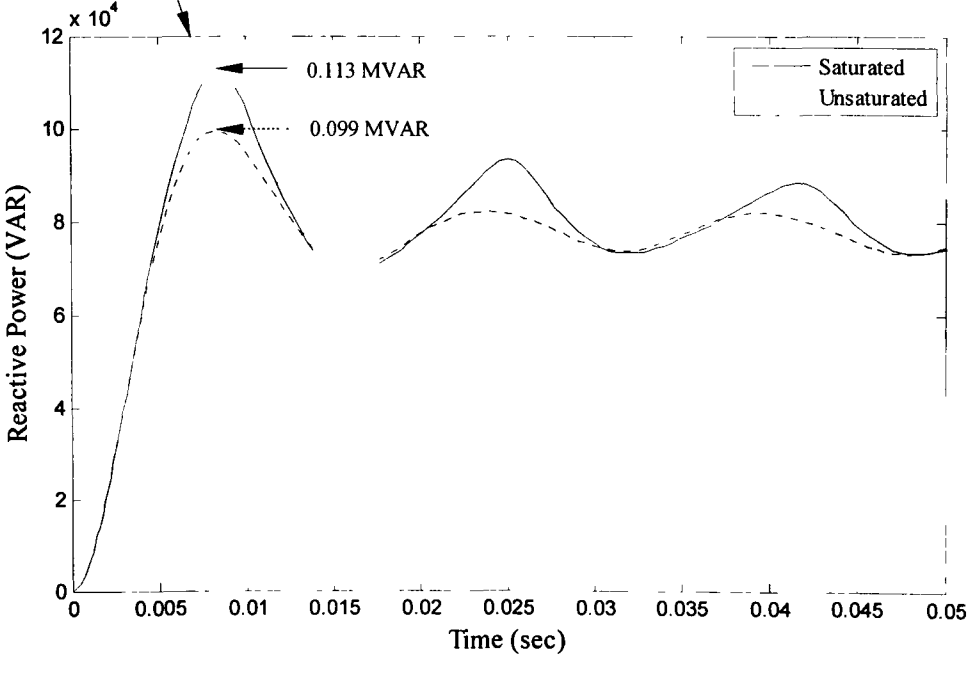

(b)

Fig. 25. Reactive power calculated by saturated and unsaturated models at full load (a) Plot for 1sec. (b) Plot (zoomed in) for 0.05 sec.

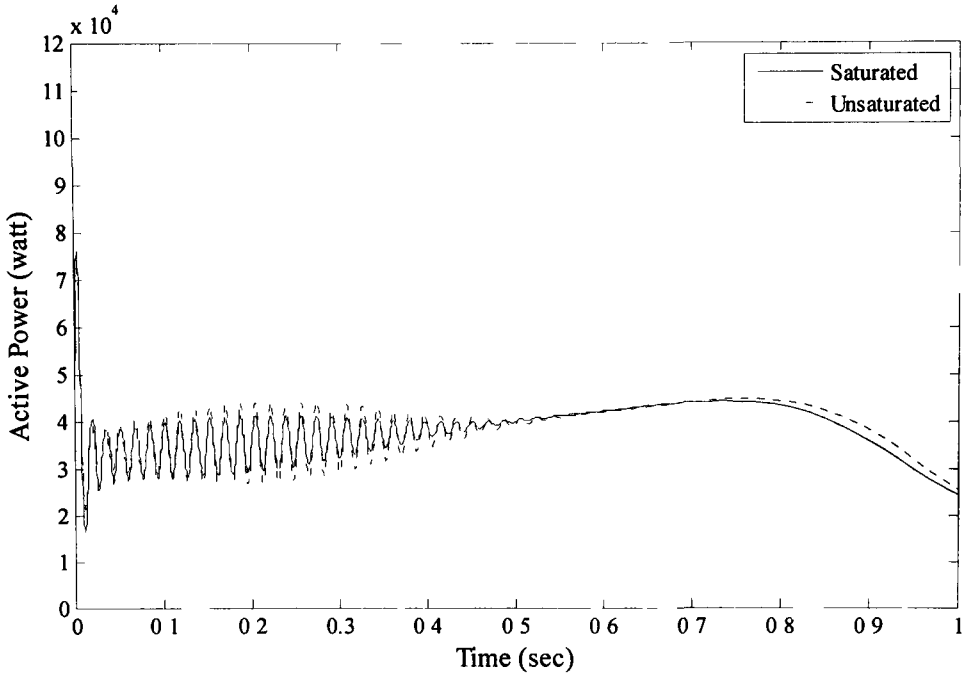

Fig. 26. Active power calculated by saturated and unsaturated models at full load.

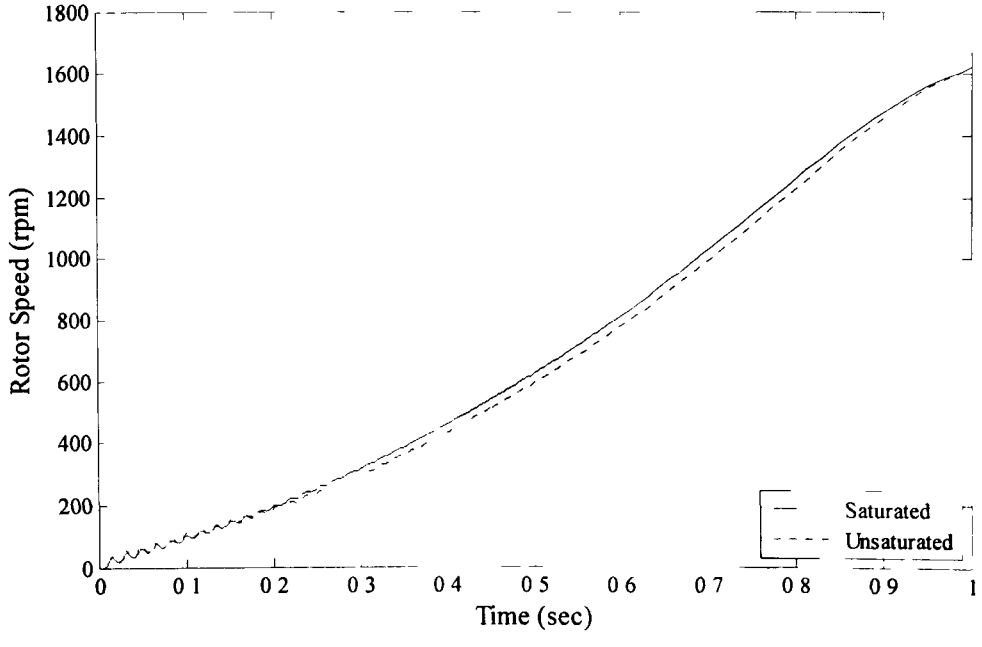

Fig. 27. Rotor speed calculated by saturated and unsaturated models at full load.

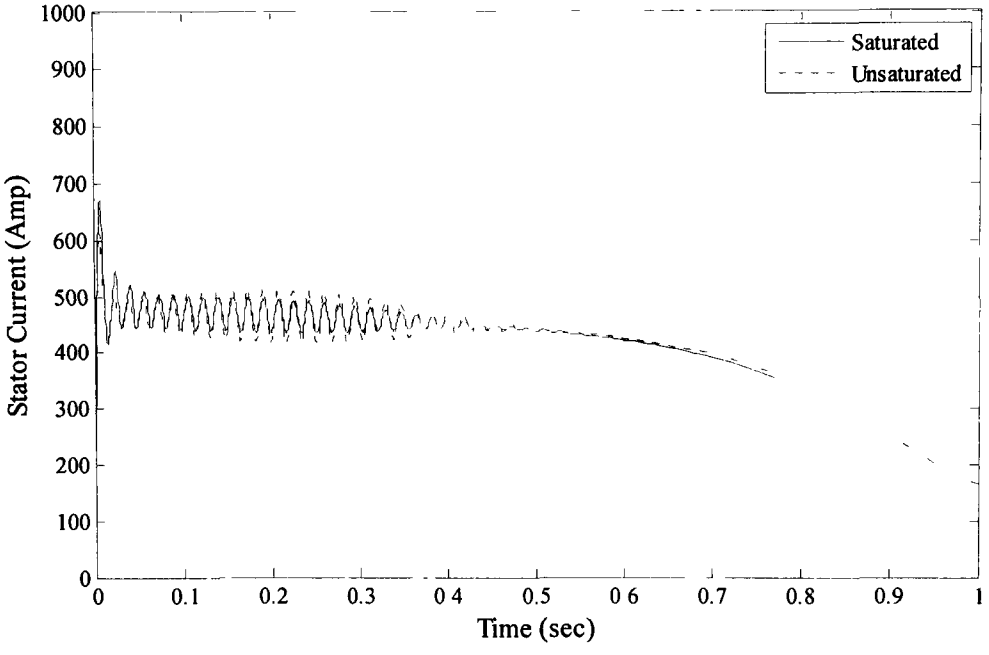

Fig. 28. Phase 'a' stator current calculated by saturated and unsaturated models at full load.

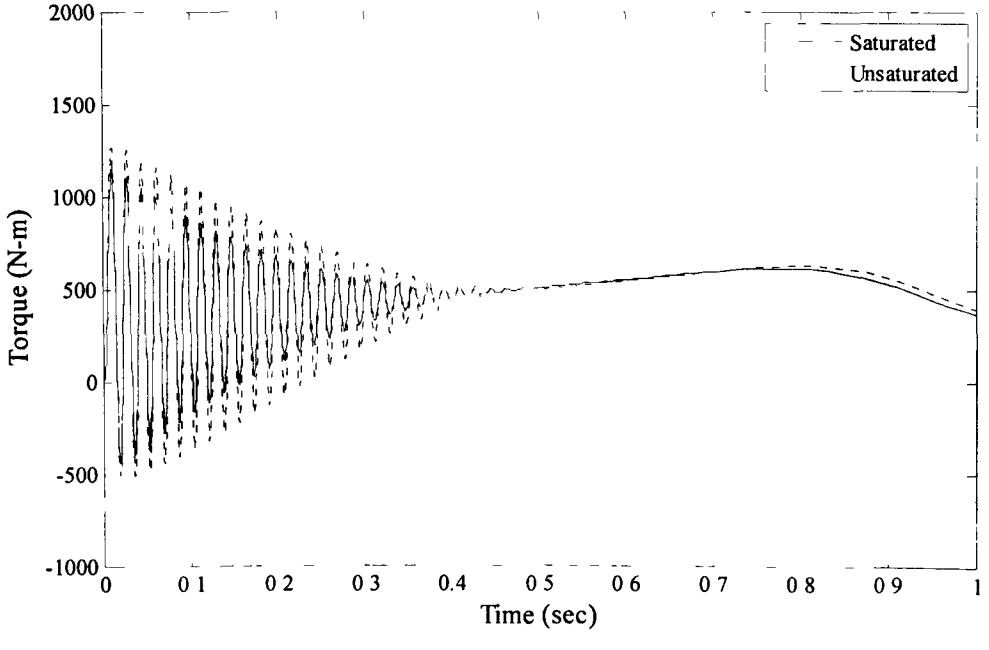

Fig. 29. Electro-magnetic torque calculated by saturated and unsaturated models at full load.

4.2.3 Direct Starting with Shunt Capacitors at No Load

In this section, the direct starting of induction motor by employing shunt capacitor bank will be investigated for both saturated and unsaturated models. The capacitor bank is connected via circuit breaker to support the necessary reactive power during starting, in order to minimize voltage dip. The capacitor bank is switched on at time t= 0.004 sec, to boost the terminal voltage as demonstrated in the Fig. 30(a). It has been examined that at time t=0.004 sec, voltage rise from 362.2 volts to 454.5 volts for both saturated and unsaturated motor models due to injection of reactive power by shunt capacitors. Maximum voltage dip calculated after switching on the capacitor bank is 445.2 volts and 448.9 volts for saturated and unsaturated respectively as can be seen in Fig. 30(b). The starting time reduced significantly to 0.4 sec

The motor consumes more reactive power by injection of VARS due to shunt capacitors during the starting as represented in Fig. 31(a). At the time of switching of capacitor bank at t= 0.004 sec, the consumption of reactive power is high as clearly demonstrated in Fig. 31(b). During the transient period at t=0.008 sec, the peak values of reactive power being consumed by the motor are, 0.195 MVARs and 0.147 MVARs for both saturated and unsaturated motor models respectively. The discrepancy between saturated and unsaturated cases is very high both during transient and steady state. The steady state value of saturated model is calculated as 0.037MVARs and for unsaturated model is 0.007MVARs which clearly indicates that for saturation case, the magnetizing current is high due to high stator current and so the steady state value is high.

The active power simulated result in Fig. 32 shows that at no load, for both the models the transient values are same, but during steady state small discrepancy has been noted. The motor gains same rated speed for both saturated and unsaturated models in t=0.004 sec as illustrated in Fig. 33. The phase 'a' stator current peak is very high during early transient state for saturated case, with a calculated value of 922 amperes, while for unsaturated model, it is 726 amperes. The same proportional discrepancy exists during the steady state as well because of the high magnetizing current. The starting torque for saturated model has been calculated low as compared to the unsaturated model. During the transient period, the torque oscillations are high for unsaturated case in comparison with saturated one as in Fig. 34.

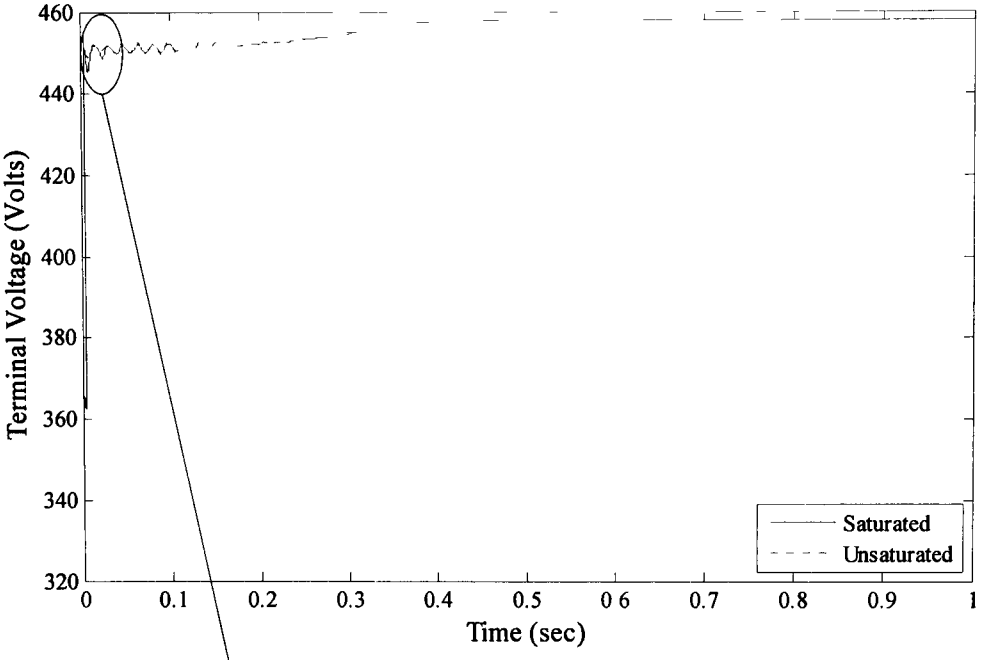

(a)

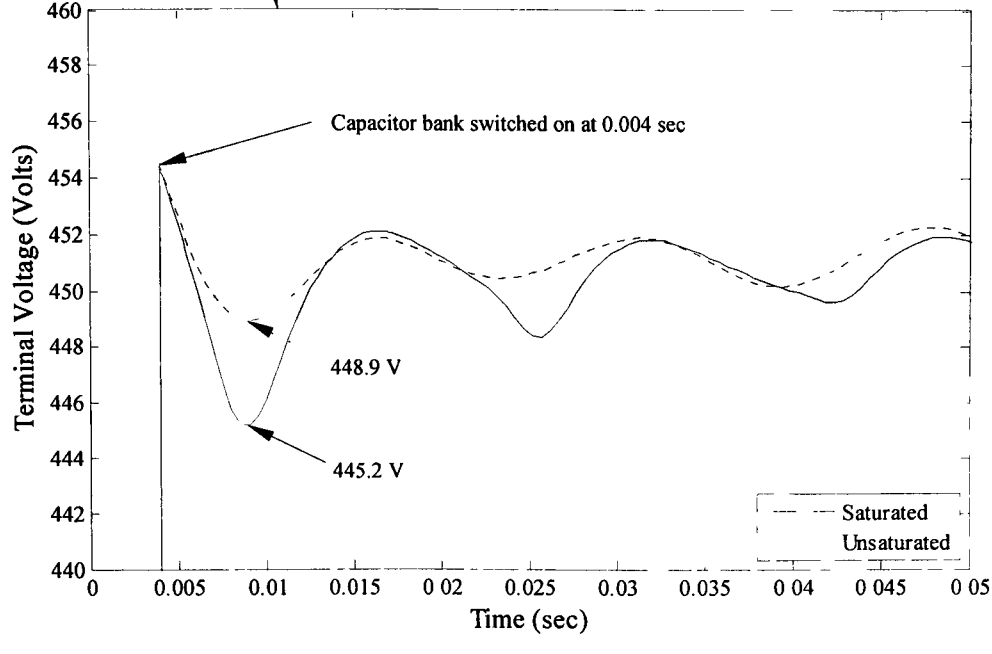

(b)

Fig. 30. Terminal voltage calculated by saturated and unsaturated model with shunt capacitors at no load. (a) Plot for 1sec. (b) Plot (zoomed in) for 0.05 sec.

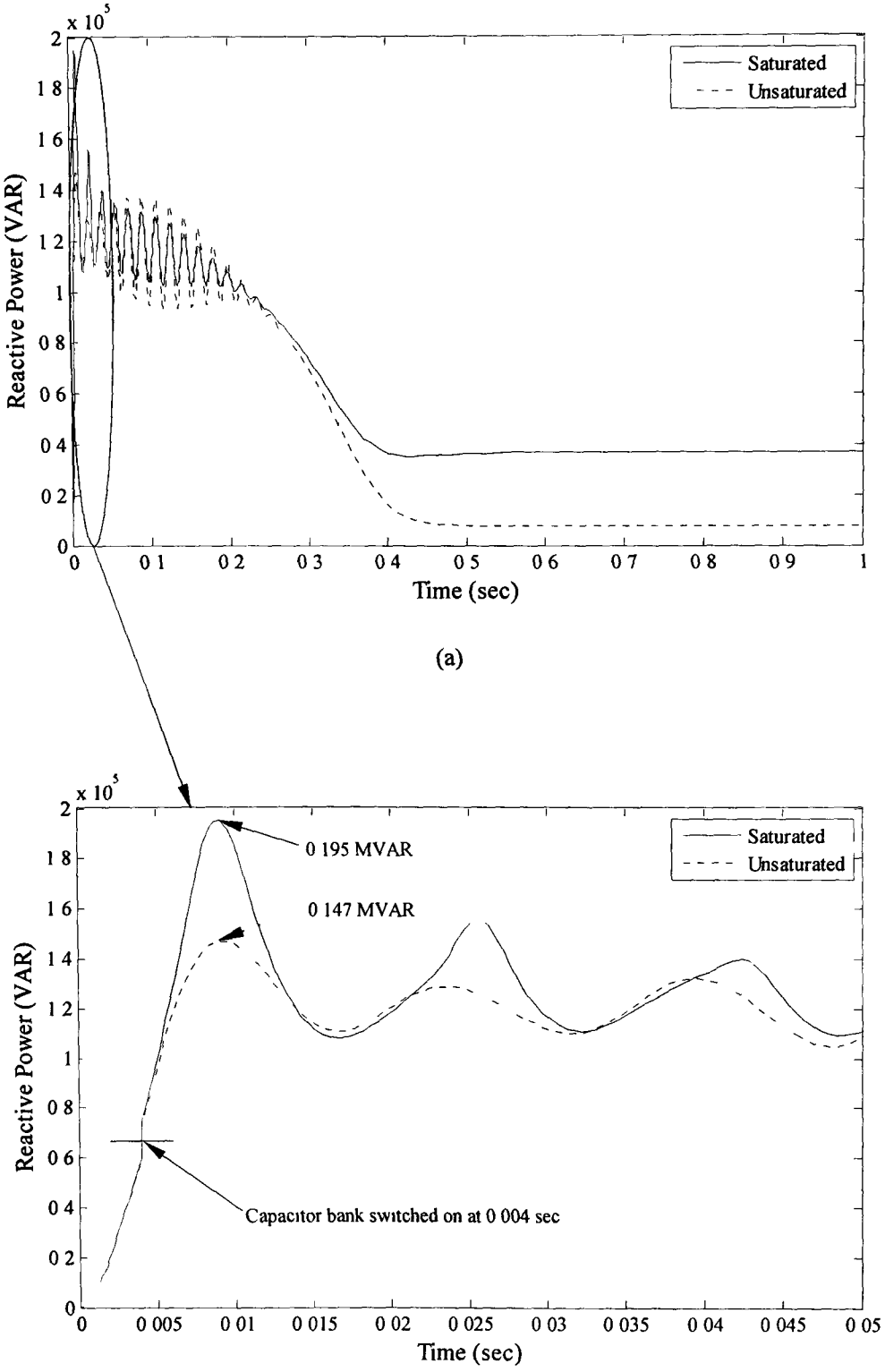

Fig. 31. Reactive power calculated by saturated and unsaturated models with shunt capacitors at no load (a) Plot for 1sec. (b) Plot (zoomed in) for 0.05 sec.

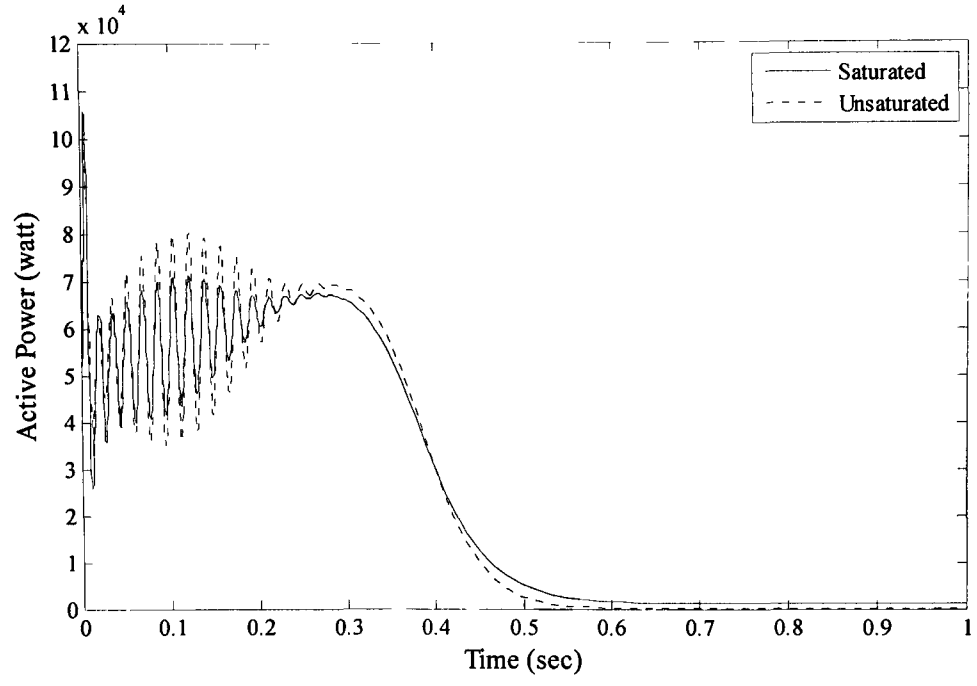

Fig. 32. Active power calculated by saturated and unsaturated models with shunt capacitors at no load.

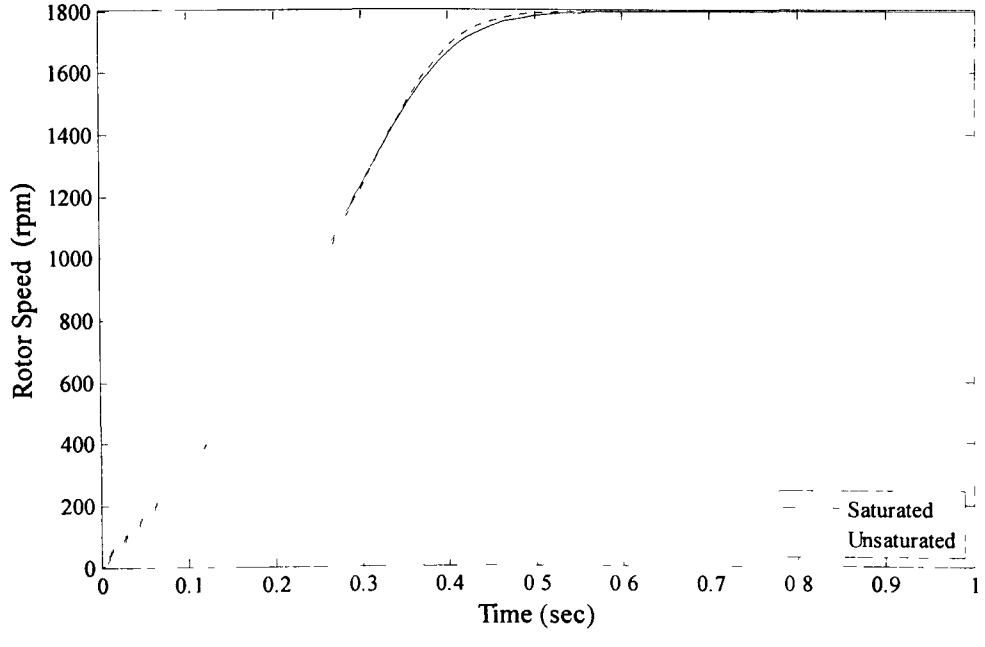

Fig. 33. Rotor speed calculated by saturated and unsaturated models with shunt capacitors at no load.

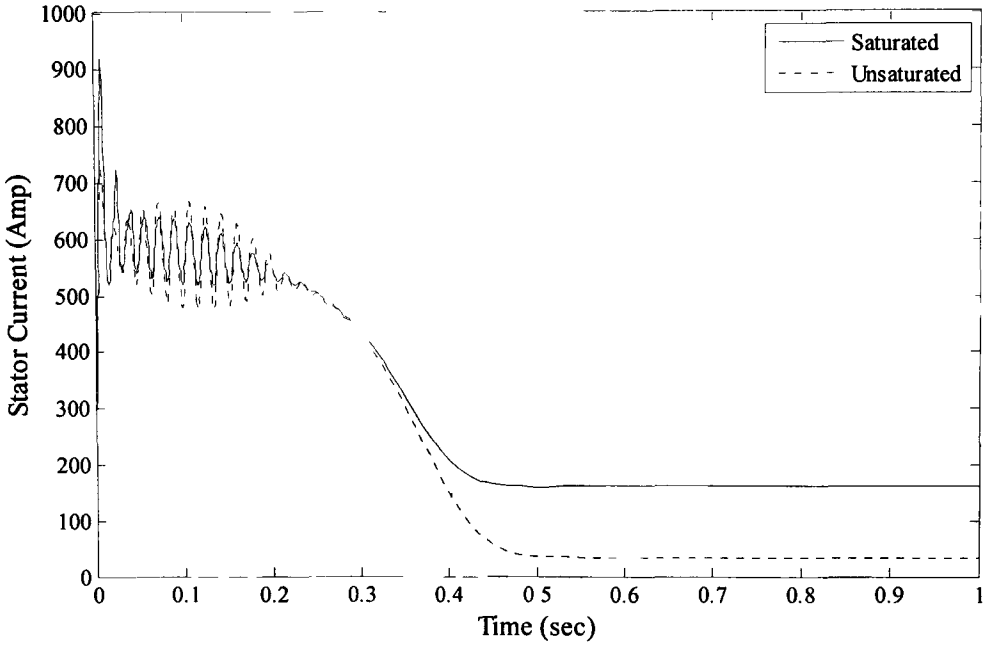

Fig. 34. Phase 'a' stator current calculated by saturated and unsaturated models with shunt capacitors at no load.

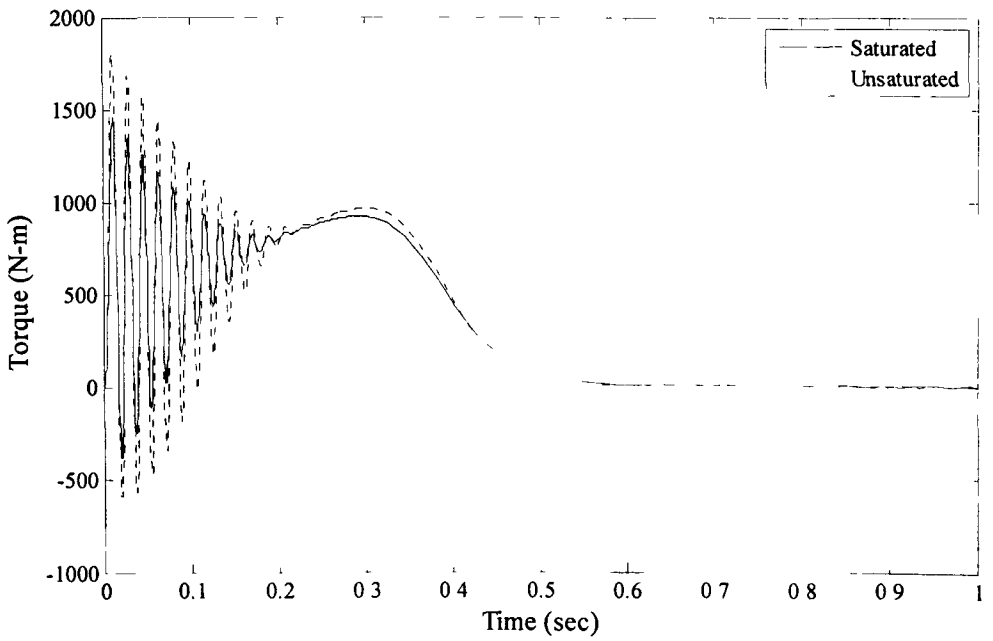

Fig. 35. Electro-magnetic torque calculated by saturated and unsaturated models with shunt capacitors at no load.

4.2.4 Direct Starting with Shunt Capacitors at Full Load

The direct starting with shunt capacitors at full load will be investigated and analyzed for considering and ignoring main flux saturation in the induction motor model. As explain in the previous section at no load condition, the injection of VARs by shunt capacitors boosts the terminal voltage while starting for both the motor models shown in the Fig. 36(a). The voltage envelope for full load is nearly same as for no load, because capacitor bank is supplying enough reactive power as demonstrated in Fig. 36(b). At full load, the acceleration time extends to 0.55 sec for motor to gain steady state. There is a discrepancy of 2 volts between the two models calculated for the steady state voltage.

The reactive power consumed during starting by the induction motor is same as for no load, as illustrated in Fig. 37. The transient period is extended due to loading condition, as a result motor draw reactive power for longer period to minimize the terminal voltage drop. The active power during the transient period is same, for both saturated and unsaturated models but there is small discrepancy between the two models in steady state as can be seen in Fig. 38. The motor rated speed for both the models drops due to loading conditions. The steady state rotor speed calculated for unsaturated model is 1747 (rpm), whereas for saturated model, it further drops to 1735 (rpm) as can be seen in Fig. 39. The phase 'a' stator current has same profile during transient and steady state, as previously explained for no load conditions except acceleration time of the motor being prolonged as represented in Fig. 40. The electromagnetic torque of the motor as shown in the Fig. 41 has less starting torque for saturated motor model, as compared to the unsaturated during the transient period.

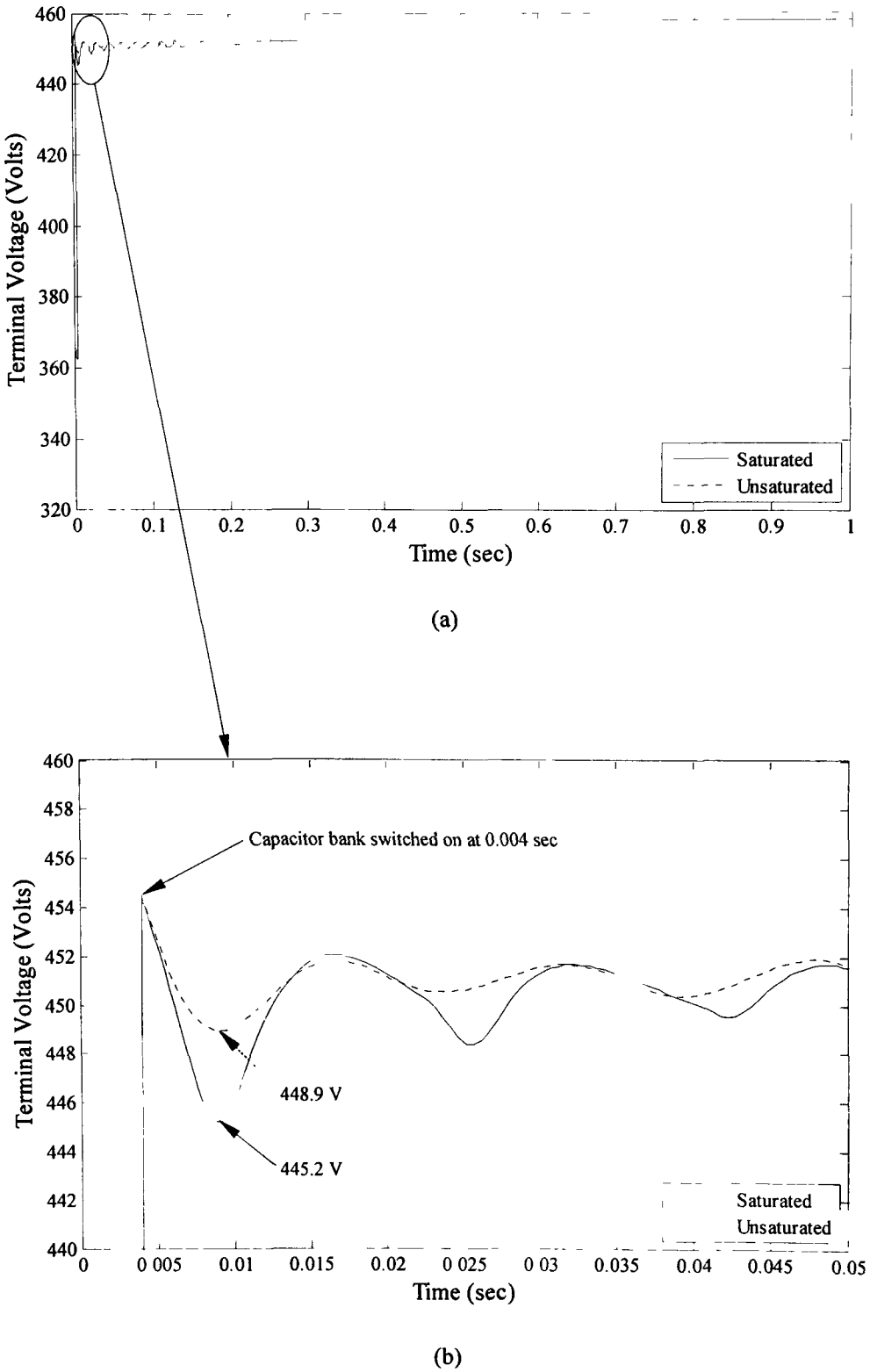

Fig. 36. Terminal voltage calculated by saturated and unsaturated models with shunt capacitors at full load. (a) Plot for 1sec. (b) Plot (zoomed in) for 0.05 sec.

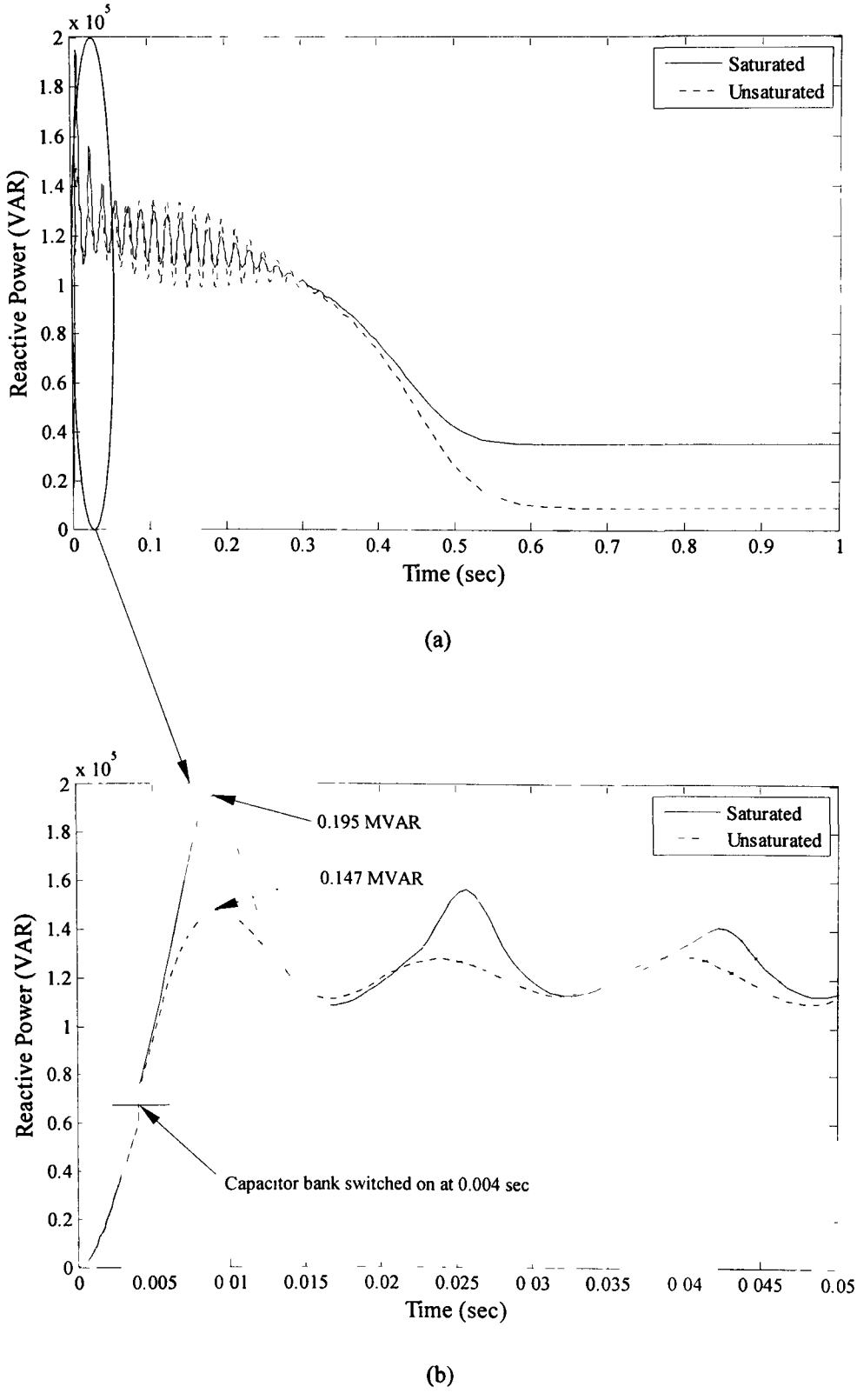

Fig. 37. Reactive power calculated by saturated and unsaturated models with shunt capacitors at full load (a) Plot for 1sec. (b) Plot (zoomed in) for 0.05 sec.

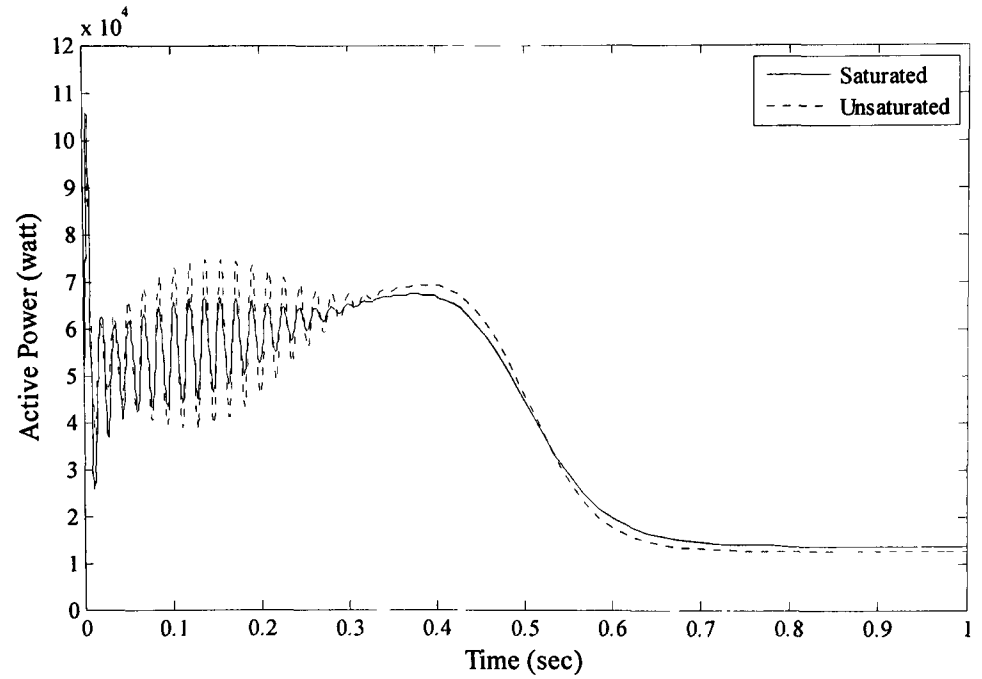

Fig. 38. Active power calculated by saturated and unsaturated models with shunt capacitors at full load.

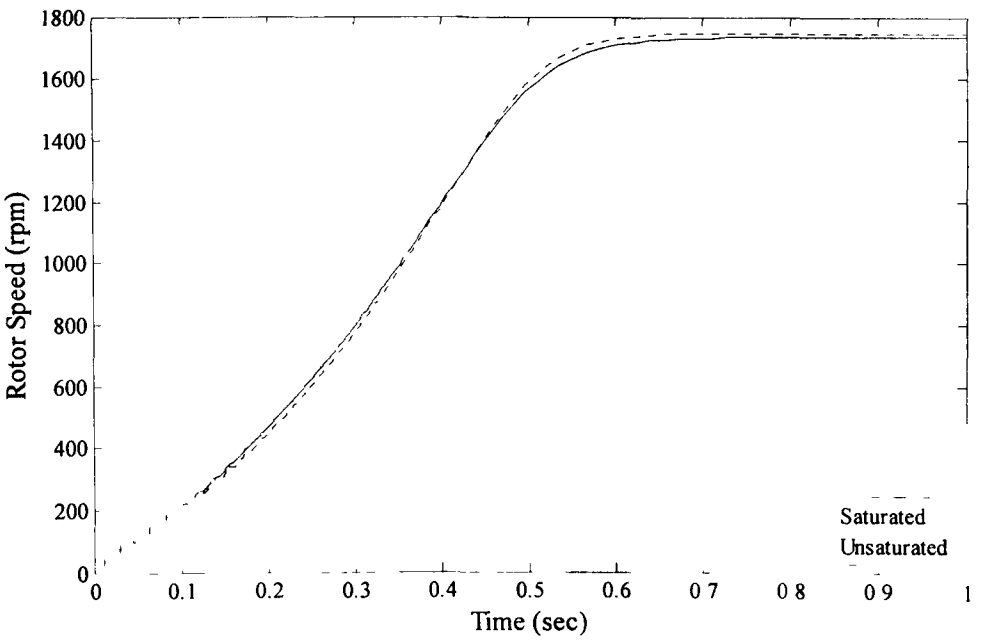

Fig. 39. Rotor speed calculated by saturated and unsaturated models with shunt capacitors at full load.

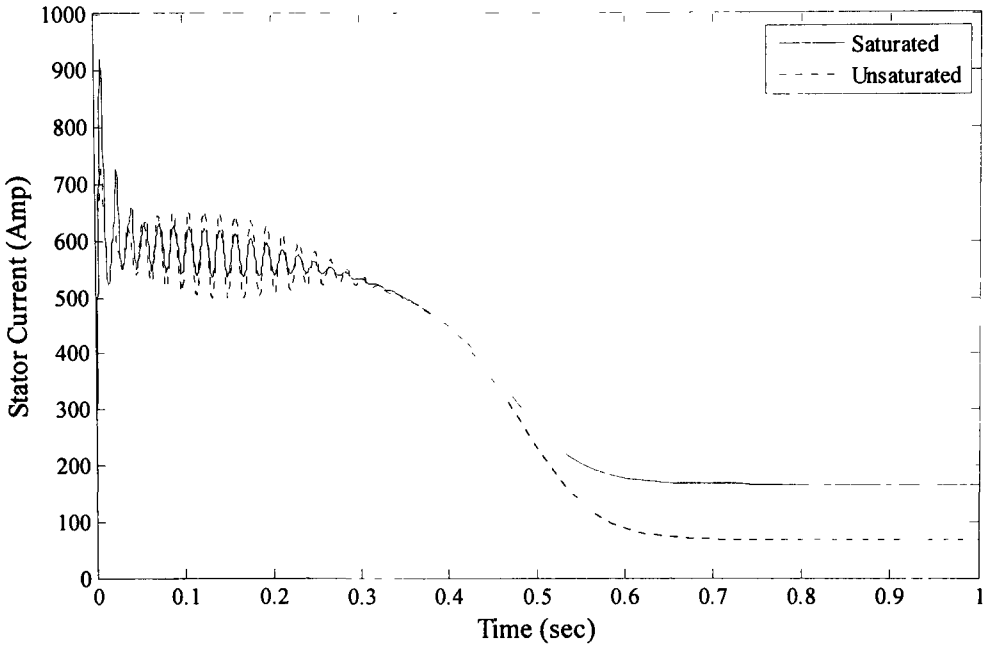

Fig. 40. Phase 'a' stator current calculated by saturated and unsaturated models with shunt capacitors at full load.

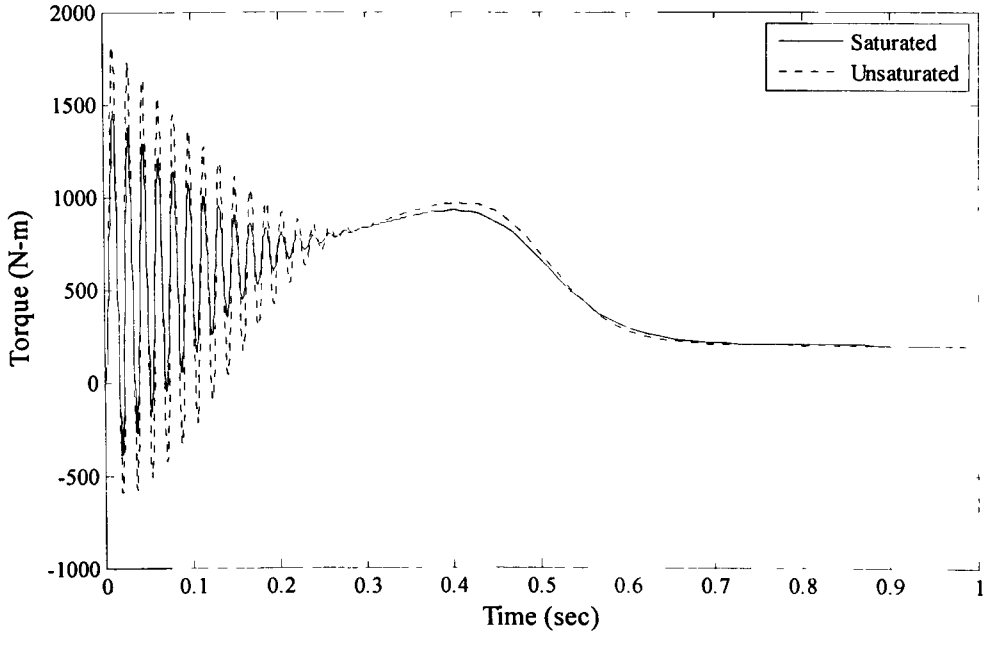

Fig. 41. Electro-magnetic torque calculated by saturated and unsaturated models with shunt capacitors at full load.

4.2.5 Direct Starting with SVC at No Load

In this section, starting performance of induction motor at no load while employing SVC will be investigated and analyzed. SVC provides the voltage regulation by supplying the necessary reactive power during starting of the motor. Voltage improves significantly, during the starting period as well as during steady state as represented in Fig. 42. TSC switched on with the time delay of 0.004 sec as can be seen in Fig. 42(b). The maximum voltage drop calculated for unsaturated model is 431.7 volts whereas for saturated case, it is 429.7 volts. After 0.008 sec, the voltage improvement calculated by unsaturated model is smoother and steady as compared to the saturated model during transient period. The synchronizing unit of SVC controls the switching of TSC in such a way to provide the continuous VARs (capacitive reactive power) to the motor while starting period in order to stabilize the voltage.

The reactive power supplied by the SVC in VAR control mode is the function of susceptance B, which can be varied according to the voltage drop as illustrated in the Fig. 43. TSC switched on at time t=0.004 sec and the amount of reactive power consumed by the motor calculated for unsaturated case is 0.141 MVAR and for saturated case, it is 0.180 MVAR. There is a discrepancy of 0.039 MVAR during the early transient period at t=0.008 sec. As explained in previous section, the discrepancy between the saturated and unsaturated values during the steady state is high, because stator current is very high for saturated case, as a function of magnetizing current. Active power and rotor speed calculated for both saturated and unsaturated motor models are nearly same at no load as demonstrated in Fig. 44 and 45. There is small discrepancy in the steady state value of active power. The phase 'a' stator current value calculated at t=0.008 sec is 856 amperes and 700 amperes for both saturated and unsaturated respectively as shown in Fig. 46. The starting torque oscillations are high for unsaturated case as compared to the saturated case during transient period as illustrated in Fig. 47.

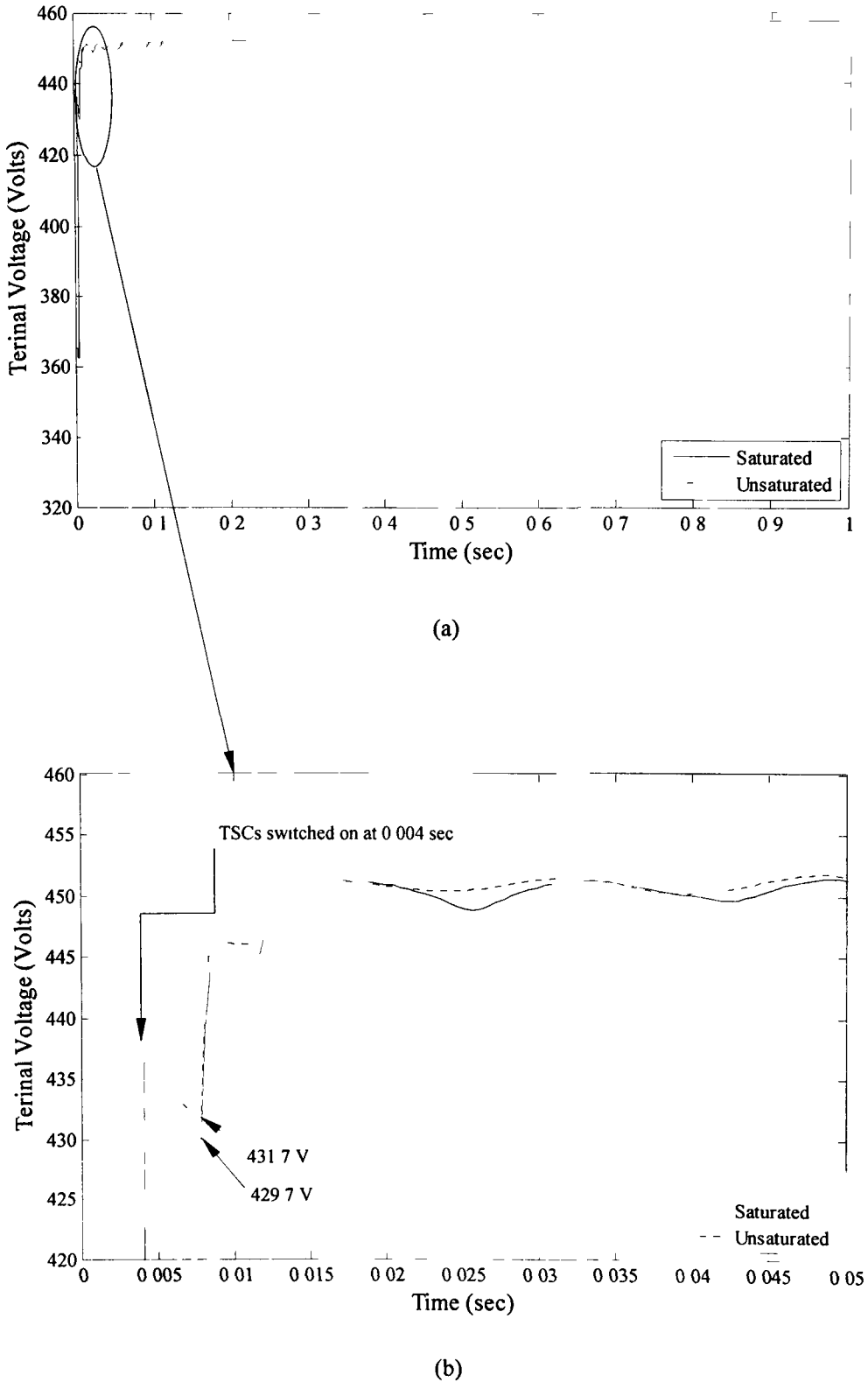

Fig. 42. Terminal voltage calculated by saturated and unsaturated models with SVC at no load. (a) Plot for 1sec. (b) Plot (zoomed in) for 0 05 sec.

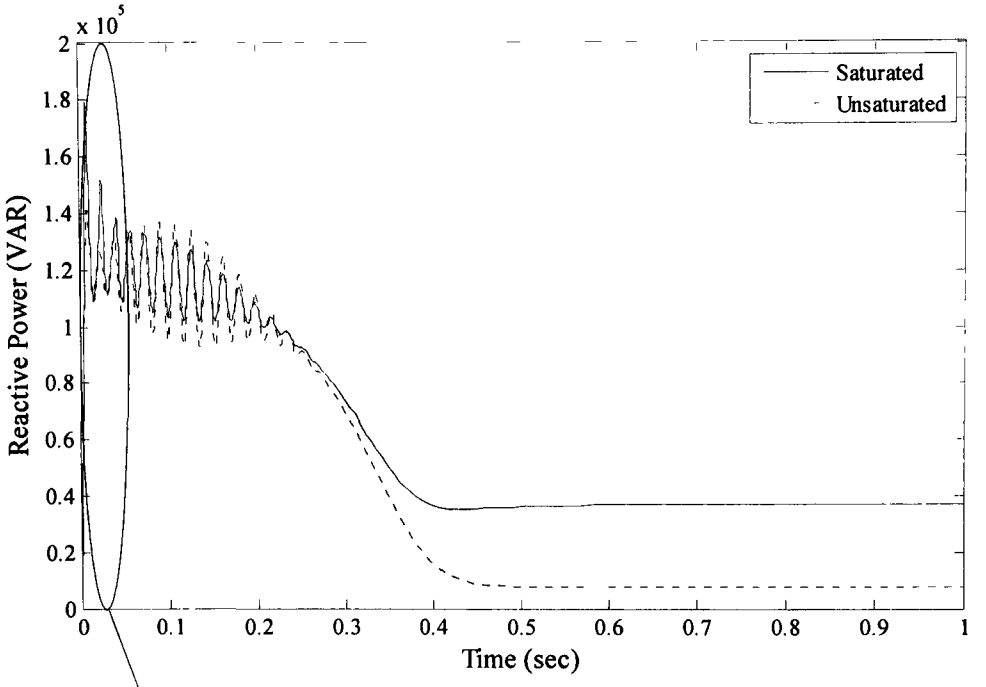

(a)

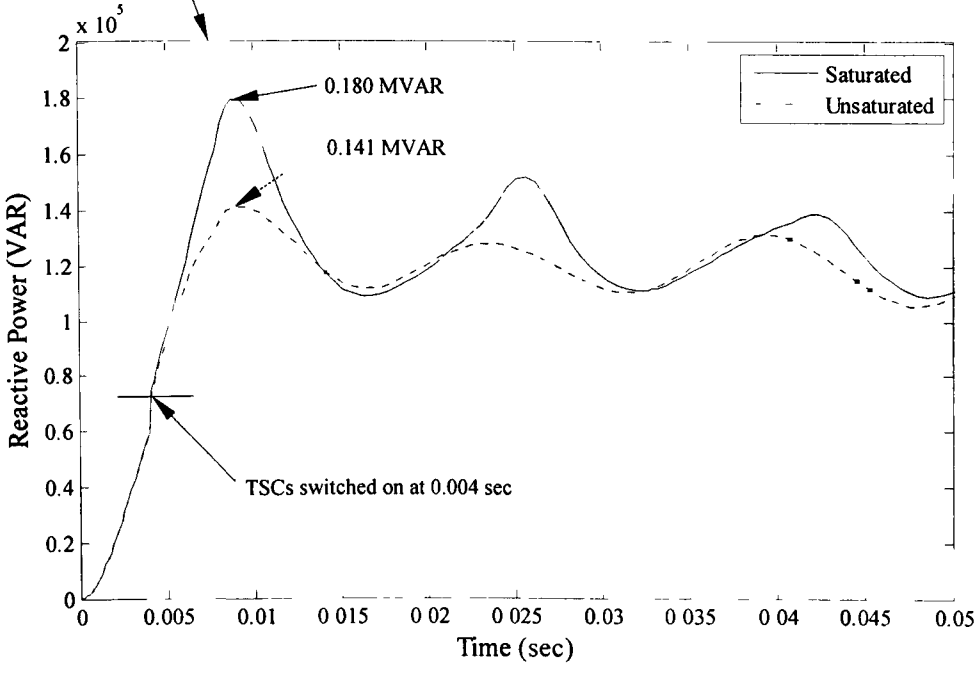

(b)

Fig. 43. Reactive power calculated by saturated and unsaturated models with SVC at no load (a) Plot for 1sec. (b) Plot (zoomed in) for 0.05 sec.

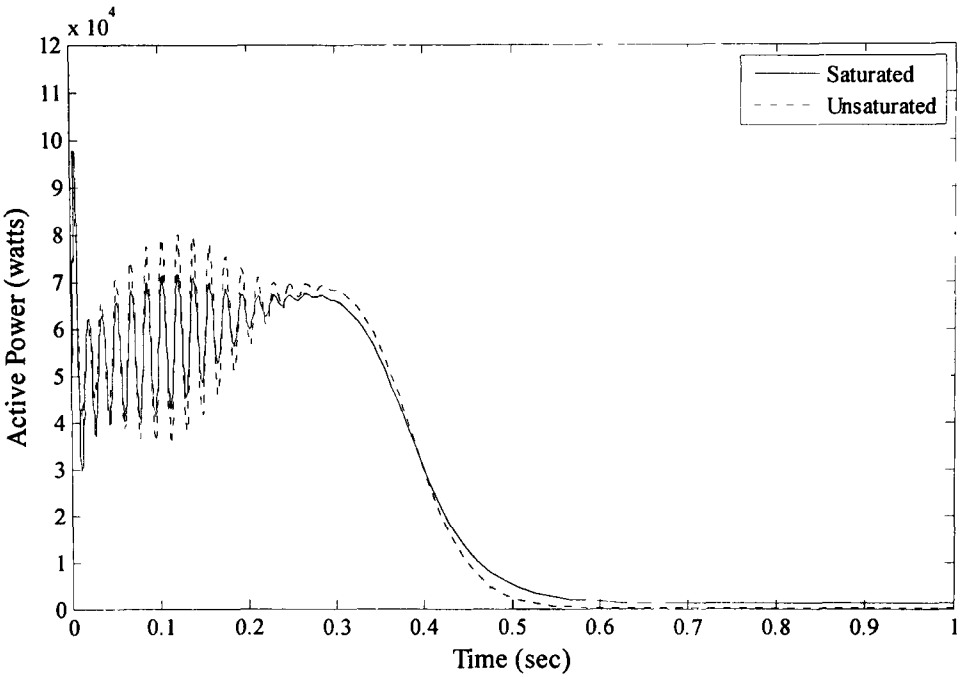

Fig. 44. Active power calculated by saturated and unsaturated models with SVC at no load.

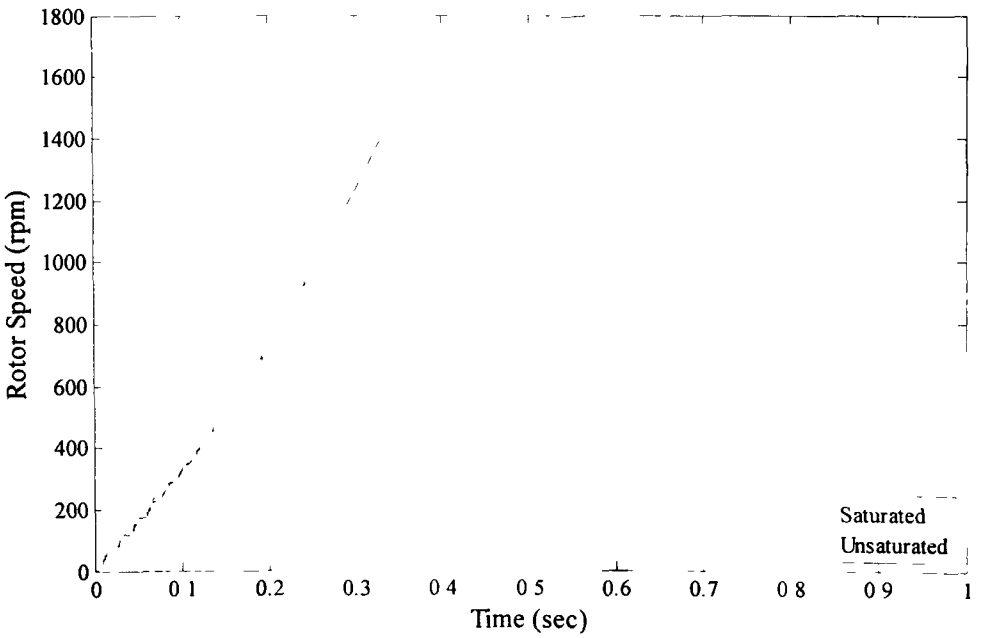

Fig. 45. Rotor speed calculated by saturated and unsaturated models with SVC at no load.

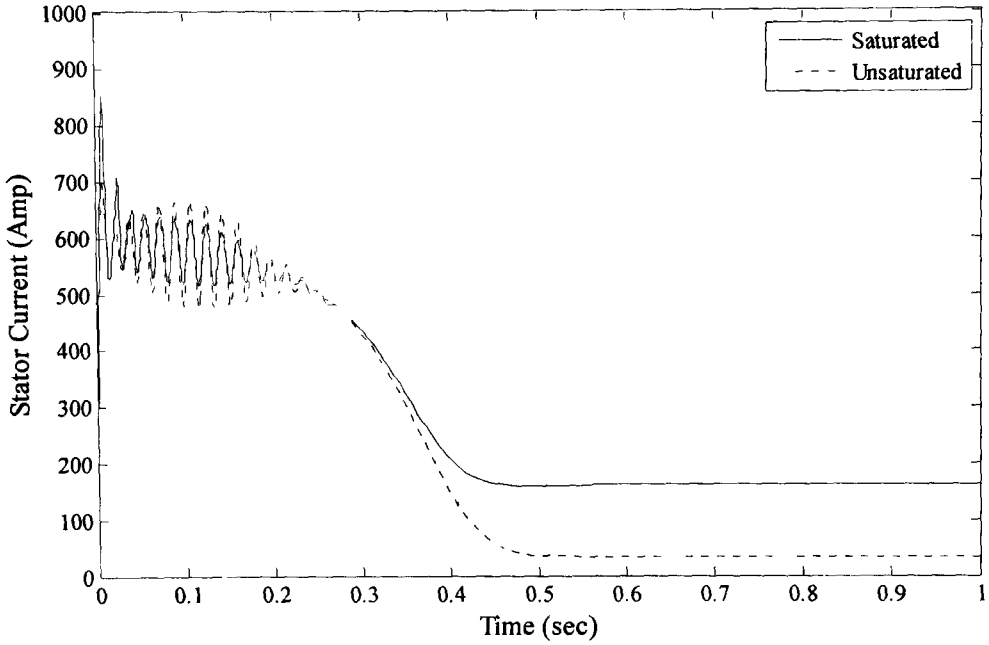

Fig. 46. Phase 'a' stator current calculated by saturated and unsaturated models with SVC at no load.

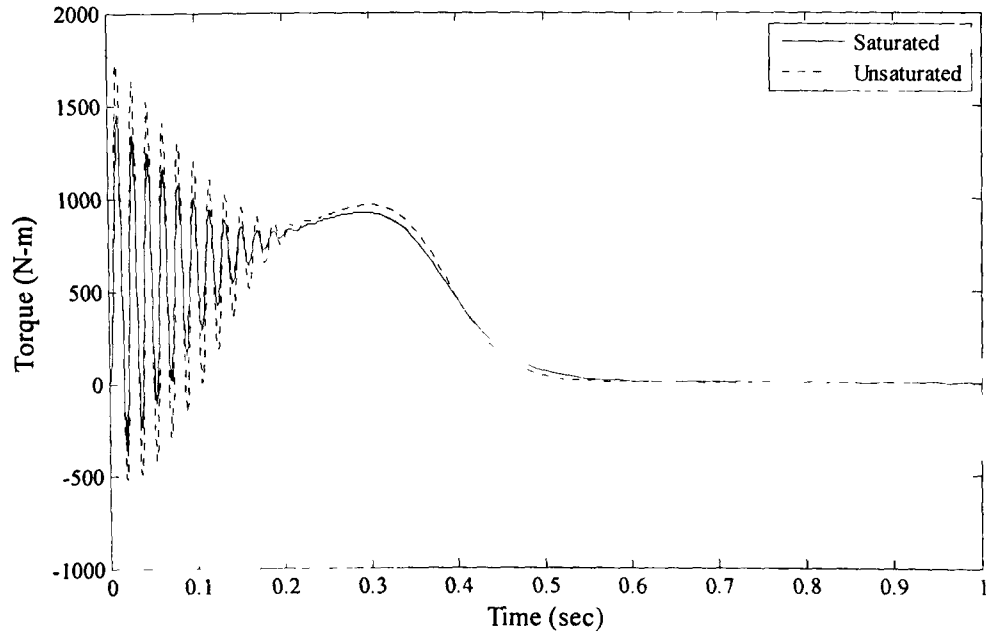

Fig. 47. Electro-magnetic torque calculated by saturated and unsaturated models with SVC at no load.

4.2.6 Direct Starting with SVC at Full Load

Direct starting of induction motor at full load by using SVC will be investigated and analyzed. As we discussed in the previous section, SVC supports the reactive power required by the induction motor during starting, by switching on TSC with the time delay of 0.004 sec. The switching on and off of TSC is controlled by the SVC control unit by using synchronizing unit. As Fig. 48 shows that voltage envelope after TSC switching is nearly same as for both no load and full load conditions. Further we can examine in the Fig. 48(b) that the voltage smoothness and steadiness is same, for both loading conditions during the transient period.

The reactive power consumed by the motor at full load is nearly same as for no load condition as presented in Fig. 49. Because voltage drop during both transient and steady state is same, so the susceptance value is nearly same for the required reactive power by the induction motor as can be seen in the Fig. 49 (b). SVC controls the reactive power during the starting transient to provide a smooth and steady start for all loading conditions.

Active power at full load while employing SVC is nearly the same during transient period for both Saturated and unsaturated cases. But the steady state value has small discrepancy of 0.01MW as can be examined in the Fig. 50. The motor rated speed drops to 1747 (rpm) and 1735 (rpm) for both saturated and unsaturated models respectively, which indicates for saturated case less drop of rotor speed due to high stator current as mentioned in the Fig. 51.The stator current envelope is nearly same as calculated for no load conditions during transient period as well as steady state as illustrated in the Fig. 52.

The starting electromagnetic torque calculated for unsaturated motor model is considerably high as compared to the saturated one. During the starting transient period, it is desirable to have enough starting and acceleration torque for the motor to meet the high inertia load requirements.

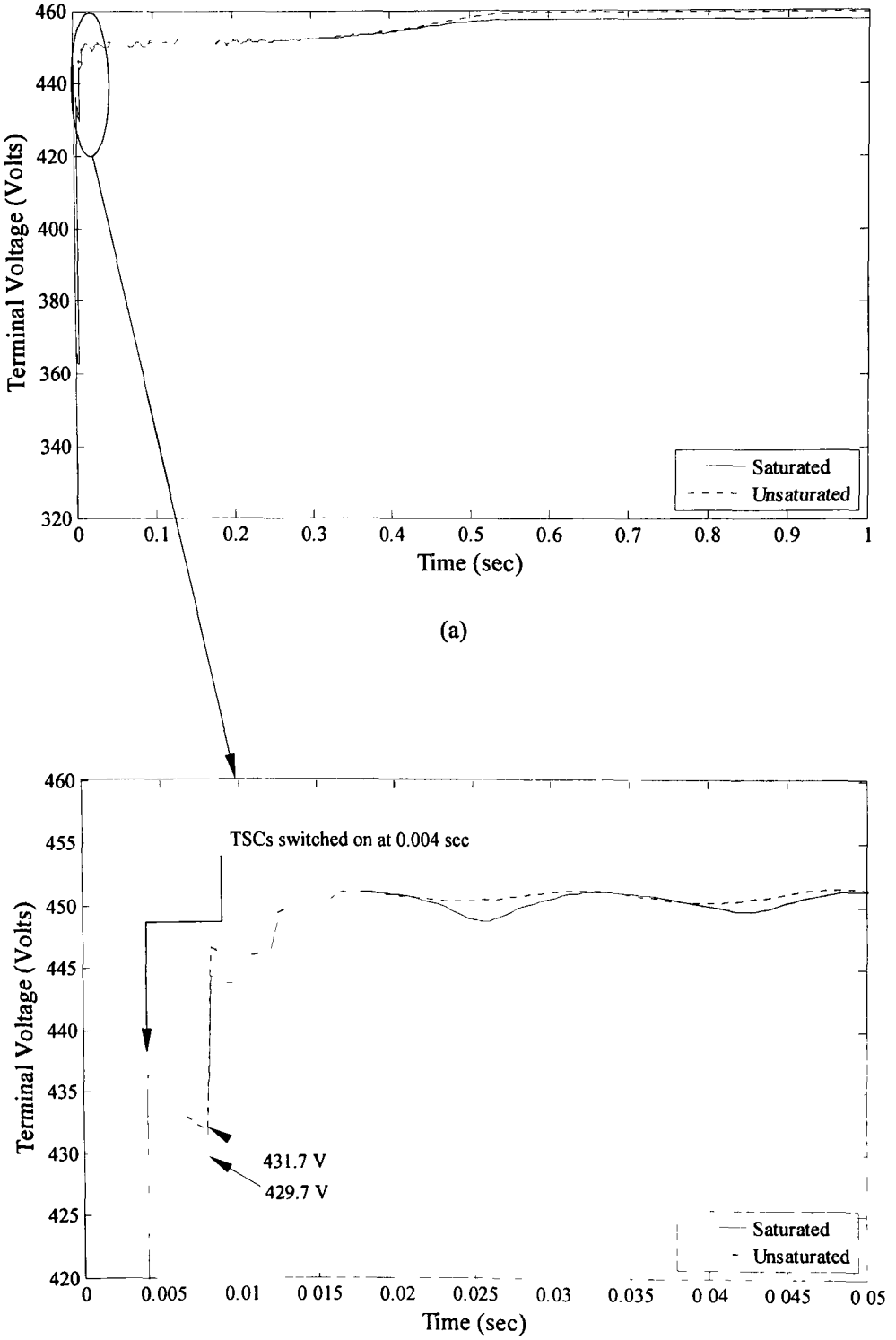

Fig. 48. Terminal voltage by saturated and unsaturated models with SVC at full load. (a) Plot for 1sec. (b) Plot (zoomed in) for 0.05 sec.

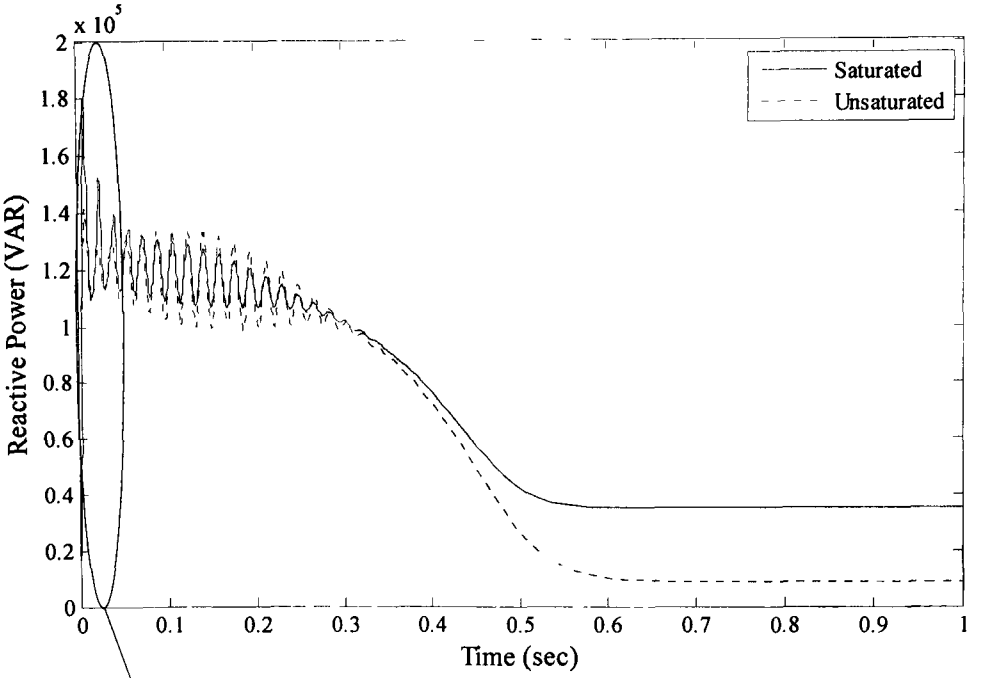

(a)

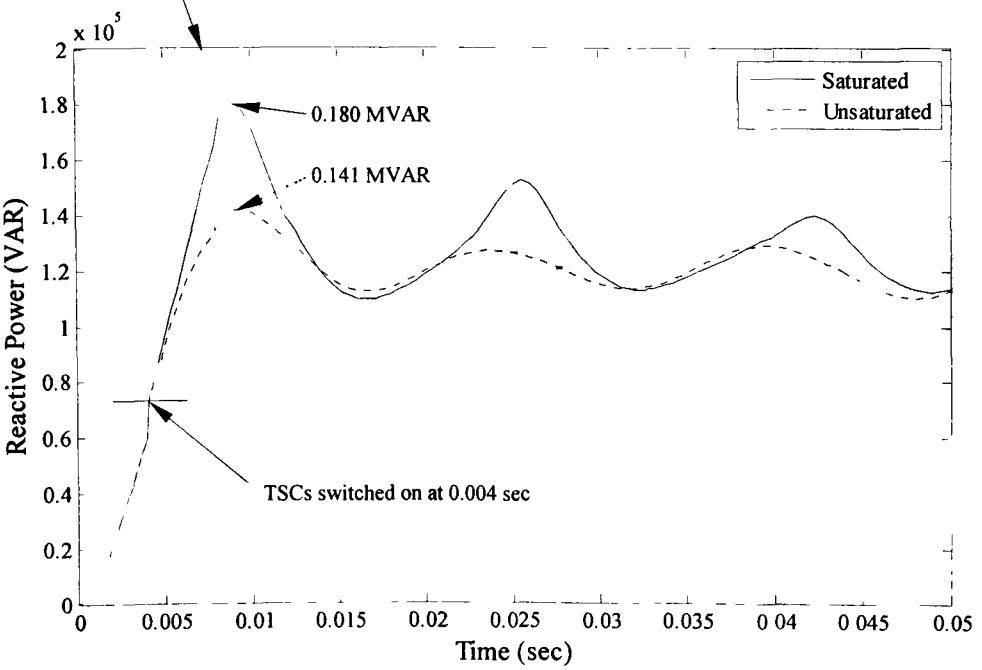

(b)

Fig. 49. Reactive power calculated by saturated and unsaturated models with SVC at full load (a) Plot for 1sec. (b) Plot (zoomed in) for 0.05 sec.

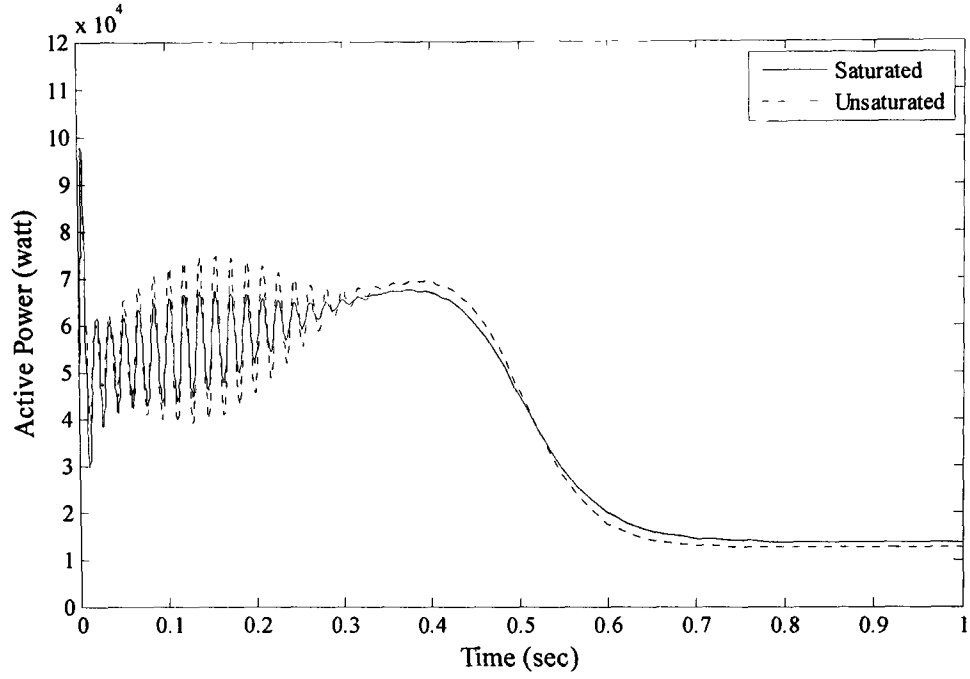

Fig. 50. Active power calculated by saturated and unsaturated models with SVC at full load.

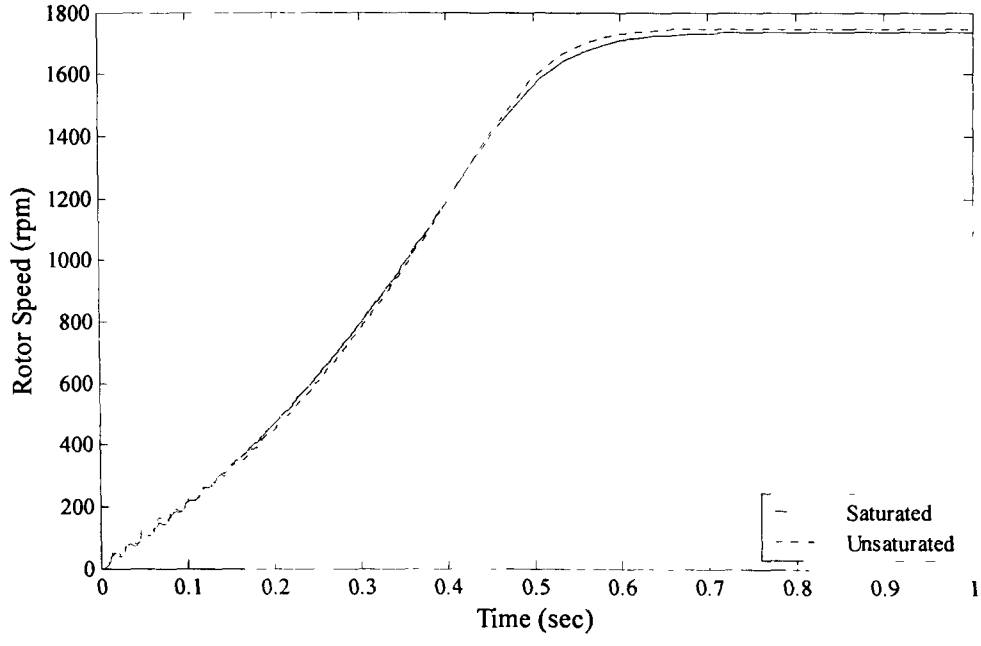

Fig. 51. Rotor speed calculated by saturated and unsaturated models with SVC at full load.

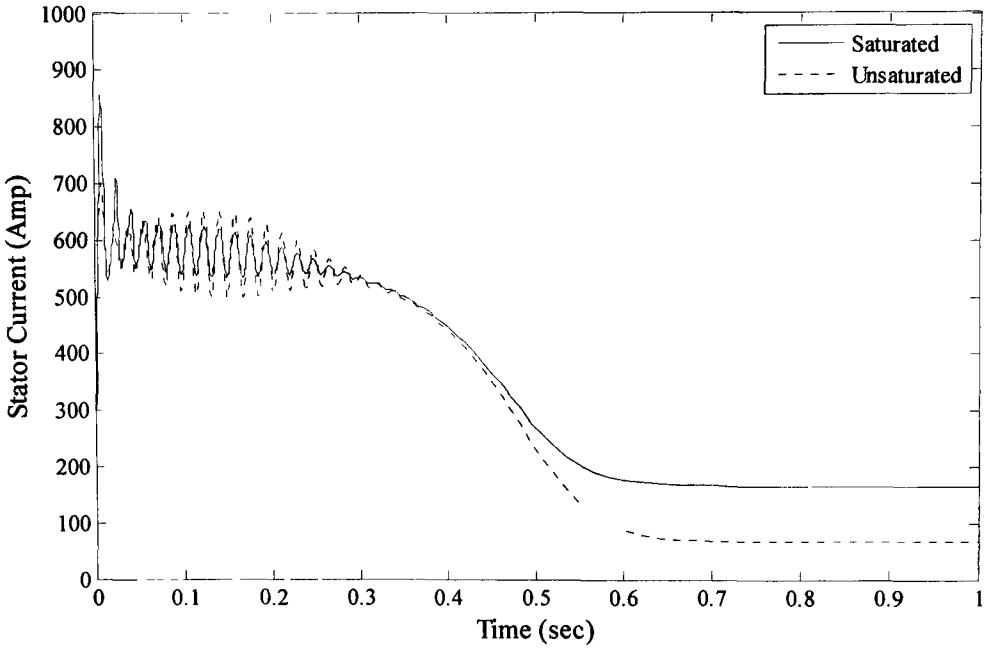

Fig. 52. Phase 'a' stator current calculated by saturated and unsaturated models with SVC at full load.

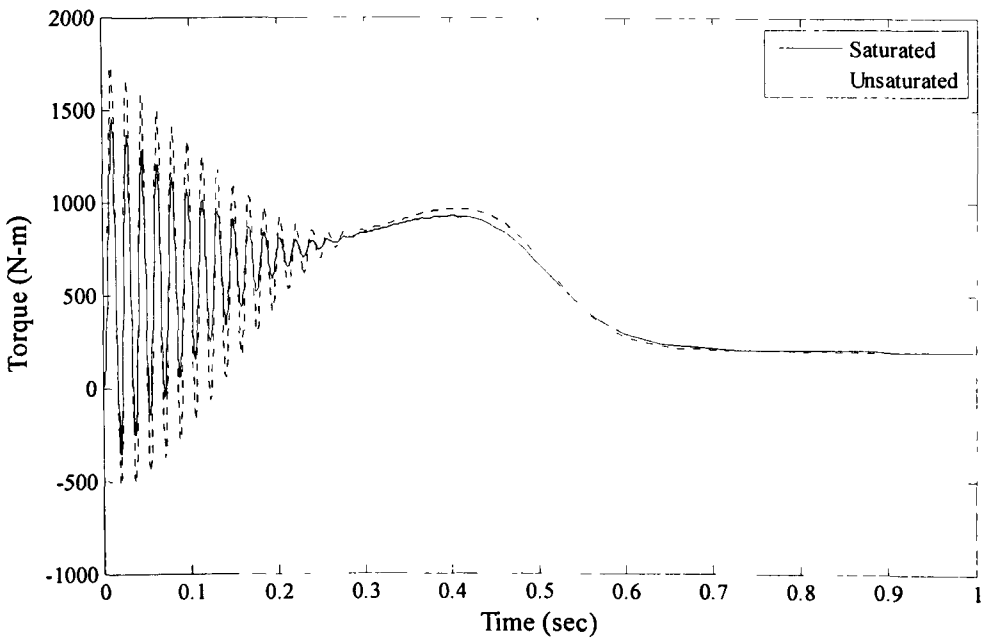

Fig. 53. Electro-magnetic torque calculated by saturated and unsaturated models with SVC at full load.

4.3 Numerical Investigations for 500 hp Motor

In this section starting performance of 500 hp motor will be investigated and analyzed. The mathematical model (unsaturated transient d-q model) and simulation methods by using MATLAB/Simulink are same as previously used for 50 hp motor. For 500 hp motor only, unsaturated model will be used for investigations as there is no saturation characteristics are available. In this part of the research work, the main objective is to further investigate the behavior of terminal voltage and reactive power demand during starting of induction motor. Moreover, it will be also investigated, how the shunt capacitors and SVC can play their role while support necessary reactive power during early starting transient period.

4.3.1 Motor Parameters and Operating Conditions for 500 hp Motor

The motor parameters and operating conditions for 500 hp induction motor are given below in the Tables 4 and 5. As mentioned in table 4. The terminal voltage of the motor is 2,300 volts, and frequency is 60 Hz.

Table 4. 500 hp Induction motor parameters.

Rated Voltage	2,300 Volts	L_m	54.02 H
Rated Current	93.60 Amperes	R_s	0.262 Ω
Rated Torque	1.98×10^3 N-m	R_r	0.187 Ω
Rated Speed	1800 (rpm)	L_{ls}	1.206 Ω
No of Poles	4	L_{lr}	1.206 Ω
Frequency	60 Hz	Inertia	11.06 Kg.m^2

Table 5. Operating conditions

Base Voltage	25 *KV*	Base Power	200 *MVA*
P	10 Watts	Transformer Ratio	$25e^3$:2,300 *V*

Table 6. SVC and shunt capacitors parameters.

Nominal Voltage	25 *KV*	Base Power	200 *MVA*
Capacitance	0.002 F	*Bref*	0.0172 pu/Pbase
Q_{lmax}	-100 *MVA*	Q_{cmax}	200 *MVA*

4.3.2 Numerical Simulation Results for 500 HP Motor

In this section starting performance of 500 hp induction motor will be investigated and analyzed by using simulated results. As in the previous section we comprehensively analyzed the starting performance for 50 hp induction motors for saturated and unsaturated models while studying the various parameters. For this large motor, we will mostly evaluate the terminal voltage and reactive power for unsaturated model only. The motor will be investigated for 'direct starting', 'direct starting with capacitor', and 'direct starting with SVC' for no load and full load conditions.

4.3.2.1 Terminal Voltage and Reactive Power at No load

The behavior of terminal voltage and consumption of reactive power of 500 hp induction motor at no load during starting period will be investigated in this section. Three-phase balance voltage is applied to the motor terminals, and a considerable voltage drop has been seen during starting as illustrated in the Fig. 54. The voltage drops to

1466.6 volts at t=0.008 sec from the initial 2300 volts as can be seen from the Fig. 54(b).The motor gains steady state at t= 2.2 sec for voltage of 1772 volts. The acceleration time of the motor is considerably high, which is most concerning issue while starting. The motor withstand high starting currents for longer period of time, which can damage the motor winding due to excessive heating. In order to reduce the starting time of the motor and minimize the terminal voltage drop, this 500 hp motor is started by employing shunt capacitors. The voltage profile during starting period with shunt capacitors can be can be seen in Fig. 55. The capacitor bank is switched on at t=0.004 sec with each capacitor has capacitance value of 0.002 Farad. The maximum voltage drop at time of switching capacitor bank is 1586 volts as can be seen in the Fig. 55(b). The acceleration time of the motor reduced from 2.2 sec to 1.4 sec with a steady state voltage of 2300 volts. SVC can also be a continuous source of reactive power while starting large motors as can be examined in Fig. 56. TSC is switched on with a time delay of 0.004 sec, when the maximum voltage drop is 1586 volts. We have noticed, a steady and quick response of SVC improves the voltage to 2300 volts in time a span of 1.4 sec.

The reactive power consumed by the motor during starting is represented in Fig. 57. It has been noticed that during early transient period, motor consumed more reactive power with a maximum value of 0.743 MVAR as illustrated in the Fig. 57(b). This maximum reactive power being consumed by the motor is not enough to maintain the terminal voltage at 2300 volts. The shunt capacitors and SVC are used to support required VARS at the time of starting as shown in the Figs. 58, 59. The maximum reactive power consumed by the motor when capacitor bank is switched on at time t=0.004 sec, is 1.082 MVAR. This value of reactive power boosts the terminal voltage to 2300 volts at 1.4 sec as can be examined in Fig. 58(b). The maximum value consumed by the motor in case of TSC is switched on at time delay of 0.004 sec is 1.100 MVAR as demonstrated in Fig. 59(b). The motor gains its required rated terminal voltage in time 1.4 sec after the application of SVC. The acceleration time of the motor at no load while applying shunt capacitors and SVC is same, but voltage envelope during transient period in case of SVC is smoother and steady.

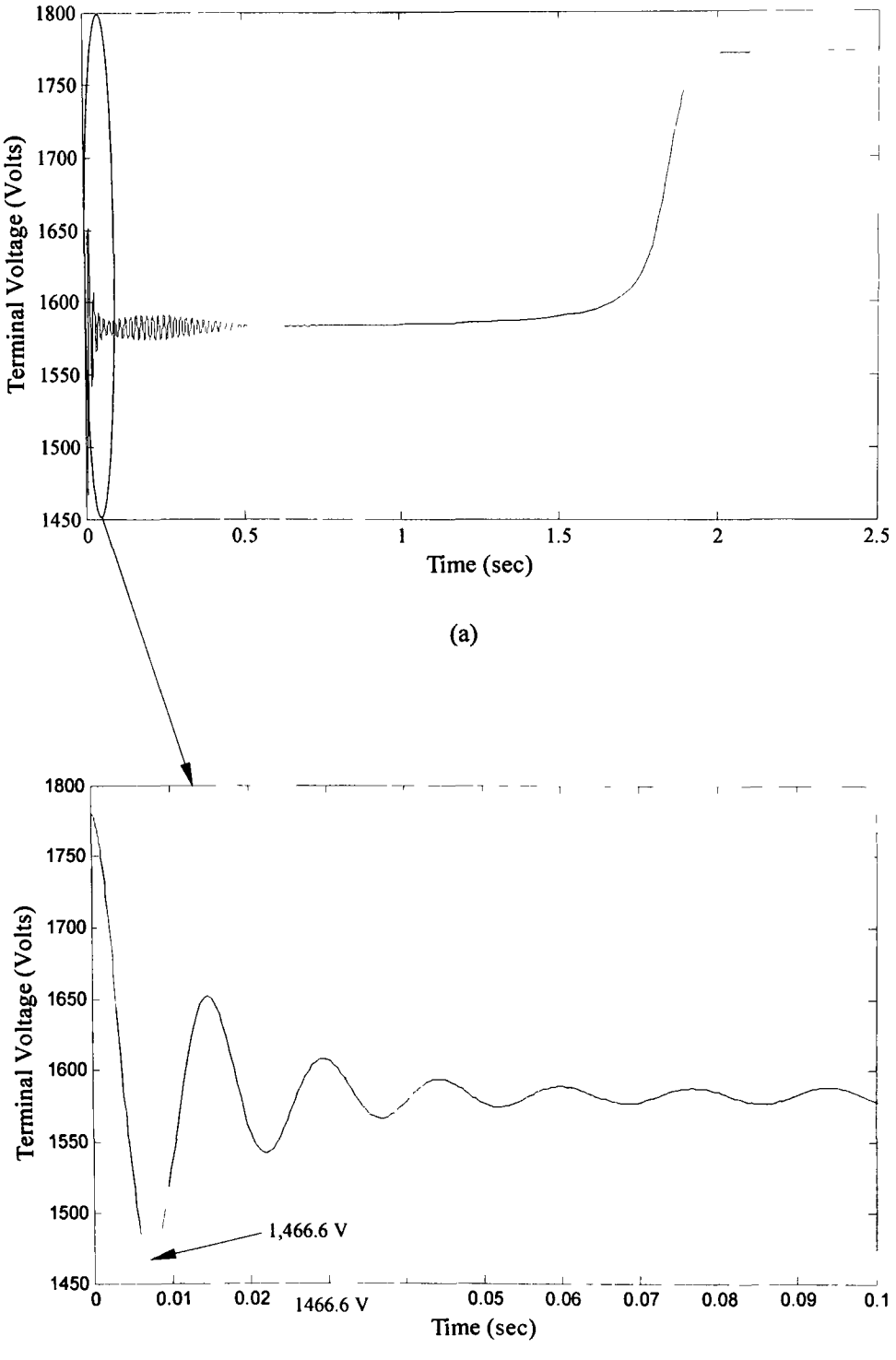

Fig. 54. Terminal voltage calculated by unsaturated model at no load. (a) Plot for 2.5 sec. (b) Plot (zoomed in) for 0.1 sec.

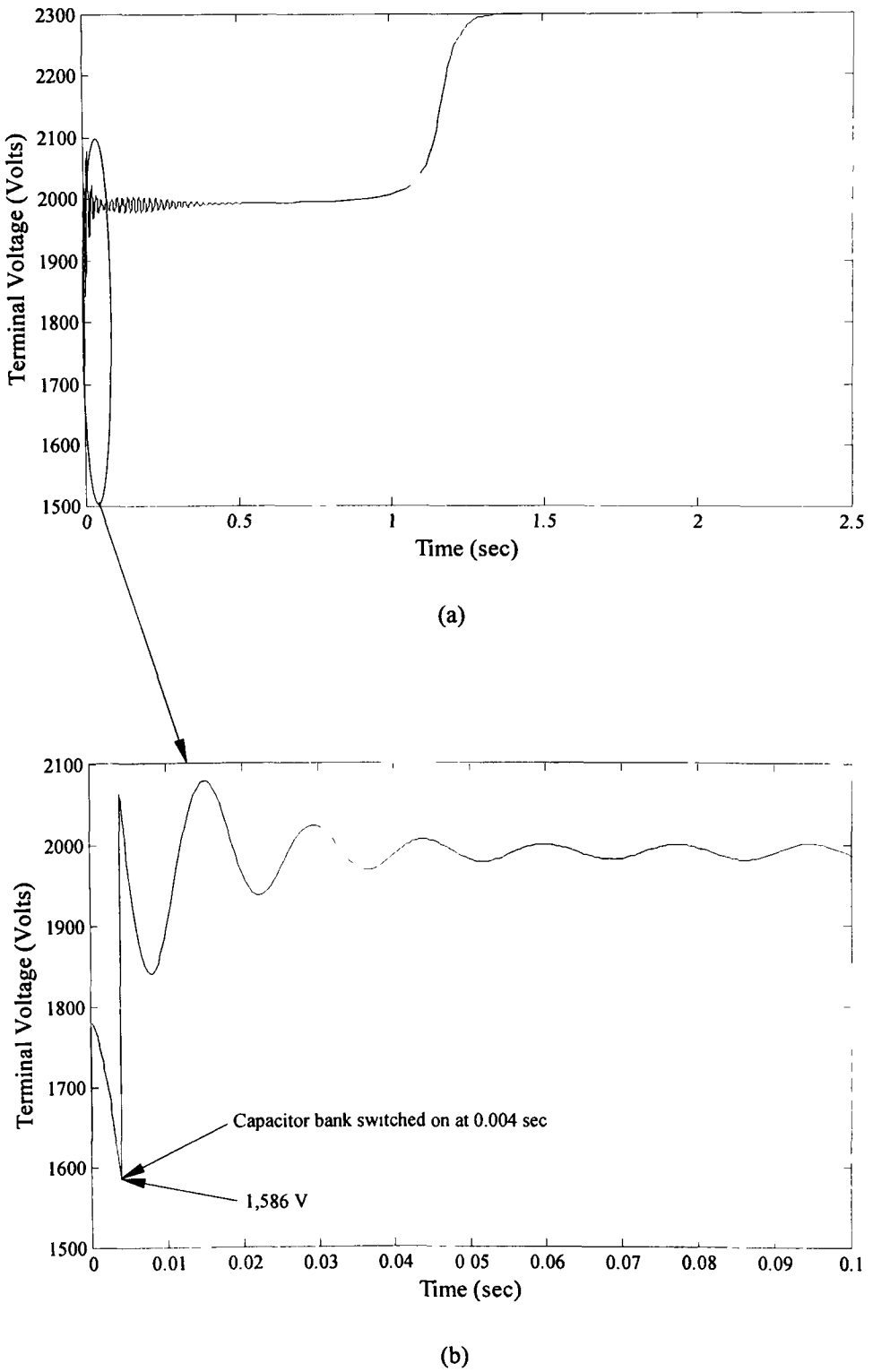

Fig. 55. Terminal voltage calculated by unsaturated model with shunt capacitors at no load. (a) Plot for 2.5 sec. (b) Plot (zoomed in) for 0.1 sec.

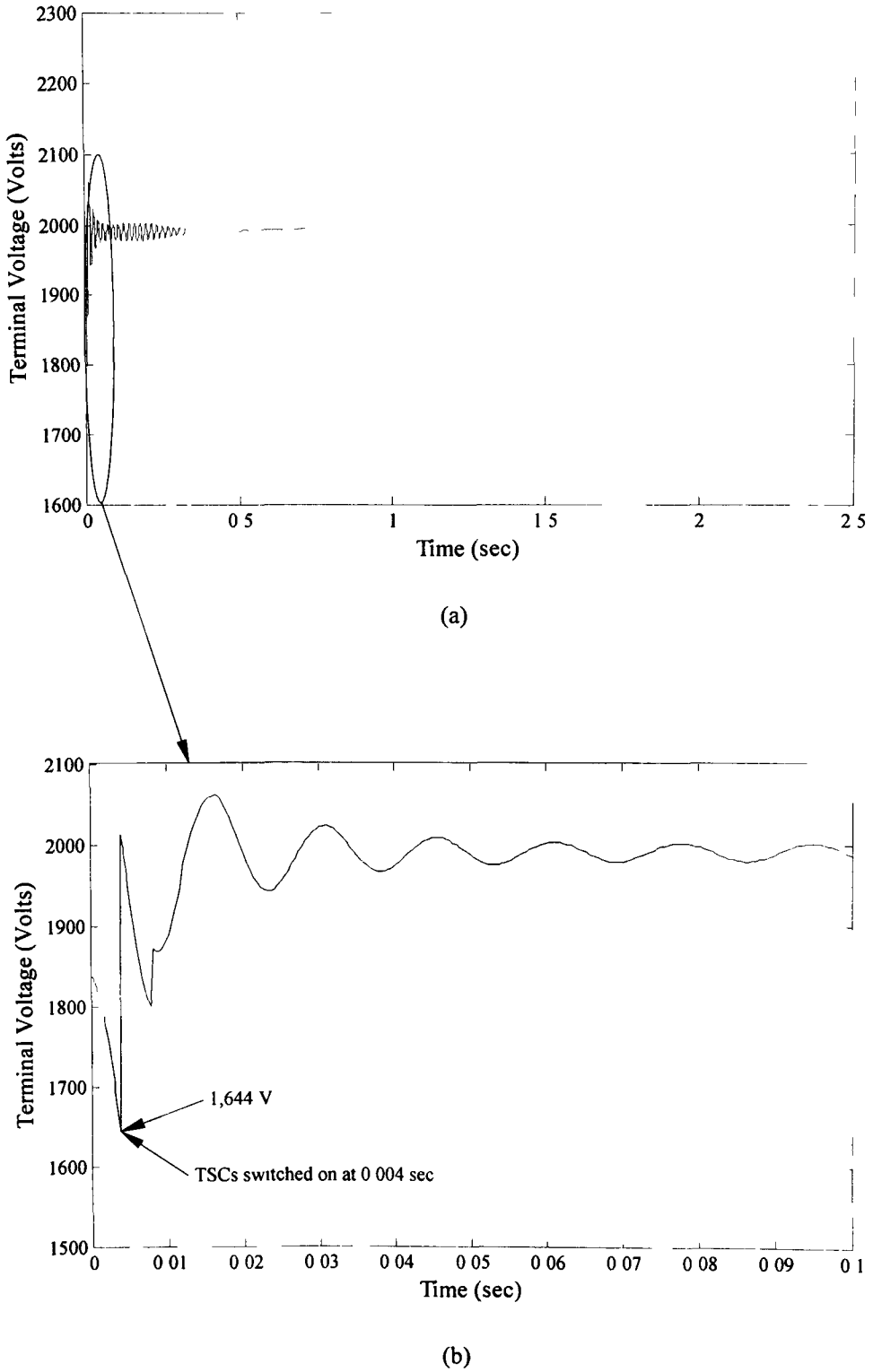

Fig. 56. Terminal voltage calculated by unsaturated model with SVC at no load. (a) Plot for 2.5 sec. (b) Plot (zoomed in) for 0.1 sec.

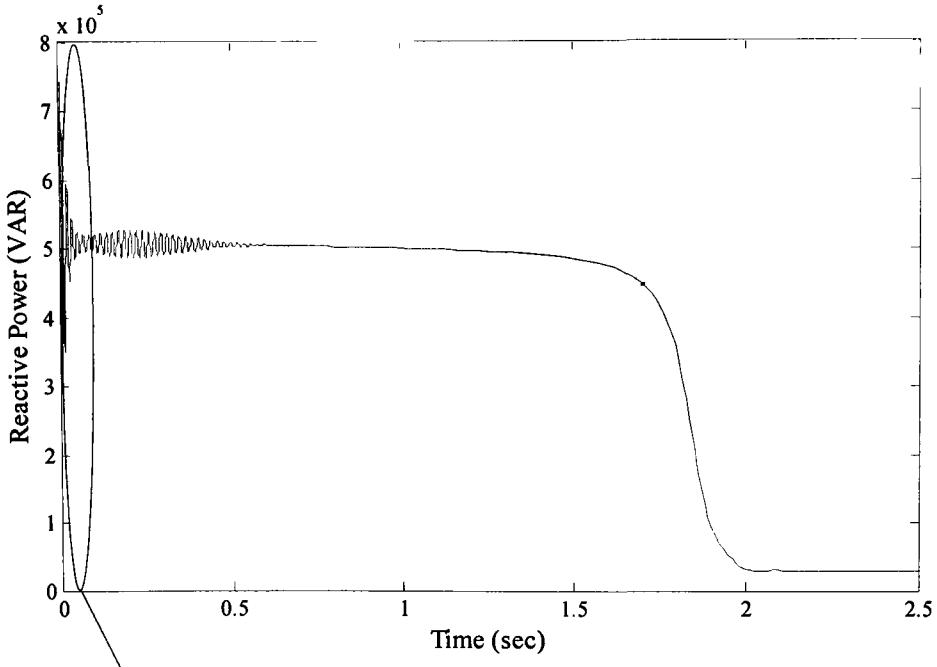

(a)

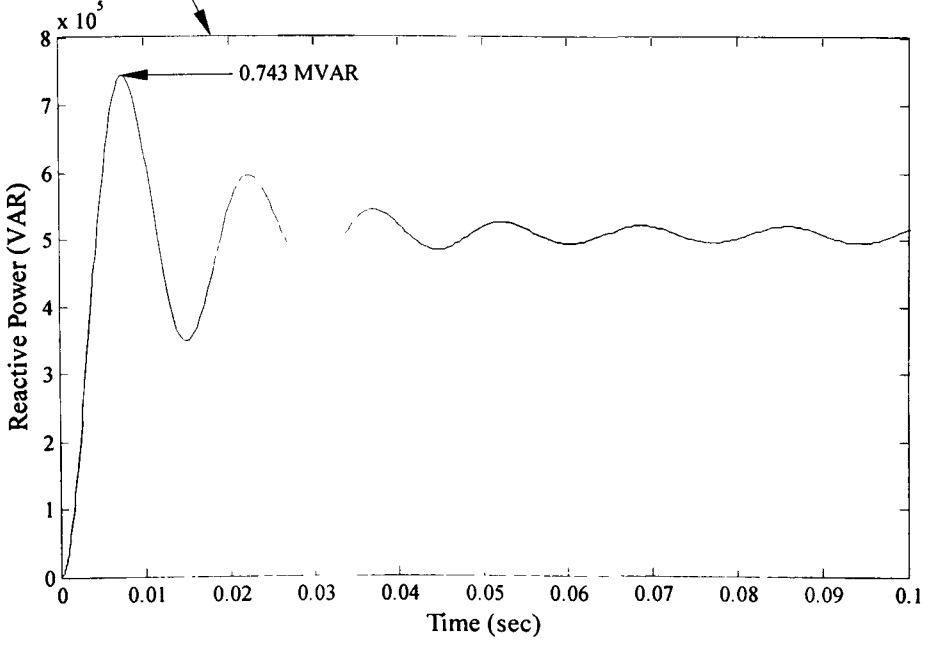

(b)

Fig. 57. Reactive power calculated by unsaturated model at no load. (a) Plot for 2.5 sec. (b) Plot (zoomed in) for 0.1 sec.

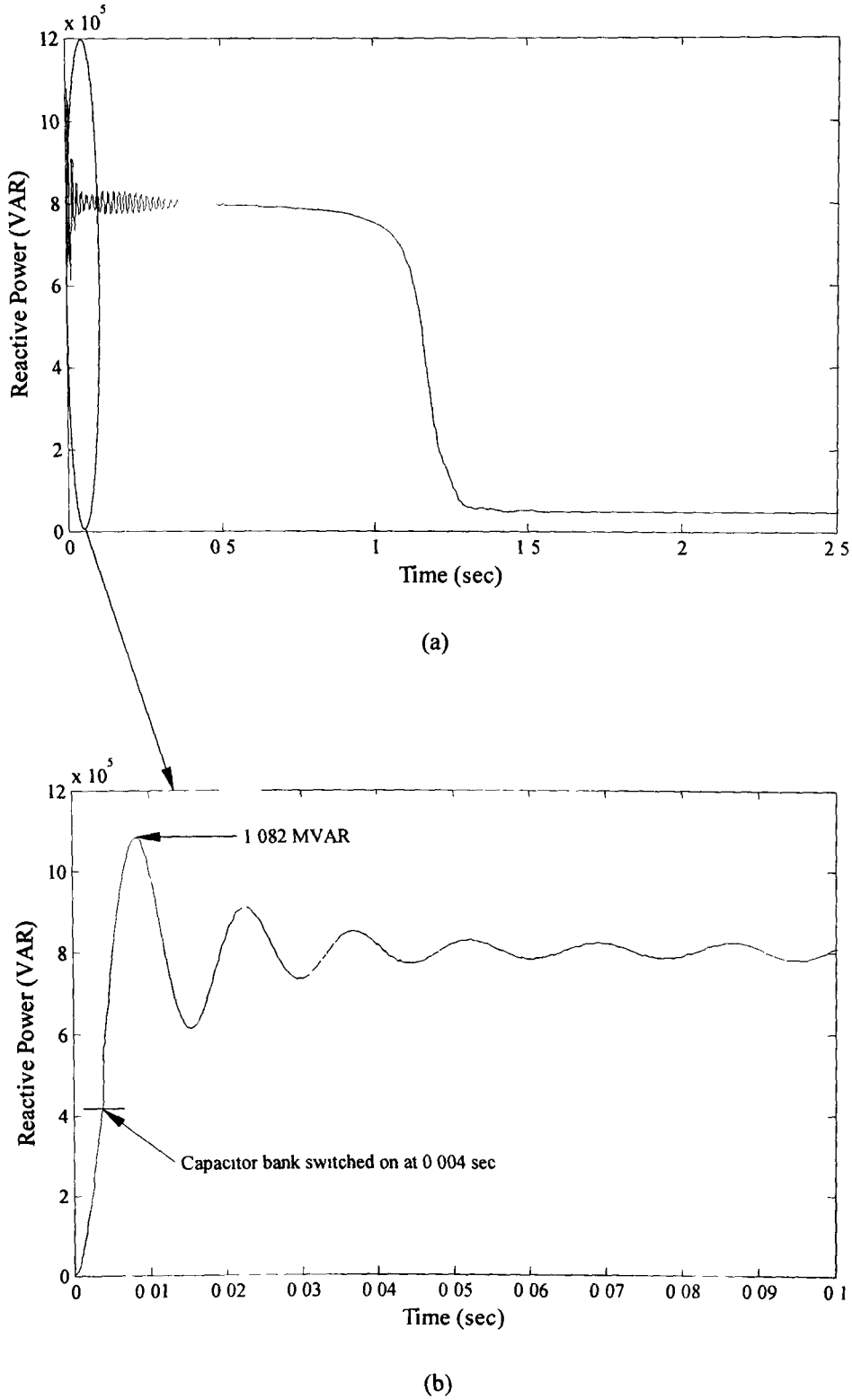

Fig. 58. Reactive power calculated by unsaturated model with shunt capacitors at no load. (a) Plot for 2.5 sec. (b) Plot (zoomed in) for 0.1 sec

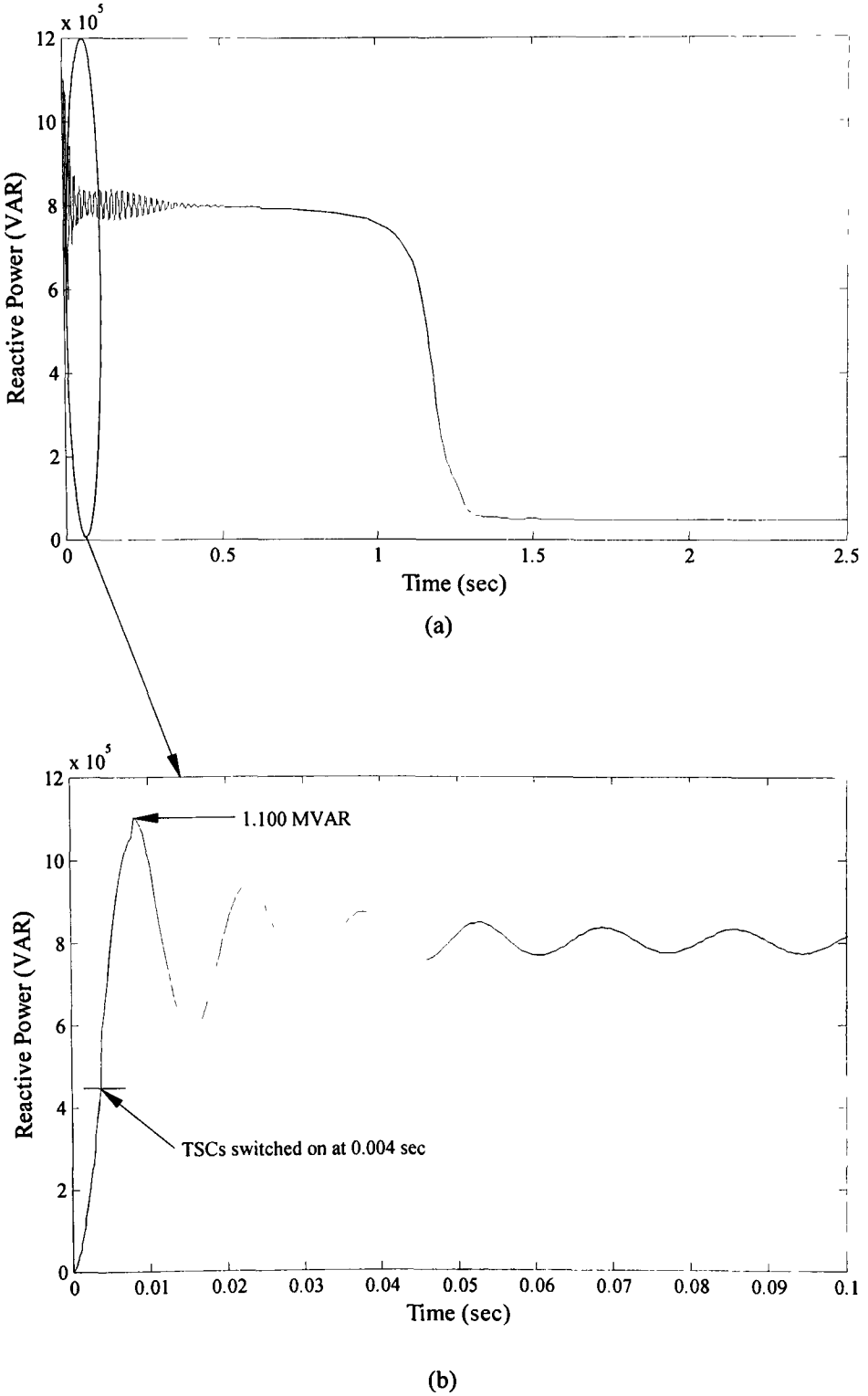

Fig. 59. Reactive power calculated by unsaturated model with SVC at no load. (a) Plot for 2.5 sec. (b) Plot (zoomed in) for 0.1 sec.

4.3.2.2 Terminal Voltage and Reactive Power at Full load

In this section, behavior of terminal voltage and consumption of reactive power of 500 hp induction motor at full load during starting period will be investigated and analyzed. As in the previous section we investigated that, motor needs some external means to boost the terminal voltage during starting transient period. During loading condition this 500 hp motor will not start from stand still condition as can be seen in the Fig. 60. Because motor itself has huge inertia of its rotor shaft, and with a coupled load it become difficult to start from at rest. The motor draws high starting current during starting, and consequently voltage drop to 1466.6 volts which is not enough for starting as can be seen in Fig. 60(b). The shunt capacitors and SVC are employed to boost the terminal voltage during starting as mentioned in the Figs. 61, 62. As explain in the last section, primary objective of both external means of supplying reactive power is the voltage regulation. Shunt capacitors are switched on at t=0.004 sec, when the maximum voltage drop is 1586.6 volts as can be examined in Fig. 61(b). At t=0.008 the voltage shoot up to 2062.75 volts, and then at t=3.5 sec at steady state voltage settles at 2300 volts. In case of SVC, the maximum voltage drop of 1643.9 volts has been seen at the time of switching TSC on at t=.004 sec, which boost the voltage to 2013.5 volts at t=0.008 sec. The steady state voltage 2300 volts will be achieved at t=3.5 sec.

The reactive power versus time plot shows in Fig. 63(a) that motor has oscillatory behavior while consuming 0.5 MVAR at 0.1 sec after the early transient. The maximum reactive power consumed by 500 hp motor at full load at time t=0.008 is 0.743 MVAR, which is equal to the value consumed during the no load conditions as plotted in Fig. 63(b). During loading condition, motor draws excessive starting current which increase the demand of reactive power. Shunt capacitors and SVC are used to support the necessary VARs during loading conditions as shown in the Fig. 64, 65. For both the cases, the acceleration time of the motor reduced considerably to 3.5 sec with loading condition. The maximum value of reactive power being consumed by the motor at full load for both shunt capacitors and SVC is same as described earlier for no load conditions which can be noticed from Figs. 64(a), 65(b).

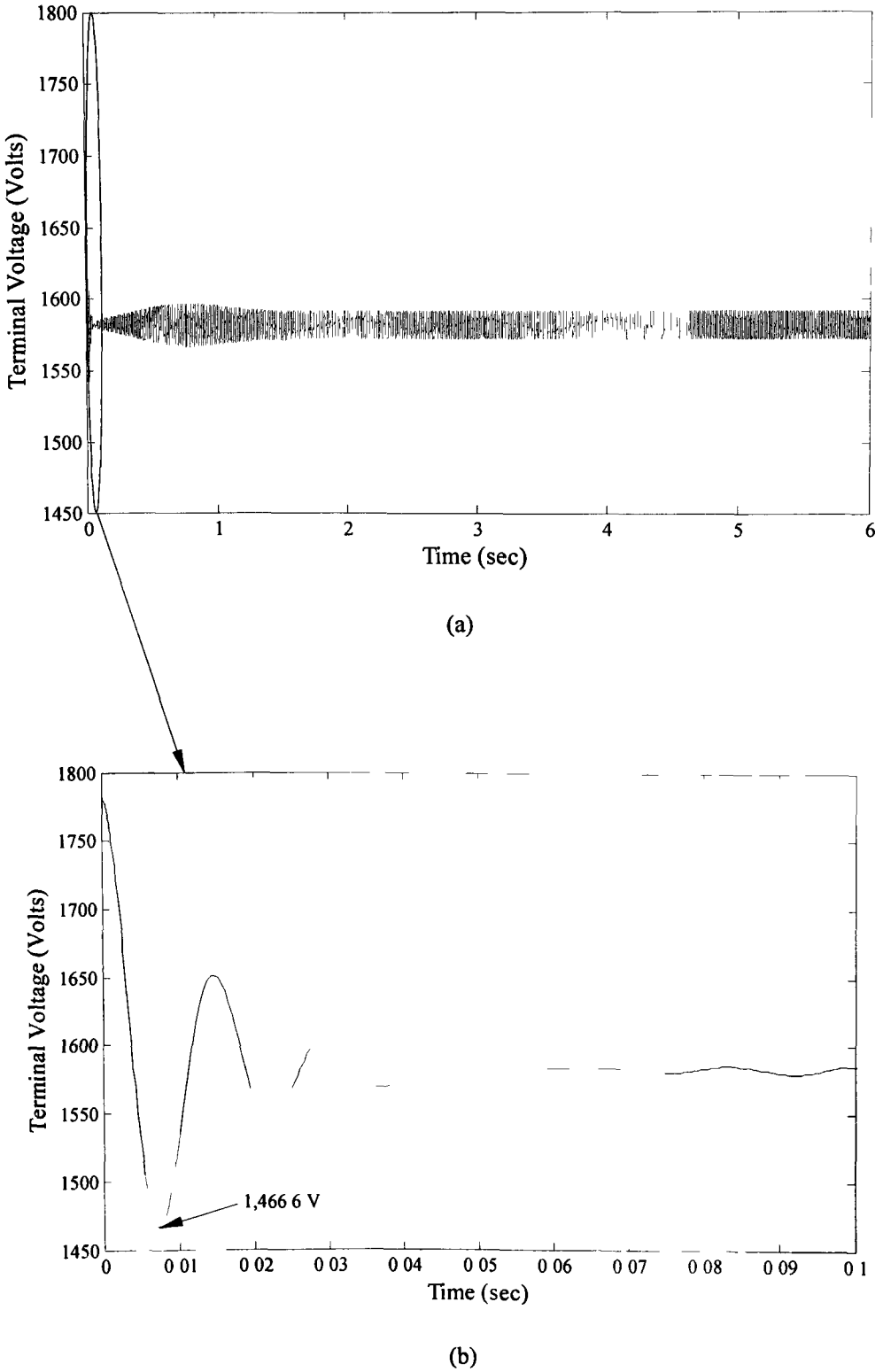

Fig. 60. Terminal voltage calculated by unsaturated model at full load. (a) Plot for 6 sec. (b) Plot (zoomed in) for 0.1 sec.

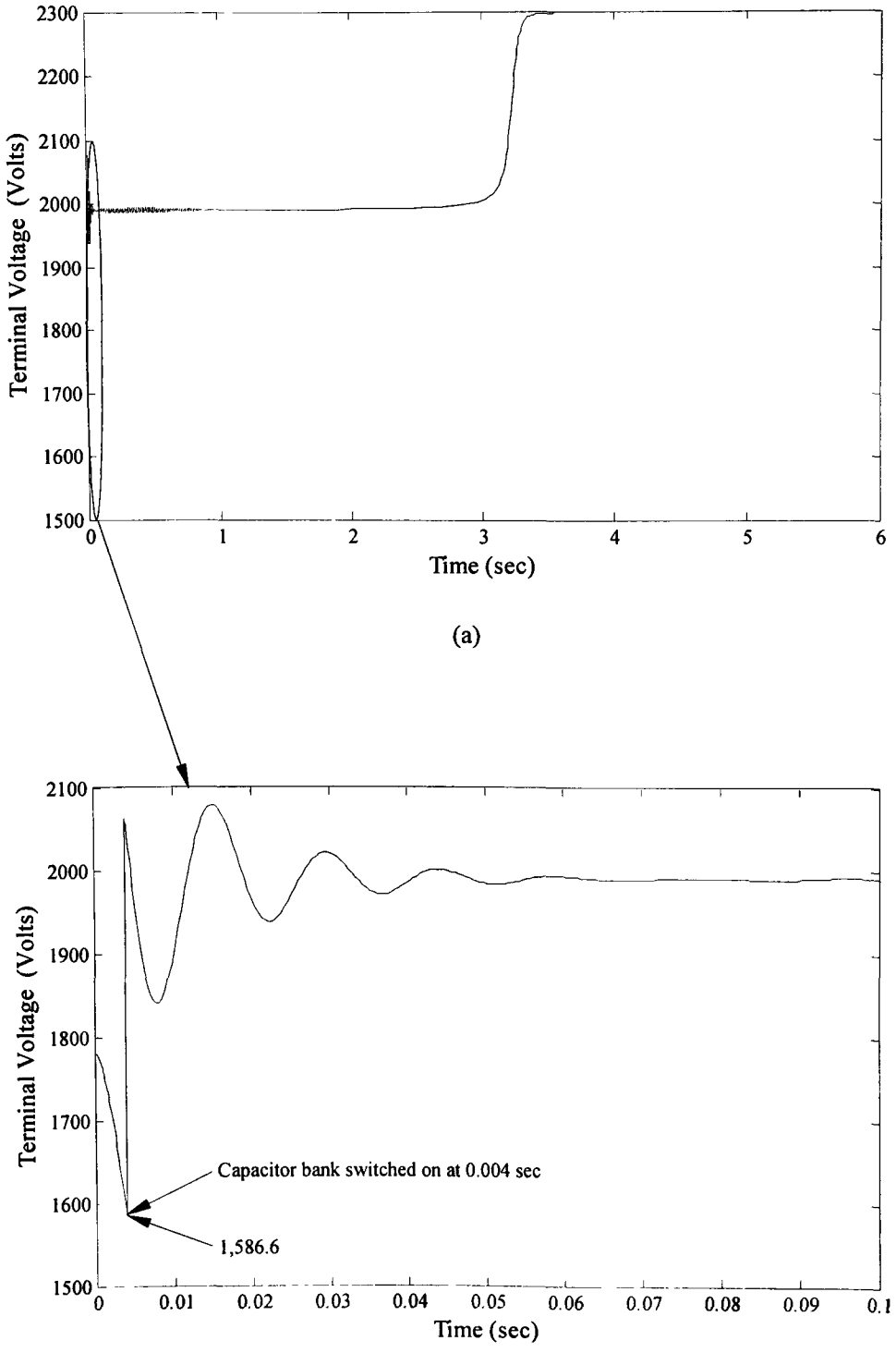

Fig. 61. Terminal voltage calculated by unsaturated model with shunt capacitors at full load. (a) Plot for 6 sec. (b) Plot (zoomed in) for 0.1 sec.

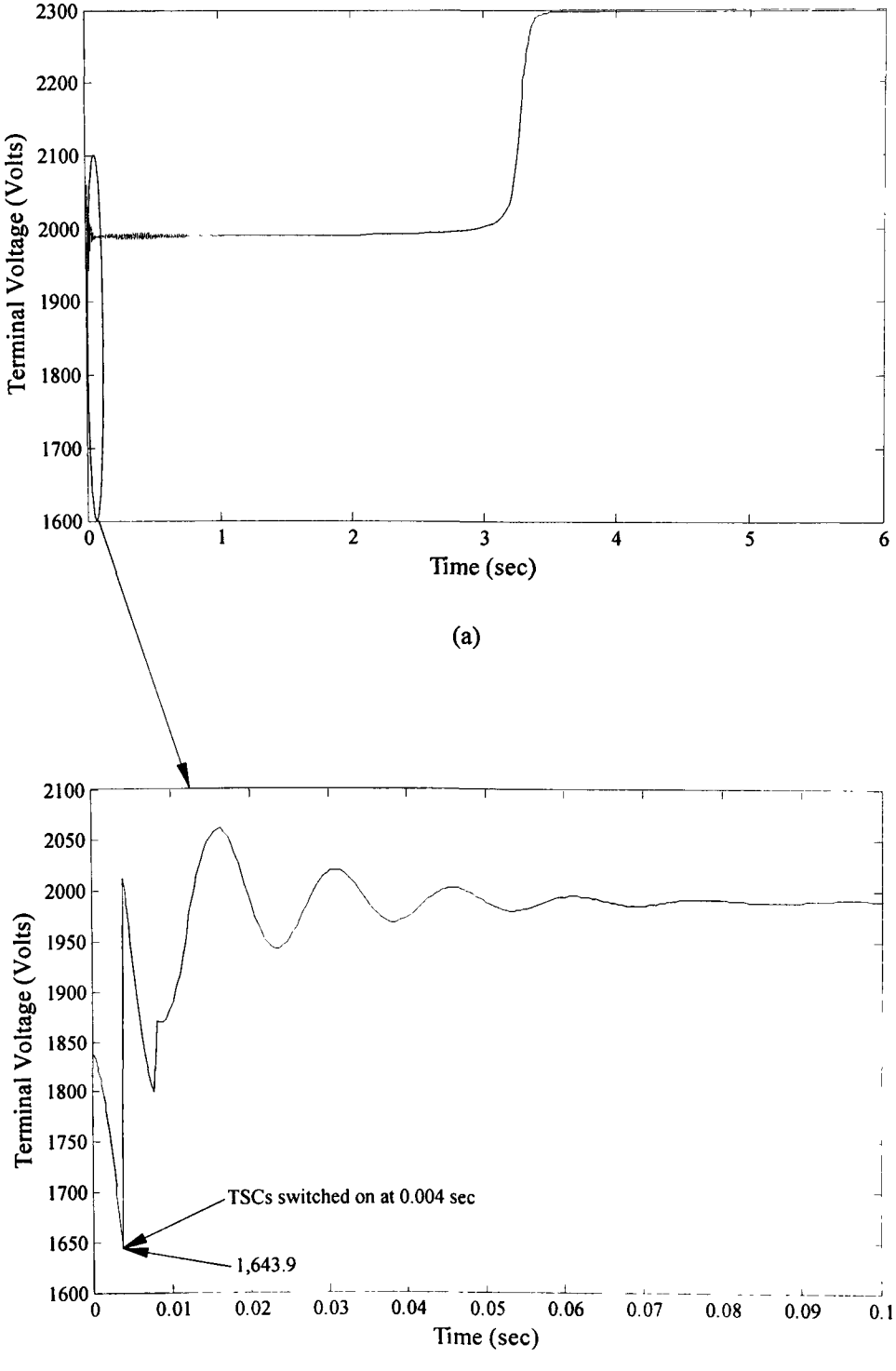

Fig. 62. Terminal voltage calculated by unsaturated model with SVC at full load. (a) Plot for 6 sec. (b) Plot (zoomed in) for 0.1 sec.

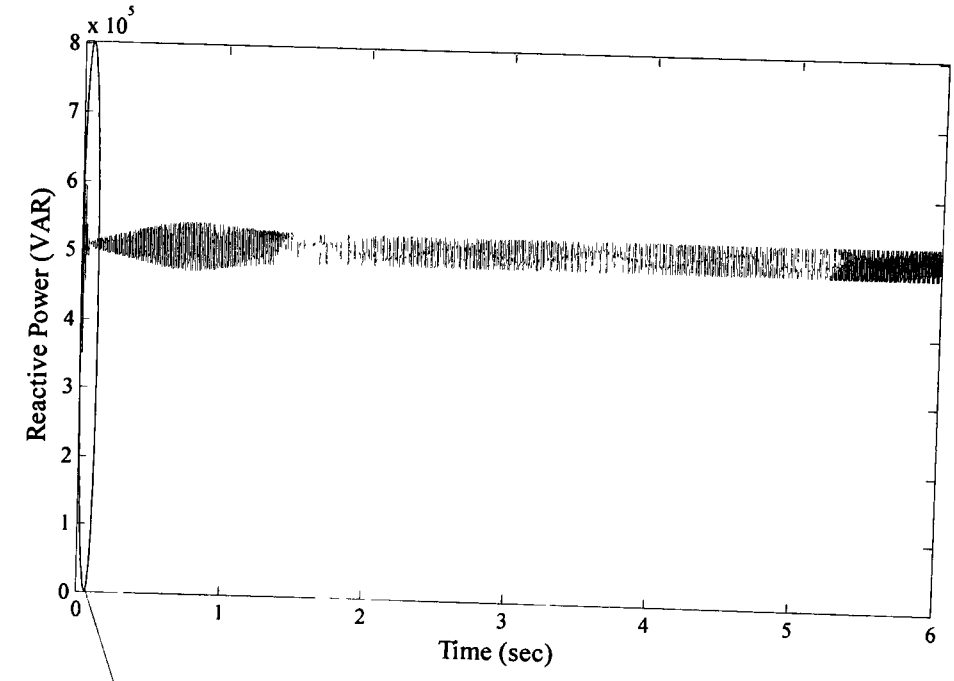

(a)

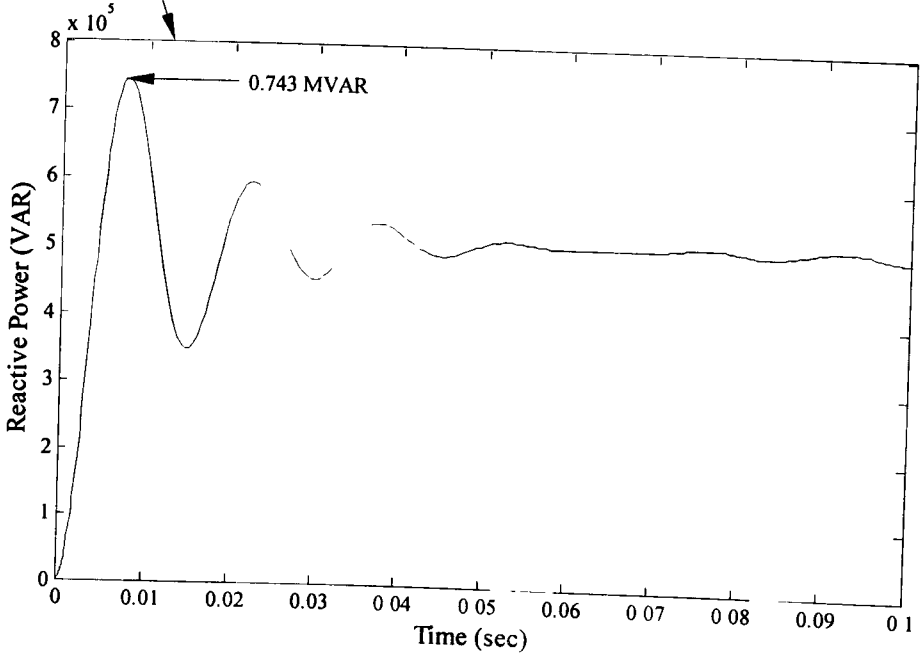

(b)

Fig. 63. Reactive power calculated by unsaturated model at full load. (a) Plot for 6 sec. (b) Plot (zoomed in) for 0.1 sec.

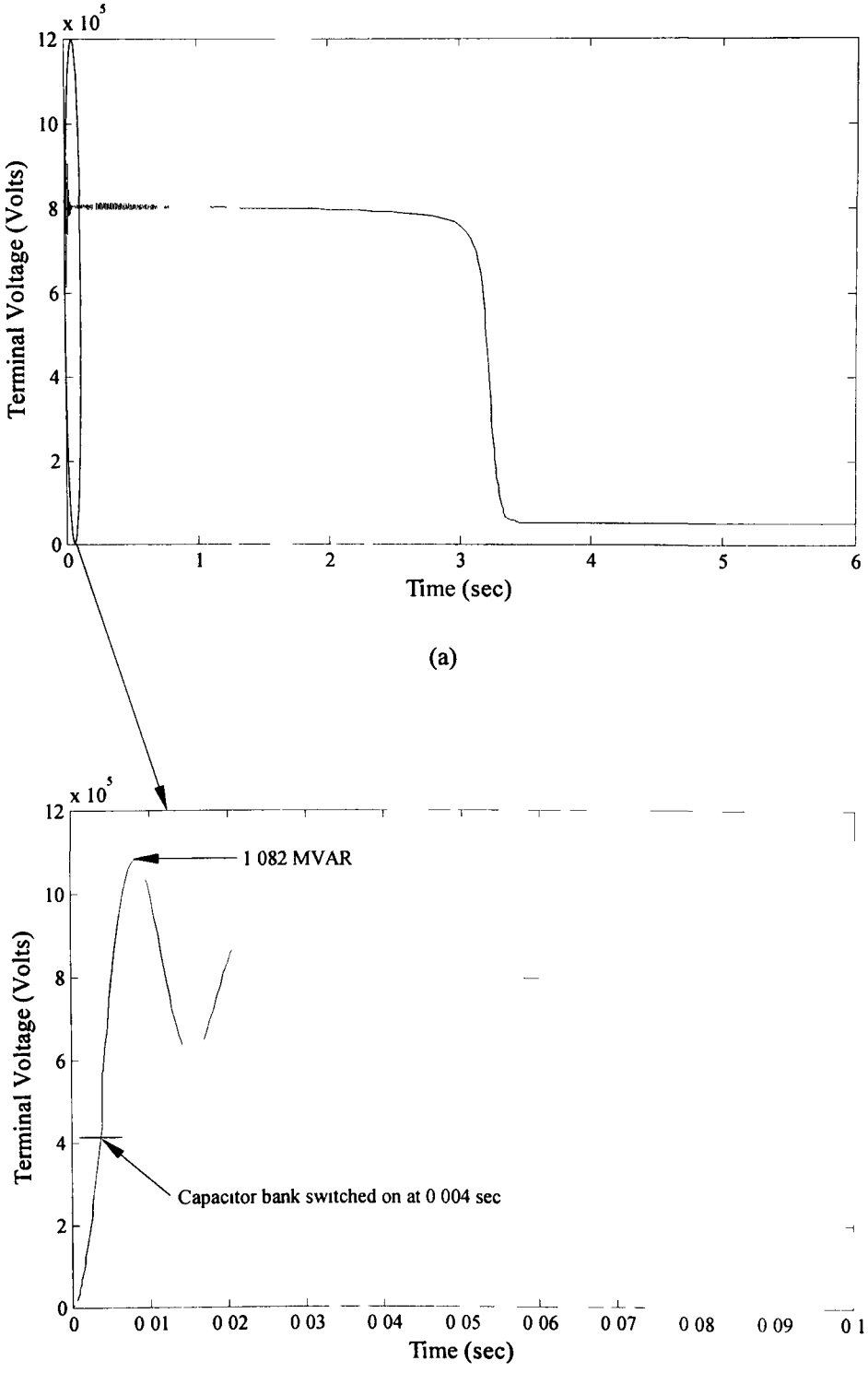

Fig 64 Reactive power calculated by unsaturated model with shunt capacitors at full load (a) Plot for 6 sec (b) Plot (zoomed in) for 0 1 sec

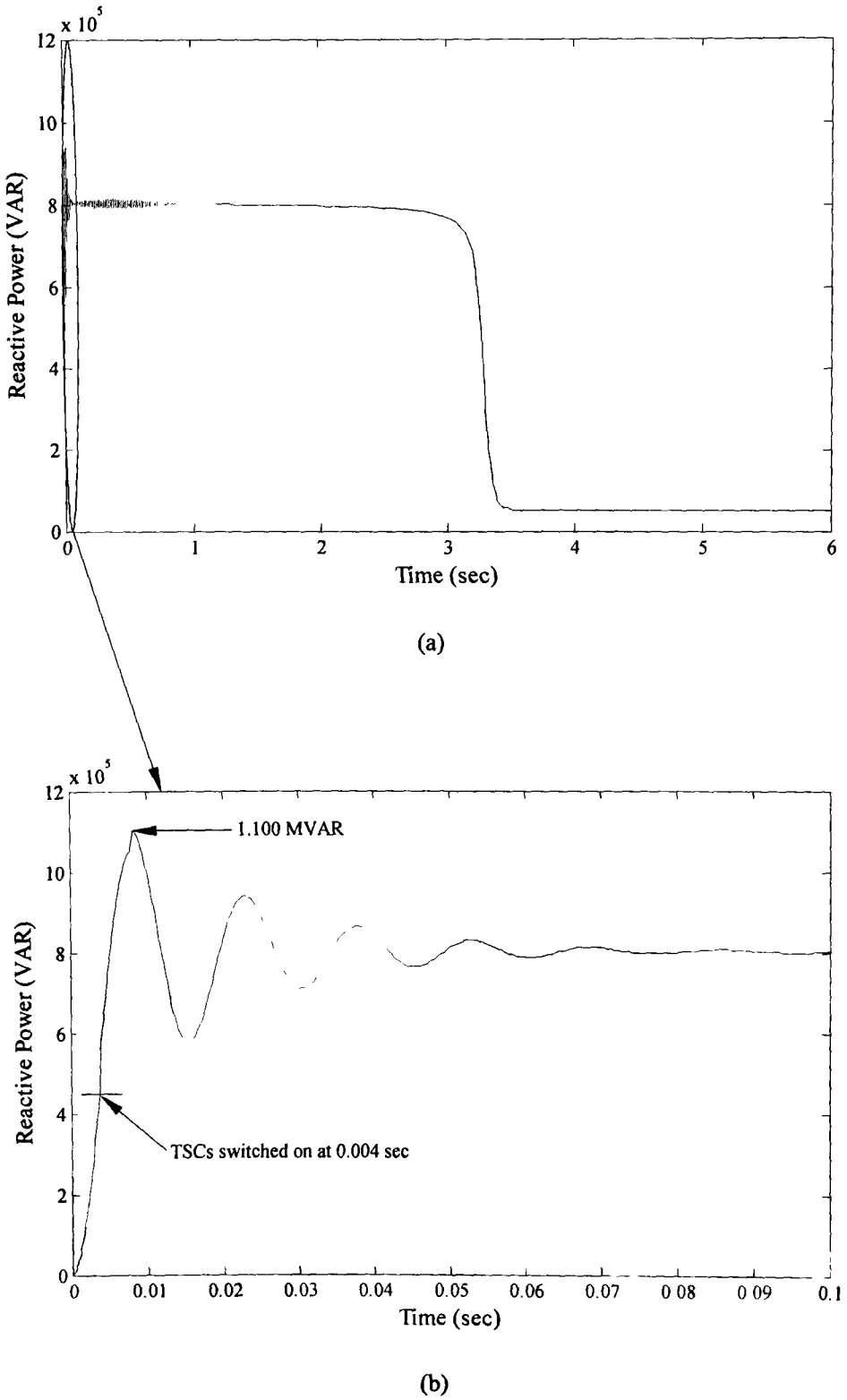

Fig. 65. Reactive power calculated by unsaturated model with SVC at full load. (a) Plot for 6 sec. (b) Plot (zoomed in) for 0.1 sec.

4.3.2.3 Comparison of Starting Performance of 50 hp and 500 hp motors

In this section the starting performance of 50 hp and 500 hp motors will be compared. The main focus will be comparing of terminal voltages behavior and consumption of reactive power calculated for unsaturated models for both the motors. As we have examined in the Fig. 18 the terminal voltage drop at no load for 50 hp motor is 21% of the rated voltage, with an acceleration time of 0.7 sec, whereas the terminal voltage drop for 500 hp motor at no load is 36.23% of the rated voltage as can be seen in Fig. 57 with an acceleration time of 2 sec. We have noticed that the terminal voltage drop for bigger motor (500 hp) is 15.23% more than the 50 hp motor of their rated voltages. For full load conditions, both the motors will have nearly same voltage drop, as for no load conditions as mentioned above, but the bigger motor will not accelerate from standstill as it needs high starting current. As calculated before, voltage drop while starting 500 hp motor at full load is 36.23% which shows that motor needs some external source (compensator) in order to boost the terminal voltage and reduce the recovery time so that motor can gain the steady state in less time.

SVC and shunt capacitors supply the necessary VARs to both the motors depending on the voltage drop and VARs requirement. SVC and shunt capacitors efficiency for both the motors is nearly same. By using of SVC and shunt capacitors, the starting time is reduced considerably for both motors. The steady state consumption ratio for bigger motor is relatively less as compared to the 50 hp motor because of comparatively low stator current. We have noticed from the analysis that SVC and shunt capacitors improve the starting performance of both motors (50hp and 500hp) nearly in the same manner. During the transient period SVC improve the terminal voltage more smoothly and steady.

4.3.2.4 Future Work

In this research work, starting performance of two induction motors is comprehensively analyzed for no load and full load conditions. Main flux saturation has been incorporated to investigate the starting characteristics of the e50 hp induction motor. In future, it will be very useful to investigate starting performance of different size of induction motors while including both main and leakage flux saturation.

5. Conclusion

This research work is an effort to study the starting performance of a saturated induction motor. Moreover, the starting performance of a relatively larger induction motor has also been investigated. Transient induction motor model is developed to investigate and analyze the starting characteristics for different loading conditions. Static VAR compensator (SVC) and shunt capacitors are employed to improve the starting performance by minimizing terminal voltage drop. Large motor (500 hp) motor is used to compare the voltage behavior with 50 hp during starting. The effects of main flux saturation on the different starting parameters have been studied. The following conclusions can be developed from the findings of these investigations:

- The terminal voltage drop during starting depends on the starting inrush current of the motor.
- The terminal voltage drop for larger motor is much higher as compared to the smaller motor.
- The acceleration time of the motor has significant impact on the motor starting performance and load.
- The acceleration time for large motor is longer as compared to the time required for the small motor to gain steady state.
- The starting and acceleration torque of induction motor is function of terminal voltage of the motor.
- The amount of reactive power motor needs during starting is a function of steady state voltage.
- Shunt capacitors can be an economical source of reactive power in order to boost the terminal voltage during starting.
- The switching time of the capacitor bank is absolutely important in order to avoid the switching transients.
- The voltage regulation of shunt capacitors is poor as compared to SVC.
- The static VAR compensator (SVC), a solid state switching device can be a useful source of supplying controlled reactive power and voltage regulation.
- SVC can limit the inrush current and improve the voltage more effectively during both transient and steady state.

- SVC improves the staring performance of 500 hp motor nearly in a same manner as for 50 hp motor.
- To analyze the dynamic behavior of induction motor while starting more accurately, the effect of saturation is significant.
- The stator current of the motor considering saturation is significantly high as compared to the unsaturated one.
- The large discrepancies in the results calculated by ignoring and considering the saturation can be attributed to the significant increase in the magnetizing current if saturation is considered.

References

[1] R. J. Kerkman, G. L. Skibinski, D. W Schlegel, "AC drives; Year 2000 and Beyond," *Record of IEEE-APEC,* March 1999.

[2] R. H. Engelmann, William. H. Middendorf, *Handbook of Electric Motor*, Marcel Dekker, Inc., 1995.

[3] A. A. Shaltout, "Analysis of tensional torques in starting of large squirrel cage induction motor," *IEEE Transactions on Energy Conversion*, Vol. 9, Issue 1, March 1994, pp. 135-142.

[4] P. C. Krause, *Analysis of Electric Machinery, McGraw-Hill, Inc.* 1988.

[5] J. Nevelsteen, H. Arogan, "Starting of large induction motors---methods and economics," *IEEE Transactions on Industry Applications,* Vol. 25. Issue 6, November 1989, pp. 1012-1018.

[6] J. Larabee, B. Pellegrino, B. Flick, "Induction motor starting methods and issues," *Petroleum and Chemical Industry Conference*, September 2005, pp. 217-222.

[7] J. Bredthauer, N. Struck, "Starting of large medium voltage motors: design, protection, and safety aspects," *IEEE Transactions on Industry Applications,* Vol. 31. Issue 5, October 1995, pp. 1167-1176.

[8] R. McElveen, M. Toney, "Starting high inertia loads," *IEEE Transactions on Industry Applications,* February 2001, pp. 257-265

[9] M. Z. El-Sadek, N. H. Fetih, F N. Abdelbar, "Starting of induction motors by static VAR compensator," *International Conference on Power Electronics and Variable Speed Derive,* July 1998, pp. 444-447.

[10] A. E. Hammad, "Prevention of transient voltage instabilities due to induction loads by static VAR compensator," *IEEE Transactions on Power Systems*, Vol. 4, Issue 3, August 1989, pp. 1182-1190.

[11] R. Natarajan, V K. Misra, M. Oommen, "Time domain analysis of induction motor starting transients", Power Symposium, Proceedings of Twenty First Annual North-American, October 1989, pp.120-128.

[12] G. Richards, M.A. Laughton, "Limiting induction motor transient shaft torques following source discontinuities," *IEEE Transactions on Energy Conversion,* Vol. 13, Issue 3, September 1998, pp. 250-256.

[13] S. Ertem, "A fast recursive solution for induction motor transients," *IEEE Transactions on industry Application,* Vol. 24, Issue 5, September 1988, pp. 758-764.

[14] R. Natarajan, V K. Misra, "Starting transient current of induction motors without and with terminal capacitor," *IEEE Transactions on Energy conversion,* Vol. 6. Issue 1, March 1991, pp. 134-139.

[15] P. Kundur, *Power system stability and control, McGraw Hill, 2004.*

[16] R. Hadidi, I. Mazhari, A. Kazemi, "Simulation of induction motor starting with SVC," *IEEE Conference on Industrial Electronics and Application*, May 2007, pp. 1135-1140.

[17] M. S. Sarma, *Electric Machinery , International Thomas Publishing*, 1994.

[18] W A. Jack, G. M. Shan, "Evaluating the effects of motor starting on industrial and commercial power systems," *IEEE Transactions on Industry Application,* Vol. 1A-14, Issue 4, July 1978, pp. 292-305.

[19] S. H. John, "Capacitor starting of large motors," *IEEE Transactions on Industry Application,* Vol. 1A-14, Issue 4, July 1978, pp. 209-212.

[20] J. F Heidbreder, "Induction motor temperature characteristics," *IEEE Transactions on Power Apparatus and Systems,* Vol. Pas-77, Issue 3, November 1958, pp. 257-265.

[21] A. N. Eliasen, "High inertia drive motors and their starting characteristics," *IEEE Transactions on Power Apparatus and Systems,* Vol. Pas-99, Issue 4, July 1980, pp. 1472-1482.

[22] P. C. Krause, *Analysis of Electrical Machinery*, New York: McGraw-Hills, 1986.

[23] J. Dixon, L. Moran, J. Rodriguez, R. Domke, "Reactive power compensation technologies, state-of-the-art review," *Proceedings of IEEE,* Vol. 93, Issue 12, December 2005, pp. 2144-2164.

[24] N. Hingorani, L. Gyuggyi, "Understanding FACTS, concepts and technology of Flexible AC Transmission System," *IEEE press, New York*, 2000.

[25] T. J. Miller, *Reactive Power Control in Electric System*, John Willey & Sons.1982.

[26] A. E. Fitzgerald, C. Kingsley C. S. D. Umans, *Electric Machinery, McGraw-Hill*, 1991.

[27] R. Natarajan, *Power System Capacitors*, Taylor & Francis Group. LLC, 2005.

[28] M. A. Badr, A. I. Alolah, M. A. Abdel-halim, "A capacitor start three phase induction motor," *IEEE Transactions on Energy conversion,* Vol. 10, Issue 4, December 1995, pp 675-680.

[29] E. Acha, V. G. Agelidis, O Anaya-Lara, T. J. E. Miller, *Power electronic control in electrical system Newnes Power Engineering Series*, 2002.

[30] B. Lockley, G. Philpott, "Static VAR compensators a solution to the big motor/weak system problem," *IEEE Industry Applications Magazine,* Vol. 8, Issue 2, March 2002, pp 43-49.

[31] A. Hammad, "New roles for static VAR compensators in transmission systems," *Brown Boveri Review,* Vol. 73, June 1986, pp 314-320.

[32] A. E. Hammad, "Analysis of power system stability enhancement by static VAR compensators," *IEEE transaction on Power Systems,* Vol. 4, Issue 1, November 1986, pp. 222-227.

[33] S. Abe, Y. Fukunaga, B. Kondo, "Power system voltage stability," *IEEE Transactions on Power Apparatus and Systems,* Vol. Pas-101, Issue10, October 1982, pp. 3830-3840.

[34] H. Dommel, N. Sato, "Fast transient stability solution," *IEEE Transactions on Power Apparatus and Systems,* Vol. Pas-91, Issue12, July 1972, pp. 1643-1650.

[35] S. Ertem, Y. Baghzouz, "Simulation of induction machinery for power system studies," *IEEE Transactions on Energy conversion,* Vol. 4, Issue 1, March 1989, pp 88-94.

[36] R. Harley, E. Makram, G. Jennings, "Induction motor model for the study of transient stability in both balanced and unbalanced multi-machine networks," *IEEE Transactions on Energy Conversion,* Vol. 7, Issue 1, March 1992, pp 209-215.

[37] H. M. Jabr, N. C. Kar, "Starting performance of saturated induction motors," *IEEE Power Engineering Society General Meeting,* June 2007, pp. 1-7.

[38] E. Levi, "A unified approach to main flux saturation modeling in d-q axis models of induction machines," *IEEE Transactions on Energy Conversion,* Vol. 10, Issue 3, September 1995, pp 209-215.

[39] J. O. Ojo, A. Consoli, "An improved model of saturated induction machines," *IEEE Transactions on Industry Applications,* Vol. 26. Issue 2, March 1990, pp 212-221.

[40] C. A. Smith, C. R. Healey, S. Williamson, "A transient induction motor model including saturation and deep bar effect," *IEEE Transactions on Energy Conversion,* Vol. 11, Issue 1, March 1996, pp. 8-15.

[41] T. A. Najafabadi, S. M. Nabavi, "The analysis of saturation and core loss effects of induction motor direct starting," *International Conference on Electrical Machines and Systems,* October 2007, pp. 1265-1268.

[42] V. Donescu, A. Charette, Z.Yao, "Modeling and simulation of saturated induction motors in phase quantities," *IEEE Transactions on Energy Conversion,* Vol. 14, Issue 3, September 1999, pp. 386-393.

[43] E. Levi , V Vuekovic, S. Vukosavic, "Study of main flux saturation effects in field-oriented induction motor drives," *International Conference on Industrial Electronics Society,* March 1989, pp. 219-224.

[44] N. Erdogan, H. Henao, R. Grisel, "The analysis of saturation effects on transient behavior of induction machine direct starting," *IEEE Symposium on Industrial Electronics*, May 2004, pp 975-979.

[45] J. M. Ferreira de Jesus, "A model for saturation in induction machines," *IEEE Transactions on Energy conversion,* Vol. 3, Issue 3, September 1988, pp. 682-688.

[46] O. I. Okoro, "MATLAB simulation of induction machine with saturable leakage and magnetizing inductances," *The Pacific Journal of Science and Technology,* Vol. 5, Issue 1, April 2003, pp. 5-15.

[47] J. E Brown, K. P Kovacs, P Vas, "A method of including the effects of main flux path saturation in the generalized equations of A.C machines," *IEEE Transactions on Power Apparatus and Systems,* Vol. PAS-102, January 1993, pp. 96-103.

[48] D. Bispo, L. Martins, J. Neto, D. A. de Andrade, "A new strategy for induction machine modeling taking into account the magnetic saturation," *IEEE Transactions on Industry Application,* Vol. 37, pp. 1710-1719, 2001.

[49] R. A. Managuli, "Motor starting with shunt capacitors an alternate approach to voltage dip control," *Master of Science Thesis Electrical and Computer Engineering,* University of Nevada, Las Vegas, December, 1996.

[50] R. Toyoshima, T. Funaki, T. Hikihara, "Anomalous phenomenon of conduction angle in TCR-SVC and its control," *35th Annual IEEE Power Electronic Conference,* pp. 3403-3408, 2004.

[51] S. Jalali, I.Dobson, R.H. Lasseter, G. Venkataramanan,"Switching time bifurcations in a thyristor-controlled reactor," *IEEE Transactions on Circuits and Systems,* Vol. 43, Issue 3, March 1996, pp. 209-218.

[52] R. J. Koessler, "Dynamic simulation of static VAR compensators in distribution systems," *IEEE Transactions on Power Apparatus and Systems,* Vol.7, Issue 3, August 1992, pp. 1285-1291.

[53] K. Keerthivasan, V S. Deve, J. Jerome, R. Ramanujam, "Modeling of SVC and TCSC for power system dynamic simulation," *International Conference on Power Engineering*, Vol. 2, December 2005, pp. 696-700.

[54] L. Gyugyi, "Reactive power generation and control by thyrisor circuits", *IEEE Transactions on Industry Applications,* Vol. 1A-15, Issue 5, September 1979, pp. 521-532.

[55] L. Gyugyi, R. Otto, T. Putman, "Principles and applications of static, thyristor-controlled shunt compensators," *IEEE Transactions on Power Apparatus and Systems,* Vol. Pas-97, Issue 5, October 1980, pp. 1935-1945.

[56] P. C. Krause, "Simulation of symmetrical induction machinery," *IEEE Transactions on Power Apparatus and Systems,* Vol. Pas-84, Issue 11, November 1965, pp. 1038-1053.

[57] R. Krishnan, *Electric Motor Drives,* Prentice Hall, Inc. 2001.

[58] O. Chee-Mun, *Dynamic Simulation of Electric Machinery*, Prentice Hall, 1998.

VITA AUCTORIS

NAME: Muhammad Choudhary

YEAR OF BIRTH: 1966

EDUCATION: Bachelor of Science in Electrical Engineering
University of Engineering & Technology Taxila,
PAKISTAN
1990-1995

Master of Applied Science in Electrical Engineering
University of Windsor, CANADA
2006-2008